FINAL Report E

TRyy1110

Project Title: Design and Evaluation of High-Volume Fly Ash (HVFA) Concrete Mixes

Report E: Hardened Mechanical Properties and Durability Performance of HVFA Concrete

Prepared for
Missouri Department of Transportation
Construction and Materials

Missouri University of Science and Technology, Rolla, Missouri

October 2012

The opinions, findings, and conclusions expressed in this publication are those of the principal investigators and the Missouri Department of Transportation. They are not necessarily those of the U.S. Department of Transportation, Federal Highway Administration. This report does not constitute a standard or regulation.

ABSTRACT

A rising concern in today's construction industry is environmental responsibility. The addition of fly ash is a leading innovation in sustainable design of concrete. Fly ash, a waste by-product of coal burning power plants, can be used to replace a portion of the Portland cement in concrete. Investigators are pushing for higher and higher total replacement levels in what is known as high-volume fly ash (HVFA) concrete. However, minor issues observed with lower fly ash replacement levels may be exacerbated as the levels increase.

Before the implementation of any new and innovative concrete, a new mix must be subjected to a series of tests and then compared to a conventional concrete mix that was subjected to the same test. In this investigation HVFA concrete was subjected to mechanical property tests such as compressive strength and modulus of elasticity as well as durability tests such resistance to freeze-thaw and chloride penetration. After being subjected to these tests, the HVFA concrete was found to be comparable to conventional concrete except for salt scaling.

TABLE OF CONTENTS

Page

ABSTRACT ii
TABLE OF CONTENTS iii
LIST OF ILLUSTRATIONS vi
LIST OF TABLES ix
1. INTRODUCTION 1
1.1. BACKGROUND, PROBLEM, & JUSTIFICATION 1
1.2. OBJECTIVES & SCOPE OF WORK 2
1.3. RESEARCH PLAN 3
1.4. OUTLINE 3
2. LITERATURE REVIEW 6
2.1. HIGH-VOLUME FLY ASH CONCRETE 6
2.2. MECHANICAL PROPERTY TESTING METHODS 10
2.2.1. Compressive Strength. 10
2.2.2. Modulus of Elasticity. 11
2.2.3. Modulus of Rupture. 12
2.2.4. Splitting Tensile Strength. 13
2.3. DURABILITY OF CONCRETE 14
2.3.1. Freezing and Thawing. 14
2.3.2. Chloride Attack. 16
2.4. DURABILITY TESTING METHODS 19
2.4.1. Resistance to Freezing and Thawing. 19
2.4.2. Rapid Chloride Penetration. 20
2.4.3. Chloride Content Analysis. 22
2.4.4. Concrete Resistivity.. 24
2.4.5. Scaling Resistance. 27
2.5. HIGH VOLUME FLY ASH CONCRETE 29
2.5.1. Mechanical Properties. 29
2.5.2. Durability Performance. 29

3. MECHANICAL PROPERTY TESTS 31
3.1. INTRODUCTION 31
3.2. MIX DESIGN 32
3.3. COMPRESSIVE STRENGTH TEST 36
3.3.1. Introduction. 36
3.3.2. Fabrication. 36
3.3.3. Testing & Procedure. 37
3.4. MODULUS OF ELASTICITY TEST 40
3.4.1. Introduction. 40
3.4.2. Fabrication. 40
3.4.3. Testing & Procedure. 41
3.5. MODULUS OF RUPTURE TEST 43
3.5.1. Introduction. 43
3.5.2. Fabrication. 43
3.5.3. Testing & Procedure. 44
3.6. SPLITTING TENSILE TEST 46
3.6.1. Introduction. 46
3.6.2. Fabrication. 46
3.6.3. Testing & Procedure. 47
4. DURABILITY TESTS 49
4.1. INTRODUCTION 49
4.2. RAPID FREEZING & THAWING TEST 50
4.2.1. Introduction. 50
4.2.2. Fabrication. 50
4.2.3. Testing & Procedure. 53
4.3. ELECTRICAL INDICATION TO RESIST CHLORIDE ION PENETRATION TEST 54
4.3.1. Introduction. 54
4.3.2. Fabrication. 55
4.3.3. Testing & Procedure. 55
4.4. PONDING TEST 58

4.4.1. Introduction. 58
4.4.2. Fabrication. 59
4.4.3. Testing & Procedure. 60
4.5. CONCRETE RESISTIVITY TEST 63
4.5.1. Introduction. 63
4.5.2. Fabrication. 65
4.5.3. Testing & Procedure. 65
4.6. SCALING TEST 66
4.6.1. Introduction. 66
4.6.2. Fabrication. 66
4.6.3. Testing & Procedure. 68
5. HARDENED PROPERTY AND DURABILITY RESULTS 70
5.1. COMPRESSIVE STRENGTH 70
5.2. MODULUS OF ELASTICITY 72
5.3. MODULUS OF RUPTURE 75
5.4. SPLITTING TENSILE 78
5.5. RAPID FREEZING & THAWING 80
5.6. ELECTRICAL INDICATION TO RESIST CHLORIDE PENETRATION ... 82
5.7. PONDING TEST 84
5.8. CONCRETE RESISTIVITY 87
5.9. SCALING 91
6. EVALUATION OF HIGH-VOLUME FLY ASH CONCRETE 93
6.1. MECHANICAL PROPERTIES 93
6.2. DURABILITY PERFORMANCE. 100
7. FINDINGS, CONCLUSIONS, AND RECOMMENDATIONS 104
7.1. FINDINGS AND CONCLUSIONS 104
7.2. RECOMMENDATIONS 106
HVFA DURABILITY TEST RESULTS DATA 108
REFERENCES 154

LIST OF ILLUSTRATIONS

Figure Page

Figure 2.5 - Electrostatic Precipitator Fly Ash Collection Process [Huffman, 2003]. 7

Figure 2.6 - Fly Ash at 4000x Magnification [Huffman, 2003] 9

Figure 2.7 – Typical Stress-Strain Diagram for Concrete, ... 11

Showing the Different Elastic Moduli [Mindess et al., 2002] 11

Figure 2.8 - Typical Modulus of Rupture Testing Setup [ASTM C 78–10]..... 13

Figure 2.9 - The Relative Volumes of Various Iron Oxides..... 17

from Mansfield [1981], Corrosion 37(5), 301-307. 17

Figure 2.10 - Typical RCT Setup..... 21

Figure 2.11 - Schematic Representation of the Four-Probe Resistivity Method [Broomfield, 2007]..... 26

Figure 3.1 - Compressive Strength Testing Setup 39

Figure 3.2 - High Strength Compressive Strength Specimens Post-Test 40

Figure 3.3 – 4 in. (102 mm) x 8 in. (203 mm) Cylinder Mold Compared to 6 in. (152 mm) x 12 in. (305 mm) Cylinder Mold 41

Figure 3.4 - Typical Compressometer 42

Figure 3.5 - Prepared Modulus of Rupture Specimen 44

Figure 3.6 - Modulus of Rupture Testing Setup 45

Figure 3.7 - Modulus of Rupture Specimen Post-Test 45

Figure 3.9 - Typical Splitting Tensile Test Setup 47

Figure 3.10 - Splitting Tensile Specimens Post-Test..... 48

Figure 4.1 - Freezing and Thawing Specimen Molds..... 51

Figure 4.2 - Freezing and Thawing Specimen with Protruding Bolt..... 52

Figure 4.3 - Setting Coating Being Applied to Concrete Specimens 56

Figure 4.4 - Typical Completed Specimen 57

Figure 4.5 – Typical RCT Setup..... 58

Figure 4.6 - Typical Ponding Specimen 60

Figure 4.7 - Concrete Core and Resulting Void in the Concrete Specimen 61

Figure 4.8 - Depths at which Powder Samples Were Collected..... 61

Figure 4.9 - Canin+ Wenner Probe 64
Figure 4.10 - Wenner Probe Grid 66
Figure 4.11 - Scaling Specimen Form 67
Figure 4.12 - Scaling Specimen Dike Keyway and Dike Construction 68
Figure 4.13 - Completed Scaling Specimen and Dike 68
Figure 5.1 - Strength Profile of HVFA Mixes 71
Figure 5.2 - Example of RCT Results 83
Figure 5.3 – Averaged Chloride Profile for HVFA Mixes 87
Figure 5.4 – Individual Specimen Results for Concrete Resistivity of Control Mix 88
Figure 5.5 – Individual Specimen Results for Concrete Resistivity of HVFA-70H Mix 88
Figure 5.6 – Individual Specimen Results for Concrete Resistivity of HVFA-70H Mix 89
Figure 5.7 – Individual Specimen Results for Concrete Resistivity of HVFA-70LA Mix 89
Figure 5.8 – Averaged Resistivity Results for HVFA Mixes 90
Figure 6.1 - Compressive Strength vs. Modulus of Elasticity 96
Figure 6.2 – Compressive Strength vs. Modulus of Rupture 97
Figure 6.3 – Compressive Strength vs. Splitting-Tensile Strength 99
Figure A.1 – Control-EC1TOP RCT Data 125
Figure A.2 – Control-EC1MIDDLE RCT Data 126
Figure A.3 – Control-EC2TOP RCT Data 127
Figure A.4 – Control-EC2MIDDLE RCT Data 128
Figure A.5 – HVFA-70H-EC1TOP RCT Data 129
Figure A.6 – HVFA-70H-EC1MIDDLE RCT Data 130
Figure A.7 – HVFA-70H-EC2TOP RCT Data 131
Figure A.8 – HVFA-70H-EC2MIDDLE RCT Data 132
Figure A.9 – HVFA-70L-EC1TOP RCT Data 133
Figure A.10 – HVFA-70L-EC1MIDDLE RCT Data 134
Figure A.11 – HVFA-70L-EC2TOP RCT Data 135
Figure A.12 – HVFA-70L-EC2MIDDLE RCT Data 136

Figure A.13 – HVFA-70LA-EC1TOP RCT Data 137
Figure A.14 – HVFA-70LA-EC1MIDDLE RCT Data 138
Figure A.15 – HVFA-70LA-EC2TOP RCT Data 139
Figure A.16 – HVFA-70LA-EC2MIDDLE RCT Data 140
Figure A.17 – Control-FT1 Data 142
Figure B.18 – Control-FT2 Data..... 143
Figure A.19 – Control-FT3 Data 144
Figure A.20 – HVFA-70H-FT1 Data..... 145
Figure A.21 – HVFA-70H-FT2 Data..... 146
Figure A.22 – HVFA-70H-FT3 Data..... 147
Figure A.23 – HVFA-70L-FT1 Data 148
Figure A.24 – HVFA-70L-FT2 Data 149
Figure A.25 – HVFA-70L-FT3 Data 150
Figure A.26 – HVFA-70LA-FT1 Data 151
Figure A.27 – HVFA-70LA-FT2 Data 152
Figure A.28 – HVFA-70LA-FT3 Data 153

LIST OF TABLES

Table Page

Table 2.1 Chemical Composition of Fly Ash as Percent by Weight [Office, 1997] 8

Table 2.2 Effect of w/cm Ratio on the Air Void System in Concrete 16

Table 2.3 Chloride Ion Penetrability Based On Charge Passed [ASTM C1202–10] 22

Table 2.4 Chloride Limits for New Construction in % Chloride by Mass of Cement [ACI, 2001] 23

Table 2.5 Correlation Between Percent Water Soluble Chloride 24

by Mass of Concrete and Corrosion Risk [Broomfield, 2007] 24

Table 2.6 Correlation Between Concrete Resistivity and the Rate of Corrosion for a Depassivated Steel Bar Embedded within the Concrete [Broomfield, 2007] 27

Table 2.7 Rating Scale for Scaling Resistance [MoDOT] 28

Table 2.8 Typical Mechanical Properties of HVFA Concrete 29

Made with ASTM Type I Portland Cement [Malhotra Mehta 2008] 29

Table 3.1 Test Matrix for Mechanical Properties 32

Table 3.5 Mix Design per Cubic Yard for High-Volume Fly Ash Investigation 33

Table 3.6 Location of Pours and Typical Fresh Concrete Properties for High-Volume Fly Ash Concrete 36

Table 4.1 Test Matrix for Durability Performance 50

Table 5.1 Individual Compressive Strength Results for HVFA Mixes 70

Table 5.2 Averaged Compressive Strength Results of HVFA Mixes 71

Table 5.3 Individual Modulus of Elasticity Results for HVFA Mixes 73

Table 5.4 Individual Modulus of Elasticity Results for HVFA-70LA Mix 73

Table 5.5 Average Modulus of Elasticity for HVFA Mixes 74

Table 5.6 Normalized Modulus of Elasticity for HVFA Mixes 74

Table 5.7 Individual Modulus of Rupture Results for HVFA Mixes 76

Table 5.8 Average Modulus of Rupture Results for HVFA Mixes 76

Table 5.9 Normalized Modulus of Rupture for HVFA Mixes 77

Table 5.11 Individual Splitting-Tensile Test Results for HVFA Concrete Mixes 79

Table 5.12 Averaged Splitting-Tensile Strength for HVFA Mixes 79

Table 5.13 Normalized Splitting-Tensile Strength for HVFA Mixes 80
Table 5.14 Individual Results of Freezing and Thawing Test for HVFA Mixes 81
Table 5.15 Average Durability Factors for HVFA Mixes 82
Table 5.16 Individual Results of RCT for HVFA Mixes 83
Table 5.17 Averaged Results of RCT and Permeability Class of HVFA Mixes 84
Table 5.18 Correlation Between Percent Chloride by Mass of Concrete and Corrosion Risk [Broomfield, 2007] 85
Table 5.19 Average Chloride Content at Specified Depths of HVFA Mixes 86
Table 5.20 Final Resistivity of HVFA Mixes 90
Table 5.21 Scaling Deterioration Classes [MoDOT] 91
Table 5.22 Averaged Scaling Performance for HVFA Mixes 92
Table 6.1 Outline of Results of HVFA Investigation 94
Table 6.2 Normalized Mechanical Properties Compared to Respective ACI Coefficients 95
Table 6.3 Normalized Mechanical Properties Compared to Respective AASHTO Coefficients 99
Table A.1 Control-R1 (Weeks 1-7) 109
Table A.2 Control-R1 (Weeks 8-14) 109
Table A.3 Control-R1 (Weeks 15-21) 109
Table A.4 Control-R1 (Weeks 22-24) 110
Table A.5 Control-R2 (Weeks 1-7) 110
Table A.6 Control-R2 (Weeks 8-14) 110
Table A.7 Control-R2 (Weeks 15-21) 111
Table A.8 Control-2R (Weeks 22-24) 111
Table A.9 Control-3R (Weeks 1-7) 111
Table A.10 Control-3R (Weeks 8-14) 112
Table A.11 Control-3R (Weeks 15-21) 112
Table A.12 Control-3R (Weeks 22-24) 112
Table A.13 HVFA-70H-1R (Weeks 1-7) 113
Table A.14 HVFA-70H-1R (Weeks 8-14) 113
Table A.15 HVFA-70H-1R (Weeks 15-21) 113

Table A.16 HVFA-70H-1R (Weeks 22-24) 114
Table A.17 HVFA-70H-2R (Weeks 1-7) 114
Table A.18 HVFA-70H-2R (Weeks 8-14) 114
Table A.19 HVFA-70H-2R (Weeks 15-21) 115
Table A.20 HVFA-70H-2R (Weeks 22-24) 115
Table A.21 HVFA-70H-3R (Weeks 1-7) 115
Table A.22 HVFA-70H-3R (Weeks 8-14) 116
Table A.23 HVFA-70H-3R (Weeks 15-21) 116
Table A.24 HVFA-70H-3R (Weeks 22-24) 116
Table A.25 HVFA-70L-1R (Weeks 1-7) 117
Table A.26 HVFA-70L-1R (Weeks 8-14) 117
Table A.27 HVFA-70L-1R (Weeks 15-21) 117
Table A.28 HVFA-70L-1R (Weeks 22-24) 118
Table A.29 HVFA-70L-2R (Weeks 1-7) 118
Table A.30 HVFA-70L-2R (Weeks 8-14) 118
Table A.31 HVFA-70L-2R (Weeks 15-21) 119
Table A.32 HVFA-70L-2R (Weeks 22-24) 119
Table A.33 HVFA-70L-3R (Weeks 1-7) 119
Table A.34 HVFA-70L-3R (Weeks 8-14) 120
Table A.35 HVFA-70L-3R (Weeks 15-21) 120
Table A.36 HVFA-70L-3R (Weeks 22-24) 120
Table A.37 HVFA-70LA-1R (Weeks 1-7) 121
Table A.38 HVFA-70LA-1R (Weeks 8-14) 121
Table A.39 HVFA-70LA-1R (Weeks 15-21) 121
Table A.40 HVFA-70LA-1R (Weeks 22-24) 122
Table A.41 HVFA-70LA-2R (Weeks 1-7) 122
Table A.42 HVFA-70LA-2R (Weeks 8-14) 122
Table A.43 HVFA-70LA-2R (Weeks 15-21) 123
Table A.44 HVFA-70LA-2R (Weeks 22-24) 123
Table A.45 HVFA-70LA-3R (Weeks 1-7) 123
Table A.46 HVFA-70LA-3R (Weeks 8-14) 124

Table A.47 HVFA-70LA-3R (Weeks 15-21) 124
Table A.48 HVFA-70LA-3R (Weeks 22-24) 124
Table A.49 Control Chloride Content Data 140
Table A.50 HVFA-70H Chloride Content Data 141
Table A.51 HVFA-70L Chloride Content Data 141
Table A.52 HVFA-70LA Chloride Content Data 141

1. INTRODUCTION

1.1. BACKGROUND, PROBLEM, & JUSTIFICATION

Concrete is one of the most widely used materials in the world. It is used in a variety of applications and produced in massive quantities. With this mass production of concrete comes the negative side effect of large amounts of carbon dioxide emissions, a greenhouse gas. These emissions are created from the production of Portland cement, a major component of concrete. Any material that would be able to partially replace Portland cement as a supplementary cementitious material might help lower emissions and be beneficial to the overall environmental impact of concrete applications.

In the 1930's, an inorganic noncombustible by-product of coal burning electric power plants known as fly ash became readily available. Researchers began testing the use of fly ash in concrete applications. The earliest study on concrete containing fly ash was published in 1937 [Davis et al., 1937]. Since this initial study, significant strides have been made to standardize the use of fly ash in concrete. Most commonly, the concrete industry uses fly ash replacement in small percentages, usually limiting the quantity to 35 percent or less of the total cementitious material. Due to growing environmental concerns over greenhouse gases, researchers have begun to evaluate whether higher replacement percentages – even up to 75 percent – are feasible in terms of concrete production, placement, and structural behavior. Referred to as high-volume fly ash (HVFA) concrete, this material offers a viable alternative to traditional Portland cement concrete and is significantly more sustainable.

Aside from its environmental impact, fly ash has been shown to improve some of the characteristics of concrete, both fresh and hardened. The physical structure of fly ash

can be described as “tiny ball bearings”. This spherical shape increased the workability of concrete while maintaining cohesiveness. Also, fly ash has a relatively low reactivity relative to Portland cement and therefore shows very low heat of hydration. This property can be useful in some concrete applications, particularly mass concrete where heat control is a major concern. However, this low reactivity of fly ash has raised concerns over its usage. Adequate early strength gains of concrete containing high amounts of fly ash can negatively impact construction schedules. Also, while concrete containing fly ash has shown comparable durability performance, some reports suggest that HVFA concrete may have poor scaling resistance. While the increased usage of fly ash in concrete would solve many environmental concerns, there are still many questions to be answered as the limits are raised on the amount of fly ash in concrete. Negative issues observed in concrete containing lower volumes of fly ash may only be magnified with an increase in fly ash. Further testing on the hardened properties and durability performance on HVFA concrete is required.

1.2. OBJECTIVES & SCOPE OF WORK

The main objective of this study is to investigate the mechanical properties and durability performance of HVFA concrete in comparison to conventional concrete.

The following scope of work was implanted in an effort to attain this objective: (1) review applicable and relevant literature; (2) develop a research plan; (3) evaluate the mechanical properties and durability of several HVFA concrete mixes; (4) compare the HVFA concrete mixes with conventional concrete mixes; (5) verify the validity of using current hardened property tests on HVFA concrete; (6) analyze the information gathered

throughout the testing to develop findings, conclusions, and recommendations; and (7) prepare this report in order to document the information obtained during this investigation.

1.3. RESEARCH PLAN

The research plan entailed the development of several concrete mixes that contained 70% fly ash by total mass of cementitious material. These mixes varied in the amount of total cementitious material used and are described in Section 3. Several standard hardened property tests were selected to evaluate the performance of the HVFA mixes in comparison to conventional concrete, including compressive strength, modulus of elasticity, modulus of rupture, and splitting-tensile strength. These tests were also used to determine their validity in predicting the performance of HVFA concrete.

Specimens were also fabricated in order to evaluate the durability performance of HVFA concrete. The tests performed on the mixes consisted of chloride penetration by electrical indication and ponding methods, freeze-thaw resistance, concrete resistivity, and scaling resistance. Both the conventional and HVFA mixes were subjected to these durability tests in order to compare their performance.

1.4. OUTLINE

This report consists of seven sections and one appendix. Section 1 briefly explains the history and benefits of using fly ash in concrete. Also within Section 1 are the objectives, scope of work, and research plan.

Section 2 summarizes how fly ash is produced as well as the chemical composition and difference among types of fly ash. The mechanical property tests are also discussed in further detail. Lastly, the durability tests as well as the mechanisms behind the durability issues are discussed.

Section 3 explains the development of the HVFA concrete mix designs including the selection of chemical admixtures. This section includes typical fresh properties measured during this investigation. Also, the mechanical property tests are discussed in more detail as well as equations used to estimate the behavior of concrete.

Section 4 consists of discussing the tests used to evaluate the durability performance in further detail.

Section 5 presents the results of both the mechanical property tests as well as the durability tests. Also presented in this section are the normalized results of the mechanical property tests in comparison to traditional relationships used to estimate the behavior of concrete.

Section 6 outlines the results of the investigation and evaluates the data based on a statistical analysis. Also, the results of the investigation are discussed to propose a theory on the outcome of the tests in order to recommend how to successfully implement HVFA concrete.

Section 7 consists of the conclusion of the investigation as well as any recommendations based on the findings from the mechanical tests as well as the durability performance of the HVFA concrete mixes in comparison to conventional concrete.

The appendix contains additional test data associated with the durability tests of the HVFA mixes.

2. LITERATURE REVIEW

2.1. HIGH-VOLUME FLY ASH CONCRETE

The use of fly ash in concrete has been in practice for nearly 100 years. In recent years, the use of fly ash has grown considerably and it is estimated that over 6 million tons are used in concrete each year. The American Concrete Institute (ACI) has limited the amount of fly ash used in concrete applications to a maximum of 25 percent by mass of total cementitious content [ACI 318-08, 2008]. Researchers are investigating the possibility of increasing the limit of the amount of fly ash that can be incorporated into concrete. It has been suggested that concrete with a minimum of 50 percent by mass of total cementitious material is considered a high-volume fly ash (HVFA) concrete [Hopkins, 2003]. It has been found that when the total amount of fly ash used crosses this 50 percent limit, the characteristic of the concrete begin to differ from concrete containing only Portland cement and may require special consideration.

Fly ash is the incombustible, inorganic, by-product of burning pulverized coal in electricity-generating power plants. This waste product is a natural pozzolanic material or a reactive aluminosilicate material created from natural processes. The most common production of fly ash is from a dry-bottom boiler that burns pulverized coal. In this process, about 80 percent of all ash leaves the furnace as fly ash and is entrained in the flue gas. The fly ash is then collected in hoppers by means of an electrostatic precipitator as shown in **Figure 2.5** or by a mechanical precipitator. Both collection processes can generate fineness, density, and carbon content variations in the fly ash from hopper to hopper. Although, typical particle size can range from 0.00004 in. (1 μm) to more than 0.008 in. (200 μm) and density of individual particles from less than 62.4 lb/ft^3 (1000

kg/m^3) hollow spheres to more than 187 lb/ft^3 (3000 kg/m^3), coal burned from a uniform source generally produces very consistent fly ash [Huffman, 2003]. A more homogenous material is created when the hoppers are emptied and the fly ash is conveyed to storage.

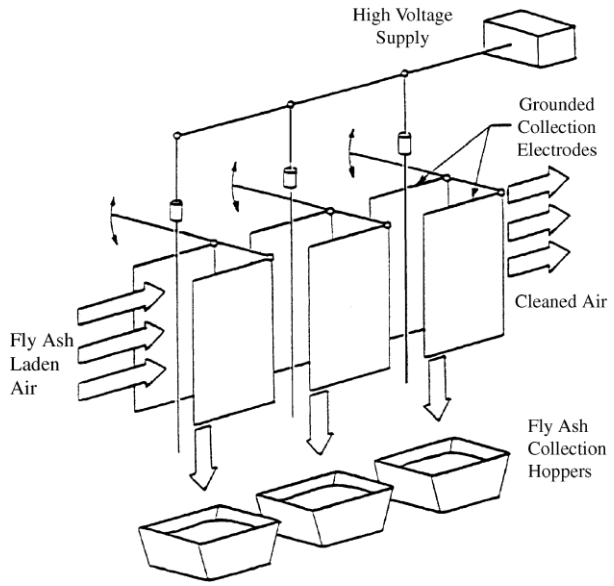

Figure 2.5 - Electrostatic Precipitator Fly Ash Collection Process [Huffman, 2003].

There are two types of fly ash as specified in ASTM C 618-12, "Standard Specification for Coal Fly Ash and Raw of Calcined Natural Pozzolan for Use in Concrete," Class C and Class F. Class C fly ashes are produced from the burning of lignitic coals, while Class F fly ash is the result of the burning of bituminous and sub-bituminous coals. These two types of fly ash are divided into these classes due to their chemical variations. Fly ash is mainly composed of silica (SiO_2), alumina (Al_2O_3), iron (Fe_2O_3), and calcium (CaO). According to ASTM C 618 Class F fly ash contains a minimum of 70% silica, alumina, and iron while Class C must contain a minimum of 50%. A complete table of the chemical composition of the different classes of fly ash can be seen in **Table 2.1**.

Table 2.1 Chemical Composition of Fly Ash as Percent by Weight [Office, 1997]

Component	***Class F***	***Class C***
SiO_2	20 – 60	40 – 60
Al_2O_3	5 – 35	20 – 30
Fe_2O_3	10 – 40	4 – 10
CaO	1 – 12	5 – 30
MgO	0 – 5	1 – 6
SO_3	0 – 4	0 – 2
Na_2O	0 – 4	0 – 2
K_2O	0 – 3	0 – 4
LOI	0 – 15	0 – 3

The chemical composition of fly ash has a noticeable impact on the hydration of concrete. Fly ash shows very little reaction when mixed with water and requires what is known as “activators”. Alkalis, sulfates, and calcium hydroxide are all used as activators. This leads to a lowered heat of hydration and delayed setting time, which can have a serious impact on finishing and removal of formwork. While the chemical composition of fly ashes may be different, their physical make up is very similar. Both classes of fly ash are very spherical in nature. Under a microscope these particles resemble tiny ball bearings. The spherical nature of these particles results in an increase in the workability of concrete containing fly ash. A microscopic photograph of fly ash can be seen in **Figure 2.6**.

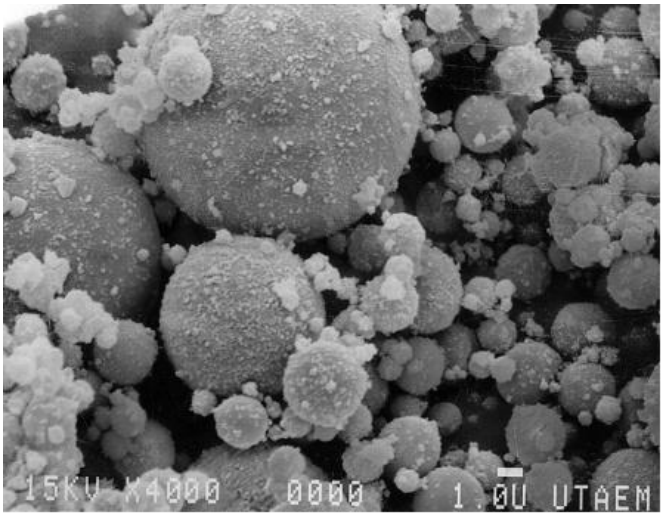

Figure 2.6 - Fly Ash at 4000x Magnification [Huffman, 2003]

The presence of fly ash also has other positive influences on concrete besides workability. Concretes with fly ash show a better plasticity as well as cohesiveness. In addition to the workability increasing, the pumpability of concrete containing fly ash increases as well. The permeability of concrete containing fly ash has been shown to decrease (Myers et al. 1998). . During the hydration process of Portland cement, calcium hydroxide may be leached out of the concrete creating voids which allow water to permeate, which can bring in unwanted and damaging chemicals. The addition of fly ash causes more of that calcium hydroxide to chemically react with water and create C-S-H, thereby preventing the calcium hydroxide from being leached. This creates an overall denser microstructure of the concrete, reducing permeability [Malhorta and Mehta, 2008].

The use of high amounts of fly ash in concrete also has environmental benefits. Currently, a majority of fly ash in the United States is disposed of in landfills. Using higher amounts of fly ash in concrete would considerably reduce the amount of fly ash

that is placed into landfills. Also, the production of Portland cement emits large amounts of carbon dioxide and consume large amount of energy. With fly ash being a by-product that is already produced from creating electricity, using higher amounts could significantly reduce these emissions and reduce energy consumption in the production of Portland cement.

2.2. MECHANICAL PROPERTY TESTING METHODS

2.2.1. Compressive Strength. The compressive strength of concrete is one of the most important of all the mechanical properties. Measuring compressive strength is influenced by many factors including specimen size, curing conditions, load rate, etc. In order to control variations in testing and consequently variations in results, a standard test method was developed by ASTM International. The standard for determining the compressive strength of concrete is outlined in ASTM C 39–11, "Standard Test Method for Compressive Strength of Cylindrical Concrete Specimens." This standard requires cylindrical specimens for testing. The specimens used in laboratory testing measure either 4 in. (102 mm) in diameter x 8 in. (203 mm) in height or 6 in. (152 mm) in diameter x 12 in. (305 mm) in height. The specimens are prepared by filling the molds in equal lifts and rodding each lift a specified number of times. The numbers of lifts and extent of rodding depends on the diameter and cross sectional area, which is specified in ASTM C 192-07 "Standard Practice for Making and Curing Concrete Test Specimens in the Laboratory." After each lift, the mold is also stuck with a mallet to ensure consolidation. After 24 hours in a moist curing chamber, the specimens are de-molded and returned to the moist curing chamber until the proper test date. Common testing dates for measuring a

concrete's strength gain profile are 1, 7, and 28 days after batching. The cylindrical specimens are ground flat or capped before testing. This flat surface reduces localized stress on the specimen. Capping can be done with sulfur capping compound or neoprene pads. Dimensions of the specimens are taken before being loaded at a constant rate until failure. The load recorded at failure is divided by the cross-sectional area to find the compressive strength of the concrete.

2.2.2. Modulus of Elasticity. Due to the nonlinear inelastic behavior of concrete, the modulus of elasticity (MOE) can be different depending on how it is measured. The MOE is the slope of the stress–strain curve between two designated points. An example of the different moduli of elasticity that can be measured can be seen in **Figure 2.7**.

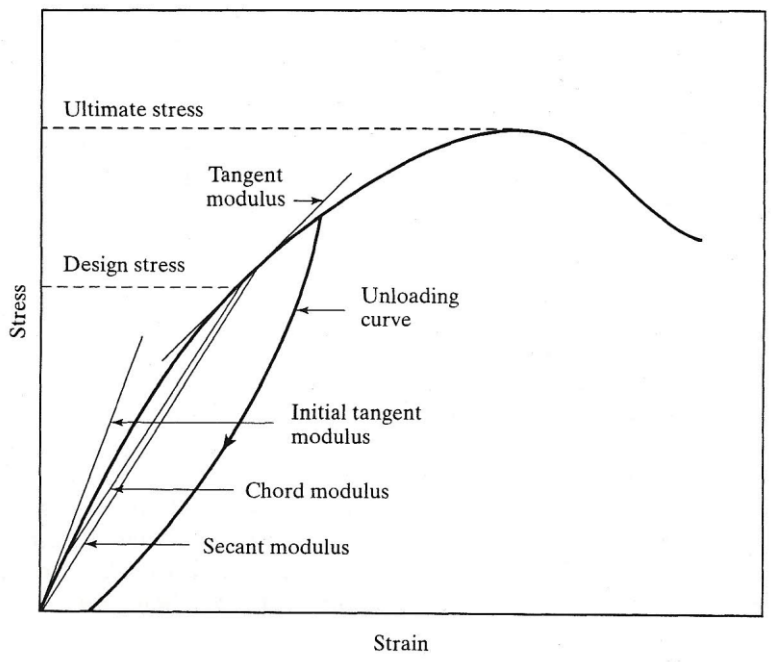

Figure 2.7 – Typical Stress-Strain Diagram for Concrete, Showing the Different Elastic Moduli [Mindess et al., 2002]

In order to standardize the measured modulus of elasticity, ASTM International developed a standard test method ASTM C 469-10, “Standard Test Method for Static Modulus of Elasticity and Poisson’s Ratio of Concrete in Compression.” This test method measures what is known as the chord modulus of elasticity. The specimens used in this test are the same type used in the compressive strength test. Either the 4 in. (102 mm) or 6 in. (152 mm) diameter cylindrical specimens can be used. Specimens are fabricated and cured in the same manner as the compressive strength specimens. After 28 days of moist curing, specimens are prepared for testing. Using a Compressometer, the strain produced at 40% of the ultimate load is recorded. Also, the stress that produces a measured strain of 0.00005 in./in. is recorded. Using these values, the chord modulus of elasticity can be calculated in accordance with **Eq. 2.2**.

$$E_c = \frac{(S_2 - S_1)}{(\varepsilon_2 - 0.00005)} \tag{2.2}$$

2.2.3. Modulus of Rupture. The modulus of rupture (MOR) is an important property in the calculation of the cracking moment of concrete and thus determining how a concrete member will behave post-cracking. ASTM International has created a standard for testing the modulus of rupture known as ASTM C 78-10, “Standard Test Method for Flexural Strength of Concrete (Using Simple Beam with Third-Point Loading).” This approach is an indirect way to measure the tensile strength of concrete. The specimen has to have an overall depth of a third of the span length. The span length shall be such that it measures three times the distance in between the load points of the testing apparatus.

Also, the specimen shall overhang the supports by at least 1 in. (25 mm). The schematic diagram in **Figure 2.8** summarizes these requirements.

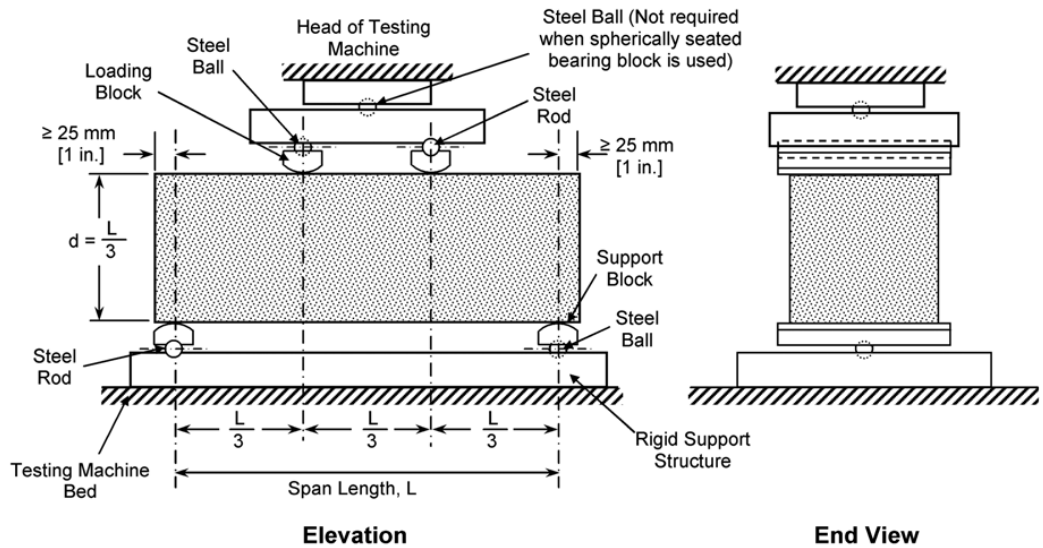

Figure 2.8 - Typical Modulus of Rupture Testing Setup [ASTM C 78–10]

The specimen is then loaded until failure. After testing, the dimensions are recorded and the modulus of rupture is computed in accordance with **Eq. 2.3**. While this test method overestimates the "true" tensile strength of concrete, the test does simulate the most common way concrete is placed into tension, through flexure.

$$R = \frac{PL}{bd^2} \tag{2.3}$$

2.2.4. Splitting Tensile Strength. While the modulus of rupture test described in Section 2.3.3 tests for the tensile strength of concrete indirectly, the splitting tensile test uses a much more direct manner. This test is outlined in ASTM C 496–11, "Splitting

Tensile Strength of Cylindrical Concrete Specimens." The cylindrical specimens measure either 4 in. (102 mm) in diameter by 8 in. (203 mm) in height or 6 in. (152 mm) in diameter and 12 in. (305 mm) in height. The method for preparing the specimens used in the splitting-tensile test is outline in ASTM C 192. Specimens are stored in a moist curing chamber and tested after 28 days. Diametral lines are drawn on the specimens to ensure that they are in the same axial plane. The dimensions of the specimens are then taken. The specimens are then placed on top of a 1 in. (25 mm) wide x 3/8 in. (10 mm) thick plywood strip within the testing apparatus. A second plywood strip is then placed on top of the specimen so the two strips align with the diametral lines. This ensures that the load is distributed in one plane of the specimen. The peak load is recorded and the tensile strength is then calculated in accordance with **Eq. 2.4**.

$$T = \frac{2P}{\pi LD} \tag{2.4}$$

2.3. DURABILITY OF CONCRETE

2.3.1. Freezing and Thawing. Concrete is a porous material which allows water to permeate into its microstructure. When concrete containing moisture is subjected to repeated cycles of freezing and thawing, severe deterioration can occur. Initially researchers believed that this damage was caused by the expansion of water when it transitioned into ice. The trapped water would freeze and expand in the capillary pores and exert hydraulic pressure on the hardened paste. This theory of hydraulic pressure was proposed by T.C Powers [Mindess et al., 2002]. Later, Powers developed a new theory based on osmotic pressure [Powers, 1956]. He proposed this theory after observing that

concrete paste, when frozen, shrank first than expanded. He also observed that air entrained cement paste would shrink indefinitely and the same deterioration is observed when liquids that do not expand when frozen were used to saturate the concrete. Investigators developed two possible explanations for these observations. The first is osmotic pressure. As water is drawn to the freezing sites through osmosis, osmotic pressure is built up. This eventually would cause the concrete to crack. Another possible explanation is vapor pressure. The ice that begins to form in the pores has less chemical potential than the supercooled water in the unfrozen pores. This creates a lower vapor pressure. This condition causes the relative humidity at the freezing pores to lower, which draws water towards them to maintain equilibrium. This pressure would also cause the concrete to begin to crack.

The introduction of air entraining admixtures has had a positive effect on the resistance of concrete to freezing and thawing deterioration. The air bubbles in the concrete allow for excess space for the water to move and freeze without damaging the concrete. These bubbles must be spaced at certain intervals to be effective in protecting the concrete. If the bubbles are too far apart, the water cannot move to these “safety valves” and the pressure cannot be relieved. The air-entraining system becomes ineffective in fully saturated concrete due to all the pores and air bubbles containing water. Many other factors influence a concrete’s resistance to freezing and thawing attack, the most important of which is the permeability of the concrete. With concretes having a low water/cement ratio and usually a low permeability, freeze/thaw resistance generally increases [Mindess et al., 2002]. This relationship can be seen in **Table 2.2**.

Table 2.2 Effect of w/cm Ratio on the Air Void System in Concrete

w/c ratio	Air content (%)	Spacing factor mm (in.)	Liner expansion per freeze – thaw cycle
0.35	4.8	0.11 (0.0043)	0.00004
0.45	4.7	0.14 (0.0055)	0.00014
0.55	5.2	0.15 (0.0059)	0.00021
0.65	4.9	0.18 (0.0071)	0.00026
0.75	5.3	0.23 (0.0091)	0.00036

1 in. = 2.54 cm.

2.3.2. Chloride Attack. Chloride ions attack the passive layer that forms on reinforcing steel placed within a high pH environment, such as concrete. Chloride ions are most commonly introduced into concrete through deicing salts. These salts can remain on bridge decks for days or even weeks, penetrating into the concrete structure and eventually destroying the passive layer of the reinforcing steel. Corrosion in steel begins with the iron being oxidized at an anode as shown in **Eq. 2.5**.

$$Fe \rightleftarrows 2e^{-} + Fe^{2+} \tag{2.5}$$

At the cathode, water is reduced into hydroxyl (OH^{-}) ions as shown in **Eq. 2.6**.

$$\frac{1}{2}O_2 + H_2O + 2e^{-} \rightleftarrows 2OH^{-} \tag{2.6}$$

These hydroxyl ions then flow from the cathode to the anode. At the anode, the ferrous ions and the hydroxyl ions react to form ferrous hydroxide as shown in **Eq. 2.7**.

$$Fe^{2+} + 2(OH)^{-} \rightarrow Fe(OH)_2 \tag{2.7}$$

When oxygen and water are introduced the ferrous hydroxide will spontaneously oxidize into hydrated ferric oxide (rust) as shown in **Eq. 2.8**.

$$2Fe(OH)_2 \rightarrow 2Fe(OH)_3 \rightarrow Fe_2O_3 \cdot nH_2O \tag{2.8}$$

This hydrated ferric oxide, or red rust that is commonly seen, is known to have six times the volume of the original iron [Broomfield, 2007]. The increased volume induces expansive stresses in the concrete, eventually leading to cracking and progressive deterioration. The volume of iron and various forms of oxidized irons can be seen in **Figure 2.9**.

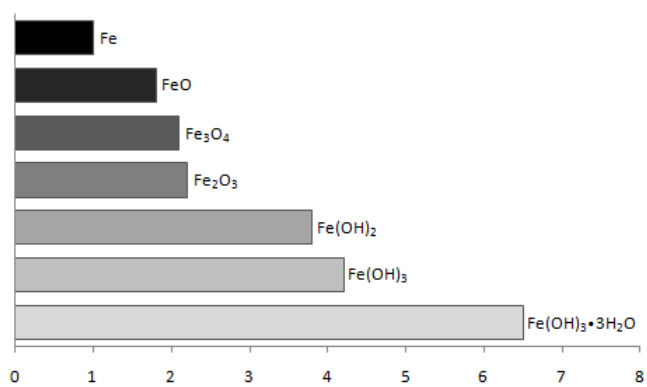

Figure 2.9 - The Relative Volumes of Various Iron Oxides from Mansfield [1981], Corrosion 37(5), 301-307.

This reaction can be largely avoided in concrete structures. Conventional concrete is highly alkaline which allows for the formation of a passive oxide film (FeOOH) on the reinforcement. The $Fe(OH)_2$ is oxidized to create this film as shown in **Eq. 2.9**.

$$2Fe(OH)_2 + \frac{1}{2}O_2 \rightarrow 2\gamma - FeOOH + H_2O \tag{2.9}$$

Chlorides effectively destroy this passive layer allowing for the reinforcement to corrode. Chlorides react with ferrous ions to create a soluble iron-chloride complex as shown in **Eq. 2.10**.

$$Fe^{2+} + Cl^{-} \rightarrow [FeCl\ complex]^{+} \tag{2.10}$$

This complex in turn reacts with the hydroxyl to form the ferrous hydroxide which oxidizes into expansive rust as shown in **Eq. 2.11**.

$$[FeCl]^{+} + 2OH^{-} \rightarrow Fe(OH)_2 + Cl^{-} \tag{2.11}$$

The largest factor influencing the effect of chlorides in concrete is the permeability of the concrete. The permeability relates to the amount and rate of oxygen, moisture, and chloride penetration into the microstructure of the concrete over time. Permeability is most influenced by the water to cementitious material ratio (w/cm). The lower the w/cm ratio of the concrete, the lower the porosity [Powers et al., 1954]. Decreasing the permeability of concrete will improve its durability. Water can carry

harmful chemicals, such as chlorides, into the concrete's pores. The diffusion of chemicals into hardened concrete is described by *Fick's Second Law* as shown in **Eq. 2.12**.

$$\frac{\partial C}{\partial t} = K_d \frac{\partial^2 C}{\partial x^2} \tag{2.12}$$

Where C is the concentration, t is the time, K_d is the diffusion coefficient, and x is the depth. The solution of this equation is shown in **Eq. 2.13** [Broomfield 2007].

$$\frac{C_{max} - C_d}{C_{max} - C_{min}} = erf\left(\frac{x}{\sqrt{4D_c t}}\right) \tag{2.13}$$

Where C_d is the chloride concentration at depth (x), x is the specified depth, t is the time, D_c is the diffusion coefficient of concrete, C_{max} is the maximum chloride content of the concrete, C_{min} is the baseline chloride content of the concrete, and erf is the error function. Using this function the chloride penetration over time can be estimated. This equation has proved to estimated chloride contents extremely accurately when compared to field results [Berke and Hicks, 1996]

2.4. DURABILITY TESTING METHODS

2.4.1. Resistance to Freezing and Thawing. In order to evaluate the potentially devastating effects of freezing and thawing cycles, ASTM International developed a standardized test to simulate these conditions in the lab. This test is outlined in ASTM C 666–03 "Standard Test Method for Resistance of Concrete to Rapid Freezing and

Thawing." Specimens used in this test are prisms that are made and cured in accordance with ASTM C 192. The dimensions requirements of these specimens are specified in ASTM C 666. The specimens are cured for 14 days before testing unless otherwise specified. This test subjects the specimens to 300 freezing and thawing cycles. Every 36 cycles, the specimens are removed and properties of the concrete are measured. These properties include the transverse frequency, total length change, and total weight change. These specimens can be tested using two different procedures, A or B. Procedure A specifies that the specimens be surrounded by water during the freezing and thawing cycles, while Procedure B specifies that the specimens be surrounded by air during freezing and water during thawing. Between the testing intervals, both the relative dynamic modulus of elasticity and the durability factor are calculated. Using these values, the concrete can be evaluated for its durability performance. The test calls for the cycles to be stopped when the measured durability factor falls below 50. Every Department of Transportation has its own criteria for acceptable durability factor and sets a minimum for acceptance. The acceptability criteria for the state of Missouri and for this investigation will be discussed during evaluation of the different concretes of this study.

2.4.2. Rapid Chloride Penetration. The diffusion of chlorides can be extremely damaging, as stated previously. However the process is very slow, and testing the chloride penetration accurately can take years. In order to test a concrete's ability to resist chloride penetration, ASTM International developed a testing method that could be performed much more quickly. This testing method is outline in ASTM C 1202–10, "Standard Test Method for Electrical Indication of Concrete's Ability to Resist Chloride Ion Penetration." This test is also known as the Rapid Chloride Test (RCT). The test

specimens consist of concrete disks subjected to a constant voltage to determine their resistance to chloride penetration. The disks are cut from concrete cylinders that are fabricated and cured according to ASTM C 192. The disks, measuring 4 in. (102 mm) in diameter and 2 in. (51 mm) thick, are prepared according to ASTM C 1202 and subjected to 60 V for 6 hours as shown in **Figure 2.10**.

Figure 2.10 - Typical RCT Setup

During the test, the current is recorded every 30 minutes. Using a plot of current versus time, the total charge passed is calculated and used to determine the permeability class of the concrete. There is a correlation between the amount of charge passed and the chloride ion penetrability of concrete. This correlation can be seen in **Table 2.3**.

Table 2.3 Chloride Ion Penetrability Based On Charge Passed [ASTM C1202–10]

Charge Passed (coulombs)	Chloride Ion Penetrability
>4000	High
2000-4000	Moderate
1000-2000	Low
100-1000	Very Low
<100	Negligible

2.4.3. Chloride Content Analysis. While the test outlined in ASTM C 1202 is an adequate test when the results are required quickly, it does not subject the concrete to realistic conditions. ASTM C 1202 is only suitable for research and development. Some studies have indicates that ASTM C 1202 gives false indications for concretes made with supplementary cementitious materials, such as fly ash, slag, silica fume, and slag [e.g., Shi, 2002]. This study showed that cement containing supplementary cementitious material would yield falsely high results than what was observed in the field. Researchers found that the change in chemical composition due the addition of supplementary cementitious material affected the results of the Rapid Chloride Test. In order to properly evaluate a concrete's ability to resist chloride penetration, it should tested directly using ASTM C 1543–10, "Standard Test Method for Determining the Penetration of Chloride Ion into Concrete by Ponding." This test method involves subjecting concrete specimens to a 5% by weight sodium chloride solution for 120 days. The specimens are then cored and powder samples are collected to determine the chloride content at multiple levels. According to Broomfield [2007], it is recommended that a minimum of four data points be used in developing a chloride profile in order to obtain an accurate representation of

the chloride distribution. A chloride content analysis is then performed on the powder samples in order to determine the chloride profile of the concrete.

Two types of chloride analyses can be performed on the concrete powder; acid-soluble and water-soluble. Acid-soluble tests will determine the total chloride content, including those chlorides trapped in the aggregate and paste (C_3A). Water-soluble tests will only determine those chlorides free to deteriorate the passive layer of the concrete, thus promoting corrosion. In some cases, the acid-soluble test will overestimate the corrosion potential of a concrete and in others provide a reasonable evaluation. ACI has developed limits on chloride content for new construction for varying applications of concrete. These limitations can be seen in **Table 2.4**.

Table 2.4 Chloride Limits for New Construction in % Chloride by Mass of Cement [ACI, 2001]

	Test method	
	Acid Soluble	Water Soluble
Concrete Application	ASTM C1152	ASTM C1218
Pre-stressed concrete	0.08	0.06
Reinforced concrete in wet conditions	0.10	0.08
Reinforced concrete in dry conditions	0.20	0.15

For in place structures classifications were developed based on chloride contents and the corrosion risk. These classifications can be seen in **Table 2.5** [Broomfield, 2007].

Table 2.5 Correlation Between Percent Water Soluble Chloride by Mass of Concrete and Corrosion Risk [Broomfield, 2007]

% Chloride by mass of concrete	Corrosion Risk
<0.03	Negligible
0.03-0.06	Low
0.06-0.14	Moderate
>0.14	High

The chloride profile determined from this test method indicates the concentration of the chloride ions in the concrete as a function of depth from the surface. As stated in Section 2.4.2, chlorides will destroy the passive layer on the reinforcement in the concrete, exposing the steel to elements that will initiate corrosion. The chloride profile determined from this test method will indicate the amount of ions at specified depth to determine a concrete's ability to resist diffusion and therefore chloride ingress. In general, this test is a comparative test and does not necessarily indicate the response of a structure in service.

2.4.4 Concrete Resistivity. Electrical resistance also refers to the ability of concrete to resist corrosion. When hydroxyl ions (OH-) are created at the cathode, they must move to the anode to cause the oxidation process to begin. The slower these ions are transported, the slower the corrosion process. This ionic current is similar to electrical current. Therefore, the rate of corrosion of the reinforcement can be estimated by the electrical resistance of the concrete [Whiting and Nagi, 2003].

Three methods have been developed to analyze the electrical resistance of concrete: single-electrode method, two-probe method, and the four probe method. Of the three methods the two-probe method is the most labor intensive and least accurate

[Broomfield, 2007]. The two-probe method works by measuring the potential between two electrodes by passing an alternating current between them. If aggregates are located near the electrodes this can cause a false reading. Aggregates have a higher resistivity than concrete paste and will therefore cause a reading to be much higher than the actual resistivity. In order to counteract this problem, shallow holes can be drilled to place the electrodes into. However this is what makes the two probe method labor intensive.

The single-electrode method is a more advanced method to determine a concrete's resistivity. This method uses a disk placed on the concrete's surface as an electrode and the embedded steel reinforcement as the second electrode. The resistivity of the concrete is measured using **Eq. 2.14**.

$$Resistivity\ (\Omega cm) = 2RD \tag{2.14}$$

Where R is the resistance drop between the embedded reinforcement and the surface electrode, and D is the diameter of the surface electrode.

The third method is the four-probe method developed by Frank Wenner. This method was developed in 1916 and was designed for geophysical studies. This method has become widely accepted by the industry and is known as the Wenner method. The probe used in this method has four equally spaced electrodes on a single rod. The two outer electrodes send an alternating current through the concrete while the middle two electrodes measure the change in potential. The resistivity is then calculated using **Eq. 2.15**.

$$\rho = \frac{2\pi sV}{I} \tag{2.15}$$

Where ρ is the resistivity (Ωcm), s is the spacing between the electrodes (cm), V is the voltage (V), and I is the applied current (A). When the current is applied through the concrete it travels in a hemispherical pattern. This can be seen in **Figure 2.11**. This allows for a greater area of concrete to be measured and thus avoids the influence of highly resistive aggregates.

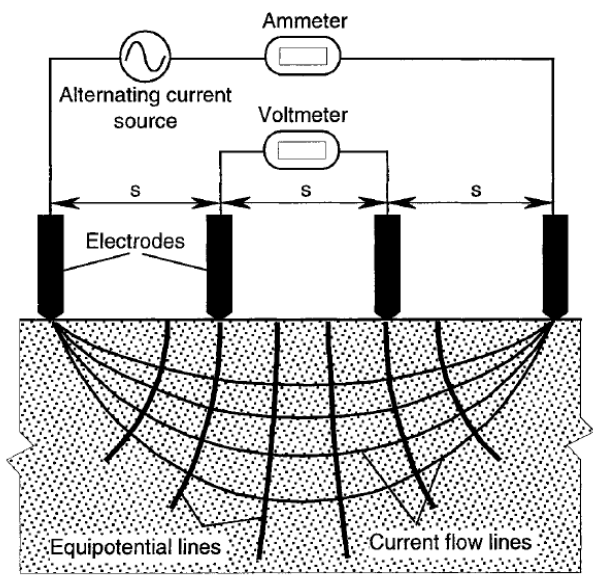

Figure 2.11 - Schematic Representation of the Four-Probe Resistivity Method [Broomfield, 2007]

The four-probe method is based on the theory that the resistivity values measured by the equation above are accurate if the current and potential fields exist in a semi-infinite volume of material [Whiting and Nagi, 2003]. This assumption indicates that larger concrete specimens will yield more accurate results. This condition has been found to be true. Measuring relatively thin concrete members or near edges produces noticeable

errors. It is recommended that the spacing between the electrodes of the probe do not exceed ¼ of the smallest concrete section dimension. Another source of error is the non-homogeneous composition of concrete. While the assumption of the Wenner method is that the material will have a consistent resistivity, this is not the case for concrete. Highly resistive aggregates are surrounded by low-resistivity paste which affects the measurements. According to research, this source of error can be avoided by using a probe where the spacing between electrodes is greater than 1.5 times the aggregate maximum size. This approach will maintain a coefficient of variation less than 5% [Whiting and Nagi, 2003]. A correlation was developed between measured concrete resistivity and the corrosion rate of embedded reinforcement. This classification can be seen in **Table 2.6**. This relationship was developed by Langford and Broomfield in 1987 and is widely used in the field.

Table 2.6 Correlation Between Concrete Resistivity and the Rate of Corrosion for a Depassivated Steel Bar Embedded within the Concrete [Broomfield, 2007]

Concrete Resistivity	Rate of Corrosion
>20 kΩcm	Low
10-20 kΩcm	Low to Moderate
5-10 kΩcm	High
<5 kΩcm	Very High

2.4.5 Scaling Resistance. The presence of salt solutions on concrete can cause additional damage besides corrosion of the reinforcing steel. The surface of the concrete can become pitted and roughened by a mechanism called scaling. In addition to leaving the surface scarred and rough, it can also increase the permeability of the concrete. To

evaluate a concrete's resistance to scaling ASTM has created a test method ASTM C 672–03, "Standard Test Method for Scaling Resistance of Concrete Surfaces Exposed to Deicing Chemicals." This test method requires specimens to have at least 72 in^2 (46,452 mm^2) of surface area and be at least 3 in. (76 mm) deep. The specimens are broom finished and a dike is built up around the perimeter of the specimen. This dike must be at least 0.75 in. (19 mm) tall and approximately 1 in. (25 mm) wide. The specimen is then moist cured for 14 days and then air cured for 14 days. When the curing duration is over the surface of the specimen is covered with a solution having a concentration of 5.34 oz /gal (0.04 g/mL) of anhydrous calcium chloride. The specimen is then subjected to 50 cycles of freezing and thawing. After every 5 cycles, the solution is completely replaced and the condition of the surface is evaluated. After 50 cycles the surface of the concrete is evaluated and given a rating based on the scaling resistance. The rating scale can be seen in **Table 2.7**.

Table 2.7 Rating Scale for Scaling Resistance [MoDOT]

Rating	Condition of Surface
1	No scaling
2	Very slight scaling
3	Slight to moderate scaling
4	Moderate scaling
5	Moderate to severe scaling

2.5. HIGH VOLUME FLY ASH CONCRETE

2.5.1. Mechanical Properties. Through several research investigations, it has been seen that HVFA concrete performs adequately in the area of mechanical properties. It has been seen that while conventional concrete reaches relative maximum strength after 28 days, HVFA continues to gain significant strength well after 28 days. This behavior is due to the increased pozzolanic reaction that occurs with the high amounts of fly ash. Typical mechanical properties for HVFA concrete using Type I Portland cement are summarized in **Table 2.8**.

Table 2.8 Typical Mechanical Properties of HVFA Concrete Made with ASTM Type I Portland Cement [Malhotra Mehta 2008]

	Age (days)	Strength (psi)
Compressive Strength	1 7 28	1160 ± 290 2900 ± 725 5076 ± 725
Flexural Strength	14	725 ± 72
Splitting-Tensile Strength	28	507 ± 72
Modulus of Elasticity	28	5,076,000 ± 290,000

1 psi = 0.00689 MPa

2.5.2. Durability Performance. It has been found through numerous investigations that HVFA concrete shows adequate durability performance when compared to conventional concrete. It should be noted that while HVFA concrete shows adequate durability performance, the scaling performance has been noted as poor. This result is due mainly to the tight microstructure and discontinuous pore structure found in HVFA concrete [Malhotra and Mehta, 2008]. HVFA concrete has performed adequately in the areas of freeze-thaw resistance and resistance to the penetration of chloride ions.

HVFA concrete has reportedly achieved durability factors as high as 90 when subject to ASTM C 666. A durability factor over 80 is typically considered to be durable concrete. HVFA has also shown a typical charge passing of 1000 coulombs when subjected to the electrical indication of chloride penetration test. Any concrete allowing only 1000 coulombs or less during the ASTM C 1202 test is considered a low permeability concrete and should perform well in the field. According to research done by Marlay [2011], HVFA concrete also showed adequate chloride penetration resistance by ponding as well as a relatively high electrical resistivity when measured using a Wenner probe.

The one area of durability that HVFA concrete may have potential problems is in the area of scaling resistance. Conflicting results have been found in the area of scaling resistance [Malhorta and Mehta, 2008]. Some research has shown that HVFA concrete shows very little scaling resistance when compared to conventional concrete while other research has indicated good scaling resistance [Malhorta and Mehta, 2008]. However field observations have indicated that HVFA concrete shows adequate scaling resistance and laboratory tests are not indicative of the actual response in service [Malhorta and Mehta, 2008].

3. MECHANICAL PROPERTY TESTS

3.1. INTRODUCTION

This section discusses the mechanical property tests used to evaluate the performance of high-volume fly ash (HVFA) concrete. The mechanical property comparison was important because these properties are essential to estimating the behavior of concrete in the field. These also serve as a good indicator of the quality of the concrete. The following mechanical property tests were included in the scope of work of this investigation:

- Compressive Strength of Cylindrical Concrete Specimens (ASTM C 39-11a)
- Static Modulus of Elasticity and Poisson's Ratio of Concrete in Compression (ASTM C 469-10)
- Flexural Strength of Concrete (Using Simple Beam with Third-Point Loading) (ASTM C 78-10)
- Splitting Tensile Strength of Cylindrical Concrete Specimens (ASTM C 496-11)

These are standard tests that are used to investigate the most commonly used mechanical properties of concrete. Running these tests on both the conventional concrete and the specialized concretes will not only assure the quality of the conventional concrete but also will serve as a baseline of comparison for the specialized concretes. These mechanical properties are used in many aspects of design, and the results of these tests will allow investigators to determine how applicable existing formulas are in estimating these properties.

An outline for all the mechanical tests performed on all experimental mixes is shown in **Table 3.1**. The outline identifies the number of test specimens fabricated for

each test for each concrete mix. All of the concrete specimens were moist cured until the designated testing date. The date tested is listed as number of days after batching of the concrete.

Table 3.1 Test Matrix for Mechanical Properties

Material Property	Number of Specimens	Moist Curing Duration, days	Testing Date(s), days
Compressive Strength	9, (3/test age)	1,7,28	1,7,28
Modulus of Elasticity	3	28	28
Flexural Strength	3	28	28
Splitting Tensile Strength	3	28	28

3.2. MIX DESIGN

The design of the HVFA concrete mixes was based on input from MoDOT as well as the results of previous research conducted at Missouri S&T. This research varied the percent of fly-ash replacement in concrete from 50% to 75% [Marlay, Wolfe, 2011]. Two HVFA concrete mixes were investigated. Both mixes used 50 and 75% replacement of cement with a Class C fly ash. One mix contained a relatively high total cementitious content (756 pcy), designated HVFA-70H and the other contained a relatively low total cementitious content (564 pcy), designated HVFA-70L. Due to the carbon content of fly ash, air-entraining admixtures do not always react the same way when used in HVFA concrete. Consequently, this present study examined the durability of HVFA concrete both with and without air entrainment. The low cementitious content HVFA concrete mix had a version both with (HVFA-70LA) and without (HVFA-70L) an air entraining admixture. The final mix designs are shown in **Table 3.5**.

Table 3.5 Mix Design per Cubic Yard for High-Volume Fly Ash Investigation

	Mix Design ID			
	Control	HVFA-70H	HVFA-70L	HVFA-70LA
Cement (Type I) (lb)	564	219	155	155
Fly Ash (lb)	0	511	360	360
w/cm	0.40	0.40	0.40	0.40
Coarse Aggregate, SSD (lb)	1860	1754	1860	1860
Fine Aggregate, SSD (lb)	1240	1080	1240	1240
HRWR (fl. oz)	16.9	21.9	15.45	15.45
Air Entrainment (fl. oz)	3.5	0	0	3.2
CaOH (lb)	0	51	39	39
Gypsum (lb)	0	21	16	16

1 lb = 0.45 kg
1 fl. oz. = 29.57 mL

The HVFA concrete mixes used a Type I cement to match typical cast-in-place concrete construction. Two types of admixtures were also used in the mix design. HRWR was added to the mix in order to achieve the necessary workability while maintaining the design w/cm. In concrete, the cement particles typical carry either positive or negative charges. The attraction between particles causes them to agglomerate. Water is trapped inside these particles and is not able to add to the workability of the concrete. HRWRs place a like charge on the cement particles causing them to repel each other. This frees the water in the paste to add to the workability of the concrete. This apparent increase in water content allows the workability to increase while maintaining relatively low w/cm. It should be noted that the batch water was adjusted to account for any moisture that was present in the aggregate. The total moisture content was found by taking a representative sample of the aggregate and weighing it. The sample was then placed into an oven and dried overnight. The dried sample was then re-weighed and the difference was taken as the total moisture content.

To provide the necessary durability of the concrete, an air-entraining admixture was also used. Concrete that is exposed to freezing and thawing temperatures is at risk of serious deterioration. One of the most effective ways to protect against that is using an air-entraining admixture. This admixture creates an air void system in the concrete paste that is composed of millions of tiny bubbles. This air void system allows for the pressure that builds up due to the freezing of water to be released into these tiny bubbles. However air entrainment was not used in every mix design. Two of the HVFA concrete mixes did not include any entrained air. This step was done because of carbon content issues when using high amounts of fly ash. With such high carbon content, it is sometimes difficult to reach the desired entrained air content. The air entrainment was purposefully left out to investigate the durability performance of the HVFA with just the entrapped air. The air entrainment was added to a third experimental mix. This was done in order to investigate if reaching the desired air entrainment was possible. The air entrainment was placed into the low cementitious content variation in order to maximize its effect due to the minimal amount of carbon found in that mix. These admixtures were added at trial dosages until the desired behavior and air contents were achieved. The proper dosages were established using 3 ft^3 mixes.

The high volume fly ash mix designs also include two supplementary materials, calcium hydroxide and gypsum. The calcium hydroxide was added to the mix in order to offset the retardation of setting time that occurs in concrete containing HVFA. This natural occurrence results in a delayed finishing time and very low early strengths. The addition of calcium hydroxide helps to maintain the hydration at a faster rate. The gypsum was added to the mix to balance out the lack of sulfates present in a high volume

fly ash mix. Typical fly ash contains a very low amount of sulfates. This leads to a delay in the hydration process as well as a decrease in the overall magnitude of the hydration peak. This leads to a decrease in early strength. With the addition of gypsum the sulfate imbalance is corrected leading to a more desirable hydration curve when compared to conventional concrete. The amount of calcium hydroxide and gypsum was determined by previous research done at Missouri S&T, [Ortega, 2012].

Fresh concrete properties were measured during each batching operation, either within the Materials Lab for mixes prepared on site or within the Structural Engineering High-Bay Research Laboratory (SERL) for mixes delivered by a local ready-mix supplier. The location of each mix is stated in **Table 3.6**. These tests were performed to ensure that certain properties were achieved such as workability and air content. The following fresh property tests were performed on all the mixes:

- Slump of Hydraulic-Cement Concrete (ASTM C 143)
- Unit of Weight of Concrete (ASTM C 138)
- Air Content of Freshly Mixed Concrete by the Pressure Method (ASTM C 173)

Typical fresh properties of the HVFA concrete mixes and locations of the pours are shown in **Table 3.6**.

Table 3.6 Location of Pours and Typical Fresh Concrete Properties for High-Volume Fly Ash Concrete

	Mix Design ID			
	Control	HVFA-70H	HVFA-70L	HVFA-70LA
Slump (in)	5	4.5	4	4.5
Air Content (%)	6.5	NA	NA	5
Unit Weight (lb/ft^3)	143.6	147.5	149.6	144.8
Pour Location	SERL	SERL	SERL	Materials Lab

1 in. = 2.54 cm.
1 lb/ft^3 = 16.02 kg/m^3

3.3. COMPRESSIVE STRENGTH TEST

3.3.1. Introduction. The compressive strength test was used in several different aspects of the research project. It was used as a quality control and quality assurance, (QC/QA) tool. The compressive strength results from the experimental mixes were compared to target values to assure the strengths were within the desired limits. These values can also be compared to other strengths of similar mixes to evaluate behavior. The compressive strength was also used to assure the quality of the concrete by observing any drastic differences between the target and actual strengths. The compressive strength of concrete is also an important factor in many tests that were used in this investigation, such as shear, bond, and creep.

3.3.2. Fabrication. A minimum of 9 compressive strength cylinders were cast for each mix design. All specimens were prepared in accordance with ASTM C 192-07, “Standard Practice for Making and Curing Concrete Test Specimens in the Laboratory” using 4 in. (102 mm) diameter by 8 in. (203 mm) long plastic cylinder molds. The molds were lubricated using form release oil prior to the placement of concrete. The concrete was rodded in order to reduce air voids and to assure the concrete would be sufficiently consolidated. The sides of the mold were also struck smartly for each lift with a rubber

mallet in order to consolidate the concrete. It should be noted that the compressive strength specimens made with the self-consolidating mixes were not rodded or struck due to the plastic highly flowable behavior of the concrete. Instead, these mixes were placed in one continuous lift. Immediately after casting, plastic lids were placed over the molds and the specimens were covered with plastic. After allowing for 16 to 24 hours of setting time, the concrete specimens were removed from the molds using compressed air and placed inside a temperature-controlled moist curing room until the designated testing date.

3.3.3. Testing & Procedure. The testing of the compressive strength of the experimental mixes was performed in accordance with ASTM C 39-11, "Standard Test Method for Compressive Strength of Cylindrical Concrete Specimens." A minimum of 3 compressive strength cylinders were used at each test age. Testing occurred at 1, 7, and 28 days after batching. These are typical testing dates for compressive strength tests. Prior to testing, the specimens had to be capped in order to provide a flat surface for testing. The two methods used to cap specimens in this project were sulfur capping and neoprene pad capping.

Neoprene pads were used to cap any specimens constructed with a high strength concrete mix. Any specimens that were constructed with normal strength concrete were sulfur capped. Prior to using the neoprene pads, the concrete specimens were ground smooth using a concrete grinding machine. Once the ends were removed off all rough spots, the cylinders were placed into steel retaining rings with a neoprene pad between the specimen and the steel. With the steel retaining rings and neoprene pads on both the top and bottom of the concrete specimen, it was loaded into the compressive strength

testing machine. Specimens that were sulfur capped were placed into liquid sulfur capping compound to create a smooth liquid cap that hardened within seconds and could be tested in a few hours. At least two hours before the compressive strength test was to occur, the concrete specimens were removed from the moist curing chamber and the moisture was removed from the ends. When the specimens were ready to be capped, an ample amount of sulfur capping compounded was poured into the capping mold. The specimen was quickly held against the mold to ensure it was level and it was gently but quickly lowered in the capping compound. The capping compound hardened very quickly, so capping the cylinders needed to be done in a swift manner. Once the capping compound hardened around the concrete specimen, it was removed and the process was repeated on the other end. Once the specimen was capped on both ends, it was returned to the moist curing chamber. In order for the capping compound to reach its maximum strength, the capped specimens had to sit in the moist curing chamber for a minimum of two hours. After this time, the concrete specimens could be tested for compressive strength.

Before the compressive strength tests were run, the dimensions of the specimens were measured. The diameter was measured three times and the average was used to compute the compressive strength. From the measured diameter, the cross sectional area was calculated. The height was also measured. The specimens were then loosely wrapped in a canvas wrap and placed in the testing apparatus, as shown in **Figure 3.1**. A Forney 600 kip (2670 kN) compression testing machine was used. Steel plates were placed on the load deck in order to minimize the distance traveled. The specimen was then placed in the apparatus, centered, and brought to just below the upper plate.

Figure 3.1 - Compressive Strength Testing Setup

When the setup was complete, the specimen was loaded at a load rate specified for 4 in. (102 mm) diameter specimens. The target load rate was 525 lb/sec. (238 kg/sec.). The specimen was loaded at the specified rate until it could no longer sustain a load and the load rate dropped to a negative value. The machine was turned off and the peak load was recorded. Completed test specimens are show in **Figure 3.2**.

Figure 3.2 - High Strength Compressive Strength Specimens Post-Test

The load was then divided by the cross sectional area to get the measured compressive strength in pounds per square inch. A minimum of three specimens were tested at a given test age and the results were averaged to get the final measured compressive strength.

3.4. MODULUS OF ELASTICITY TEST

3.4.1. Introduction. The modulus of elasticity is an important property to investigate as it is used to determine the anticipated amount of deflection in design. This is important in designing for serviceability of a structure. The modulus of elasticity of concrete is determined by testing specimens in the liner elastic range. Specimens are loaded to a specified stress while the strain is measured. The slope of the stress–strain curve is taken as the modulus of elasticity.

3.4.2. Fabrication. Specimens used to measure the modulus of elasticity were fabricated according to ASTM C 192–07.These are the same type of specimens that were used for compressive strength testing. A minimum of three specimens were created for

each mix design. For the modulus of elasticity test, the specimens could be fabricated either using 4 in. (102 mm) diameter by 8 in. (203 mm) long cylinders or 6 in.(152 mm) diameter by 12 in.(305 mm) long cylinders. The two types of cylinder molds can be seen in **Figure 3.3**. It should be noted that for the SCC mixes, 4 in. (102 mm) x 8 in. (203 mm) specimens were used, while for the HVFA concrete mixes, 6 in. (152 mm) x 12 in. (305 mm) specimens were used.

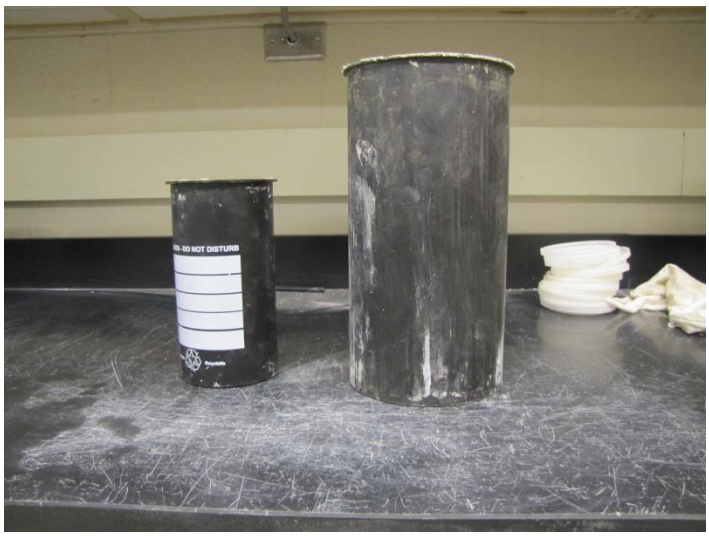

Figure 3.3 – 4 in. (102 mm) x 8 in. (203 mm) Cylinder Mold Compared to 6 in. (152 mm) x 12 in. (305 mm) Cylinder Mold

Specimens were de-molded after 24 hours and placed in the moist curing chamber for 28 days before testing. Before the test was conducted, all test specimens were sulfur capped in the same manner as the compressive strength cylinders.

3.4.3. Testing & Procedure. After the specimens were allowed to cure for 28 days, the specimens were tested in accordance with ASTM C 469–10, "Standard Test Method for Static Modulus of Elasticity and Poisson's Ratio of Concrete in Compression." The dimensions of the specimens were measured, and before loading, the

specimen was fitted with a compressometer in order to measure the deflection of the cylinder during loading. A typical compressometer can be seen in **Figure 3.4**.

Figure 3.4 - Typical Compressometer

The specimen was then placed into a compression loading apparatus and loaded at a constant rate. The load was recorded when the deflection of the specimen reached 0.0004 in. (0.01 mm). The specimen was continually loaded until the load reached 40% of the ultimate strength of the concrete. The value of the ultimate strength was determined from compressive strength tests of companion specimens. When the load on the specimen reached 40% of the measured ultimate load, the deflection was recorded. This test was then performed three additional times on the same specimen. The data recorded during the first test run on each specimen was disregarded and only the following three tests were used for averaging. Using these deflections, the strains were calculated and the corresponding stresses were used to calculate the modulus of elasticity using Eq. 3.1.

$$E_c = \frac{(S_2 - S_1)}{(\varepsilon_2 - 0.00005)} \tag{3.1}$$

Where S_2 is the stress measured at 40% of the ultimate load and S_1 is the stress measured when the deflection of the specimen reached 0.0004 in. (0.01 mm) and ε_2 is the strain produced by S_2. The results from the individual tests were then averaged and the averages from the three tests were then averaged to obtain the measured modulus of elasticity.

3.5. MODULUS OF RUPTURE TEST

3.5.1. Introduction. The modulus of rupture test is used to determine the flexural strength or tensile strength of the concrete. This is an important mechanical property to investigate. The modulus of rupture is important in design for estimating the cracking moment of the concrete when subjected to flexure.

3.5.2. Fabrication. The specimens used for the modulus of rupture test were fabricated in accordance with ASTM C 78–10, "Standard Test Method for Flexural Strength of Concrete (Using Simple Beam with Third-Point Loading)." Three specimens were fabricated for every concrete mix. The specimens measured 6 in. (152 mm) x 6 in. (152 mm) in cross section with a length of 24 in. (610 mm). The specimens were filled with two lifts, each lift being rodded 72 times. It should be noted that the SCC was not rodded when specimens were cast. The specimens were cast in one single lift. The specimens were de-molded after 24 hours and stored in a moist curing chamber for 28 days. After 28 days they were prepared for testing.

3.5.3. Testing & Procedure. After 28 days, the specimens were removed from the moist curing chamber. The supports on the testing apparatus were 18 in. (457 mm) apart. In order to align the specimen on the supports, it had to be divided into thirds. The first 3 in. (76 mm) of either end of the specimen were not included in the measuring. This caused the 18 in. (457 mm) span to be divided into 3, 6 in. spans. The load points would be placed on the 6 in. mark and the 12 in. mark, creating the third-point loading. The prepared specimen can be seen in **Figure 3.5**.

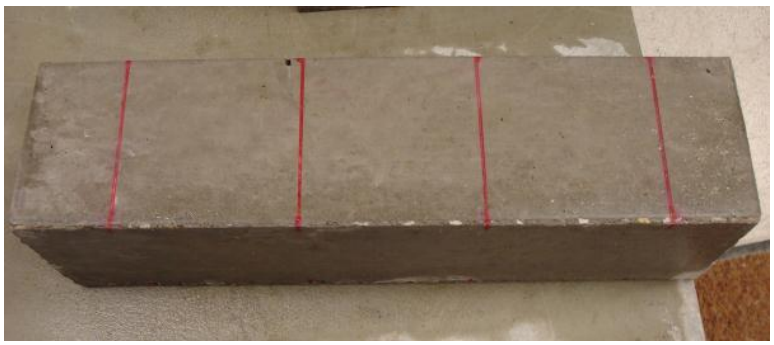

Figure 3.5 - Prepared Modulus of Rupture Specimen

The specimen was rotated and loaded into the testing machine on a formed side to provide the smoothest surface and thus prevent localized forces on the beam. The load was applied at the aforementioned points. A leather pad was placed in between the concrete specimen and the load points in order to help distribute the load. The test setup can be seen in **Figure 3.6**. It is important to note that during the set-up, the specimen was kept moist in order to prevent any internal stresses from developing.

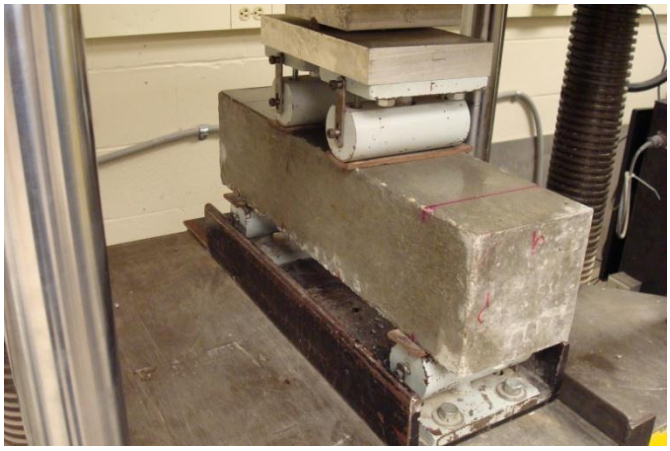

Figure 3.6 - Modulus of Rupture Testing Setup

The load head was then lowered until it made contact with the leather pads. The beam was then loaded at a constant rate until failure. If the beam failed within the middle third, the test was accepted. It should be noted that all beams tested in this investigation failed in the middle third of the beam. A post failure specimen can be seen in **Figure 3.7**. The failure load was recorded and subsequently used to calculate the modulus of rupture using **Eq. 2**.

Figure 3.7 - Modulus of Rupture Specimen Post-Test

The beam was removed from the testing apparatus and its dimensions were measured. The width and depth of the beam were measured three times and averaged. The modulus of rupture was then calculated using **Eq. 3.2**.

$$R = \frac{PL}{bd^2} \tag{3.2}$$

Where P is the peak load, L is the distance between supports, b is the average width of the beam after testing, and d is the average depth of the beam after testing.

3.6. SPLITTING TENSILE TEST

3.6.1. Introduction. ASTM has not yet specified a standardized test to find the direct tensile strength of concrete. There is a standardized test for an indirect tension test known as the splitting tensile test. This test involves loading a cylindrical specimen along its longitudinal axis until failure. This test is thought to measure a greater tensile strength than a direct tensile strength. However it is usually lower than a measured strength from a modulus of rupture test. The splitting tensile test is a good indication of a concrete's tensile strength but should be performed alongside other tests such as the modulus of rupture test.

3.6.2. Fabrication. The specimens used for the splitting tensile test were fabricated in accordance with ASTM C 496–11, "Standard Test Method for Splitting Tensile Strength of Cylindrical Concrete Specimens." A minimum of three specimens were made for each concrete mix. The specimens were made using a 4 in. (102 mm) diameter by 8 in. (203 mm) long cylindrical molds. The specimens used for the splitting

tensile test were the same types of specimens used for the compressive strength test. The specimens were fabricated according to ASTM C 192. After 24 hours, the specimens were de-molded and placed in a moist curing chamber for 28 days, at which time they were then tested.

3.6.3. Testing & Procedure. After the specimens were allowed to cure for 28 days, the specimens were removed from the curing chamber for testing. The diameter and height of the specimens were recorded. The diameter of the specimen was marked the top of the specimen. Two lines were then drawn down the long side of the specimen from the previously drawn line. This was done to assist in lining up the specimen in the testing apparatus. The specimen was then loaded into the testing apparatus on the line drawn down its vertical axis. The specimen was placed on a piece of plywood. Another plywood strip was placed on the top of the specimen between it and the load platen. These strips were used so the load would be distributed along the axis of the specimen. The test setup can be seen in **Figure 3.9**.

Figure 3.9 - Typical Splitting Tensile Test Setup

The specimen was then loaded at a rate between 100 (45 kg) and 200 lb /min. (91 kg/min.) until failure. The load at failure was recorded as the peak load, and the tensile strength was calculated using **Eq. 3.3**.

$$T = \frac{2P}{\pi LD} \tag{3.3}$$

Where P was the peak load, L is the length of the specimen, and D is the diameter of the specimen. A post failure specimen can be seen in **Figure 3.10**.

Figure 3.10 - Splitting Tensile Specimens Post-Test

4. DURABILITY TESTS

4.1. INTRODUCTION

This section discusses the durability tests used to evaluate the performance high-volume fly ash (HVFA) concrete. The durability performance of these specialized concretes is a crucial aspect in investigating the possibility of implementing these new materials into transportation-related infrastructure, such as bridges, roadways, culverts, and retaining walls. The following durability tests were included in the scope of work for this investigation:

- Resistance of Concrete to Rapid Freezing and Thawing (ASTM C 666-08)
- Electrical Indication of Concrete's Ability to Resist Chloride Ion Penetration (ASTM C 1202-10)
- Determining the Penetration of Chloride Ion into Concrete by Ponding (ASTM C 1543-10)
- Concrete Resistivity (Non-ASTM)
- Scaling Resistance of Concrete Surfaces Exposed to Deicing Chemicals (ASTM C 672-03)

The outline for the durability tests is shown in **Table 4.1**. The outline identifies the number of test specimens fabricated for each test for each concrete mix. The table also includes the required curing conditions and durations, as well as the specimen age at the start of testing and the duration of the test, if applicable.

Table 4.1 Test Matrix for Durability Performance

Durability Property	Number of Specimens	Moist Curing Duration, days	Dry Curing Duration, days	Testing Date, days	Testing Duration, days
Freezing and Thawing	3	35	0	35	N/A[1]
Electrical Chloride Penetration	2 (4) disk	28	0	28	N/A[2]
Ponding	3	14	14	28	120
Concrete Resistivity	3	14	21	35	168
Scaling	3	14	14	28	50

Notes: 1. Test duration based on cycles
2. Duration of test is 6 hours

4.2. RAPID FREEZING & THAWING TEST

4.2.1. Introduction. The rapid freeze-thaw test was one of the most critical durability tests performed in this investigation. The climate in Missouri is susceptible to multiple freeze-thaw cycles, which is a more severe environment for concrete durability than continuous freezing. The test involves subjecting specimens to multiple freeze-thaw cycles in order to measure the resistance of the material to deterioration caused by the expansion of the free water freezing inside the specimens. This resistance was measured using three parameters: the length change of the specimens, change in the fundamental transverse frequency of the specimens, and mass change of the specimens. A decrease in the values for these parameters indicates freeze-thaw deterioration.

4.2.2. Fabrication. The specimens for the rapid freeze-thaw test were fabricated according to ASTM C 666–03, “Standard Test Method for Resistance of Concrete to Rapid Freezing and Thawing.” The molds used in the fabrication of these

specimens were loaned to the project by the Construction Materials Department of the Missouri Department of Transportation (MoDOT) and can be seen in **Figure 4.1**. These stainless steel molds measured 3.5 in. (8.9 cm) in width, 4.5 in. (11.43 cm) in height, and 16 in. (40.64 cm) in length and conformed to ASTM C 666 requirements for specimen dimensions.

Figure 4.1 - Freezing and Thawing Specimen Molds

The ends of each mold contained a threaded hole to install a specialized bolt. This bolt contained a rounded end, and when the concrete specimens were de-molded, the end of this bolt protruded from both either end of the prism as shown in **Figure 4.2**. The embedded bolt provides a mechanism to measure the length change of the concrete prism as it was subjected to freezing and thawing cycles.

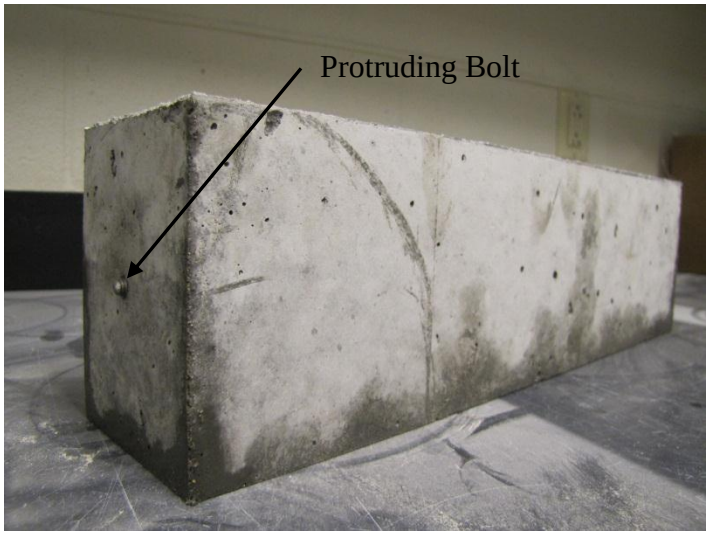

Figure 4.2 - Freezing and Thawing Specimen with Protruding Bolt

Once the specimens were formed and de-molded, they were placed in a temperature controlled moist curing room for 35 days prior to testing. It should be noted that this moist curing duration is a standard for MoDOT and a modification from ASTM C 666. The ASTM specifies that the prisms should be moist cured for 14 days unless otherwise specified. It should also be noted that the typical MoDOT procedure requires that specimens that will be subjected to the rapid freeze-thaw test be submersed in a lime water solution while they cure for the 35 days. However, due to space restraints in the University laboratory, the specimens were only moist cured. This change was deemed acceptable provided all specimens received the same treatment. Between 14 and 21 days, the prisms were transported from the University's moist curing chamber to the Construction Materials testing lab of MoDOT in Jefferson City, Missouri. To be transported, the specimens were wrapped in burlap that was saturated in a 5% by weight lime water solution. The specimens were then placed into a cooler and immediately driven to the MoDOT lab and placed into the moist curing chamber to complete the 35-

day moist curing regime. All rapid freezing and thawing test were performed by MoDOT employees of the Construction Materials Department.

4.2.3. Testing & Procedure. All specimens were tested in accordance with ASTM C 666, Procedure A. When the specimens reached the appropriate age, they were brought to the target thaw temperature. The fundamental transverse frequency, mass, length, and cross section of the specimen was measured. The freeze-thaw specimens were then subjected to the appropriate freezing and thawing cycles. Each specimen was subject to 300 cycles of freezing and thawing while submerged in water. Every 36 cycles the specimens would be removed at the thawed state and properties of the specimen would be measured. The properties measured were fundamental transverse frequency, length change, and mass change. The specimens were then placed back into the testing apparatus and the cycles continued. The test could be ceased if the specimen deteriorated so extensively that the test could not continue. The relative dynamic modulus of elasticity was then calculated using **Eq. 4.1**.

$$P_c = \frac{n_1^2}{n^2} x100 \tag{4.1}$$

Where P_c is the relative dynamic modulus of elasticity at, c, cycles of freezing and thawing. N_1 is the fundamental transverse frequency after, c, cycles of freezing and thawing and n is the fundamental transverse frequency after 0 cycles of freezing and thawing. Using the relative dynamic modulus of elasticity, the durability factor of the freezing and thawing specimen was also calculated using **Eq. 4.2**.

$$DF = \frac{PN}{M} \tag{4.2}$$

Where DF is the durability factor, P is the relative dynamic modulus of elasticity at N cycles, N is the number of cycles at which the specified value of P is reached or the specified number of cycles is reached, whichever is less, and M is the number of cycles which the test is to be terminated. The higher the measured durability factor, the greater resistance the concrete will have to freezing and thawing attack.

4.3. ELECTRICAL INDICATION TO RESIST CHLORIDE ION PENETRATION TEST

4.3.1. Introduction. Chloride penetration of concrete is one of the leading durability issues facing many concrete specimens. Concrete members that are exposed to chlorides such as concrete piers in the ocean or concrete bridge decks exposed to de-icing salts all face chloride penetration. If sufficient chloride is allowed to penetrate into a concrete member, it can cause the embedded steel reinforcement to corrode and the expanding corrosion product will results in internal stresses, which in turn will cause cracking of the concrete. Over time this will cause concrete spalling and eventual failure. The electrical indication of concrete's ability to resist chloride penetration is a rapid method to determine the permeability of the concrete and its ability to withstand chloride penetration. This test is often used in correlation with the ponding test as it was in this investigation. Due to the ponding test's longer duration, this electrical test is a rapid method to estimate the durability of concrete. This test is also known as the Rapid Chloride Test (RCT).

4.3.2. Fabrication. The test specimens consisted of cylinders fabricated and prepared according to ASTM C 192–07, “Standard Practice for Making and Curing Concrete Test Specimens in the Laboratory.” Two 4 in. (10.16 cm) diameter x 8in. (20.32 cm) long cylinders were used for this test for every concrete mix. These cylinders were prepared alongside the compressive strength specimens. These specimens were de-molded after 24 hours and placed in the moist curing chamber for 28 days. In between 14 and 21 days after batching, these cylinders were transported to the Construction Materials testing lab in Jefferson City to finish the curing cycle and begin testing. These specimens were wrapped in burlap that was saturated in a 5% by weight lime water solution. The specimens were then placed into a cooler and immediately driven to the MoDOT lab and placed into the moist curing chamber to complete the 28-day moist curing regime. All electrical chloride tests were performed by MoDOT employees of the Construction Materials Department.

4.3.3. Testing & Procedure. The testing of specimens for the electrical indication of a concrete’s ability to resist chloride ion penetration is outlined in ASTM C 1202-10, “Standard Test Method for Electrical Indication of Concrete’s Ability to Resist Chloride Ion Penetration.” The test specimens consist of 4 in. (102 mm) diameter by 2 in. (51 mm) thick concrete disks. These disks were cut from specimens cast according to ASTM C 192. Two disks were cut from each concrete cylinder, with two concrete cylinders cast from each mix, which resulted in a total of 4 concrete disks for each concrete mix. One disk was cut from the top of the cylinder and the other from the middle. These disks were labeled with the mix design name and noted as either middle or

top. The specimens were allowed to surface dry for at least 1 hour before the sides of the disks were coated with a setting coating as seen in **Figure 4.3**.

Figure 4.3 - Setting Coating Being Applied to Concrete Specimens

After the coating dried, the specimens were placed into a vacuum desiccator and vacuumed for 3 hours. The pressure of the vacuum was at least 0.96 psi (6650 Pa). At the end of the 3 hour desiccation period, de-aerated water was poured into the water stockpot of the vacuum until the specimen was covered. The stockpot was closed and the vacuum was maintained for another hour. The vacuum was then turned off and air was allowed to enter the desiccator. The specimen was then allowed to soak in the de-aerated water for 18 ± 2 hours. The specimen is then blotted dry and placed into the voltage cell. A sealant is then applied to the specimen-cell boundary. The exposed face of the specimen is then covered while the sealant is allowed to dry. Once the sealant is dry, the process is repeated to the other face of the specimen. The final specimen can be seen in **Figure 4.4**.

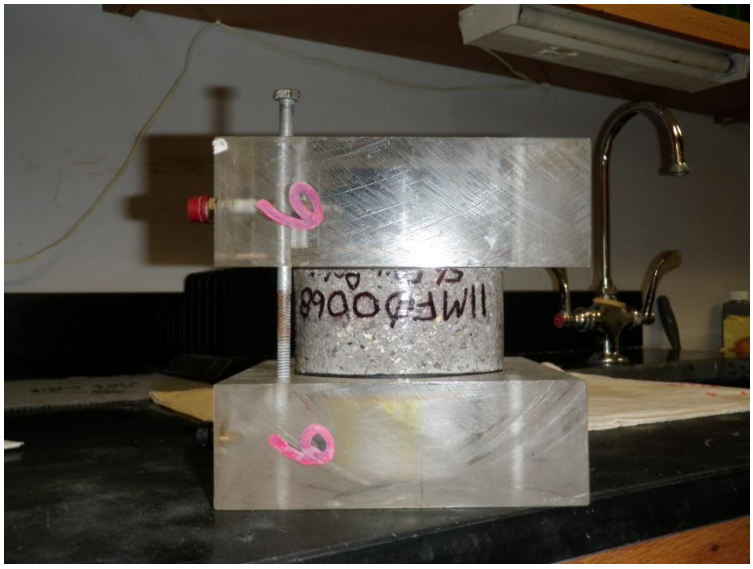

Figure 4.4 - Typical Completed Specimen

The side of the cell that is connected to the negative terminal is then filled with 3.0% NaCI solution while the side connected to the positive terminal is filled with 0.3 N NaOH solution. The test setup can be seen in **Figure 4.5**. The power is then turned on and the voltage is set to 60 V. The initial current is recorded and then recorded at 30 minute intervals.

The test is conducted for 6 hours unless the temperature in the solution exceeds 190°F. This temperature is only exceeded when the concrete is extremely permeable. The data that is recorded is then used to calculate the total charge passed through the specimen in coulombs. This is discussed further during evaluation of the different concretes.

Figure 4.5 – Typical RCT Setup

4.4. PONDING TEST

4.4.1. Introduction. A serious problem facing Missouri concrete bridge decks is spalling and deterioration caused by chloride penetration and subsequent corrosion of the underlying steel. During winter months, de-icing salts are used to remove snow and ice from bridge and roadway surfaces. The chlorides contained in these de-icing salts diffuse into the concrete, eventually breaking down the passive layer of the reinforcing steel and causing corrosion. The corrosion product expands to approximately six times the original volume, resulting in internal stresses and eventually cracking. Over time, this process will lead to spalling and deterioration of the concrete. The ponding test subjects concrete specimens to a similar environment to investigate the ability of the concrete to resist chloride penetration. This test is a valuable indicator of the resistance of the concrete to chloride ingress and thus the durability of the material. Although this test

requires a longer period of time compared to other methods to predict the resistance of concrete to chloride penetration, it is the most realistic test method.

4.4.2. Fabrication. The concrete specimens for the ponding test were fabricated according to ASTM C 1543-10, "Standard Test Method for Determining the Penetration of Chloride Ion into Concrete by Ponding." Three specimens were made for each concrete mix. The test requires that the specimens have a surface area of at least 45.6 in^2 (30,000 mm^2). The specimens must also be at least 3.54 ± 0.6 in. (90 ± 15 mm). tall. The specimens created for the ponding test in this investigation measured 18 in. (457 mm) wide x 18 in. (457 mm) long x 4 in. (102 mm) tall. Also, the test procedure required a dike along the top of the specimen with a height of at least 0.79 in. (20 mm) high. To accomplish this, a 0.75 in.-thick (19 mm) foam panel measuring 16 in. (406 mm) x 16 in. (406 mm) in plan was placed on a sheet of plywood that would serve as the base of the mold. Walls constructed from 2 in. (51 mm) x 4 in. (102 mm) pieces of wood were then connected to the panel to arrive at the overall dimension of 18 in. (457 mm) x 18 in. (457 mm) in plan. When the concrete was placed in the mold, the foam created a void in what would become the top of the specimen. The foam formed the reservoir for the chloride solution. The concrete was placed into the formwork and consolidated as necessary. After 24 hours, the concrete specimens were de-molded and placed in a moist curing chamber. After 14 days of moist curing, the specimens were transported to a temperature and humidity controlled environment where they would dry cure for another 14 days. After 28 days of curing, the specimens would then begin the ponding test.

4.4.3. Testing & Procedure. The test procedure involved placing a 5% by weight chloride solution into the ponding specimen reservoir. The solution had to be at a depth of 0.6 ± 0.2 in. (15 ± 5 mm). A typical ponded specimen can be seen in **Figure 4.6**. When the required amount of solution was poured into the reservoir, the concrete specimens were covered with plastic sheeting and the sheets were secured with elastic bands to prevent evaporation of the solution.

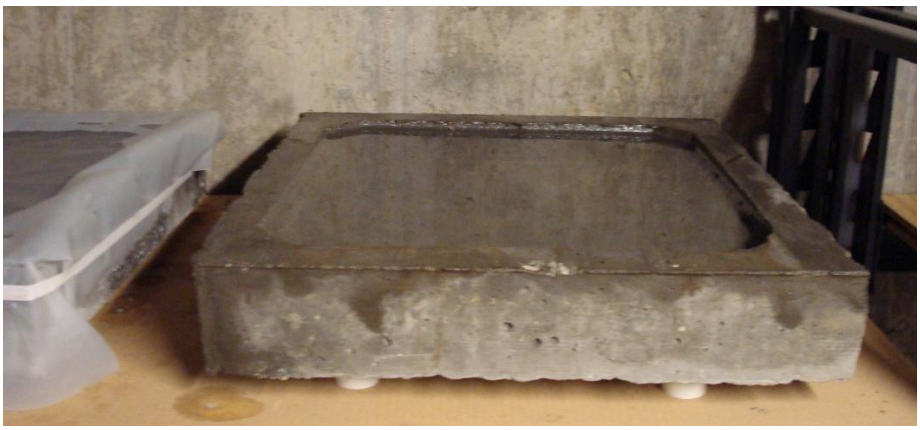

Figure 4.6 - Typical Ponding Specimen

Every two weeks the specimens were checked to ensure that the proper depth of the solution was maintained. If the reservoir was low, additional solution was added. After 60 days of ponding, the reservoir was vacuumed dry and fresh solution was added. The sheeting was replaced and the specimens were monitored every two weeks. After another 60 days, the chloride solution was vacuumed off and the specimen allowed to air dry. A few days later, a core was taken from the center of the specimen. A typical core and core location can be seen in **Figure 4.7**.

Figure 4.7 - Concrete Core and Resulting Void in the Concrete Specimen

The core was removed using an industry standard core driller with a medium flow of water to ensure proper blade lubrication as well as creating the proper slurry. Powder samples were then taken from the cores at specified depth intervals. The intervals were 0.25 in. (6 mm), 0.75 in. (19 mm), 1.5 in. (38 mm), and 2 in. (51 mm) from the surface of the core. A sample was also taken from the surface of the core. These depths are shown in **Figure 4.8**.

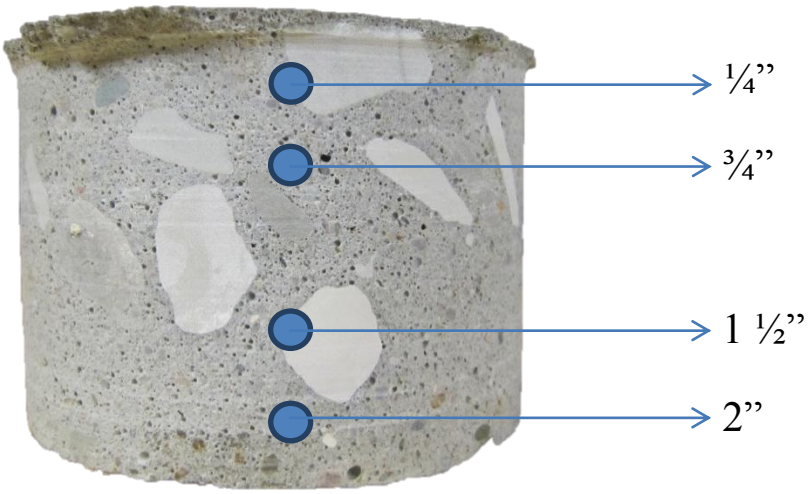

Figure 4.8 - Depths at which Powder Samples Were Collected
1 in. = 2.54 cm.

The samples had to measure at least 0.053 oz. (1.5 g) to be considered sufficient. Samples were collected using a 3/8 in. (9.5 mm) drilled bit at all locations except at the 0.25 in. (6 mm) location. At this location a 3/16 in. (5 mm) drill bit was used. A paper plate was used to collect the dust and a steel plate was placed in between the core and the vice to confine the concrete and prevent spalling. After each hole was drilled, it was sealed using masking tape to prevent cross contamination with the other samples. Samples were also taken from the surface of the core. This was done by drilling the surface of the core to a depth of no deeper than 0.125 in. (3 mm). Samples were collected from several locations on the surface of the core to obtain the necessary sample size. A chloride analysis was then performed on the powder samples to obtain the chloride content in the concrete at the respective sample depths.

The chloride analysis of water soluble chlorides was performed using the Rapid Chloride Testing (RCT) equipment made by Germann Instruments, Inc. The 0.053 oz. (1.5 g) sample was poured into a vial containing 0.304 fl-oz. (9 mL) of the extraction liquid. The vial was shaken vigorously for 5 minutes. The extraction liquid and powder slurry were then filtered into a buffer solution. While the slurry was filtering the electrode was prepared and calibrated. The preparing of the electrode began with filling it with a wetting agent. After any air bubbles were removed the wetting agent was allowed to be released in order to fully wet the circumference of the electrode tip. After the electrode had been refilled with the wetting agent, it had been prepared. In order to calibrate the electrode and build a scale to determine the chloride content of the specimens, the electrode was inserted into four calibration solutions of known chloride content. The four calibration liquids contained 0.005%, 0.02%, 0.05%, and 0.5% chloride content. The

electrode was inserted into each solution and the voltage was read. The four calibration liquids produced a voltage of approximately 100 mV, 72 mV, 49 mV, and -5 mV respectively. This data was used then plotted on a log chart in order to build a scale for the rest of the testing. An example of this log chart can be seen in Appendix B. After the preparing and the calibrating the electrode was ready to use. When the filtering process was complete the electrode was inserted into the vial and was held steady until the voltage reading stabilized. Using the recorded voltage and the scale determine by the log, the chloride content was determined. After every use the electrode was sprayed with distilled water, blotted dry and stored in an empty vial. This data collected from each depth was used to develop a chloride profile and determine chloride penetration into the concrete.

4.5. CONCRETE RESISTIVITY TEST

4.5.1. Introduction. A concrete's electrical resistance may be measured in an attempt to quantify the rate at which a bare, depassivated steel bar, embedded within the concrete, corrodes. The corrosion process is dependent upon the ability of charged ions, such as hydroxyl ions (OH^-), to flow from the cathode to the anode. The faster the ions can flow from the cathode to the anode, the faster the corrosion process may proceed, provided the cathode is supplied with a sufficient amount of oxygen and water. The transport of electricity through concrete closely resembles that of ionic current; therefore, it is possible to classify the rate of corrosion of a bar embedded within concrete by quantifying the electrical resistance of the surrounding concrete.

The four probe resistivity meter, also known as the Wenner probe and shown in **Figure 4.9**, is generally regarded as the most accurate method of measuring concrete resistivity. The probe contains four equally spaced electrodes that are positioned along a straight line. The two outer electrodes send an alternating current through the concrete while the inner electrodes measure the drop in potential. The resistivity is then calculated using **Eq. 3.3**.

$$\rho = \frac{2\pi sV}{I} \tag{3.3}$$

Where ρ is the resistivity (Ωcm) of the concrete, s is the spacing of the electrodes (cm), V is the recorded voltage (V), and I is the applied current (A).

Figure 4.9 - Canin$^+$ Wenner Probe

4.5.2. Fabrication. The concrete specimens for the resistivity test were fabricated according to ASTM C 1543–10 “Standard Test Method for Determining the Penetration of Chloride Ion into Concrete by Ponding”. The molds used to create these specimens were the same molds to create the specimens for the ponding test. The specimens were prepared the same way, using the same procedure. They were cured in the moist curing chamber for 14 days then transported to a humidity and temperature controlled environment to dry cure for an additional 21 days before testing. Testing began when the specimens reached an age of 35 days.

4.5.3. Testing & Procedure. One day prior to the beginning of the test, the specimens were ponded with just enough distilled water to coat the bottom of the reservoir. The specimens sat with water in them for 24 hours. The following day the water was vacuumed off using a shop vacuum cleaner. The Wernner probe was then used to take the initial resistivity measurements. The measurements were taken in a systematic manner, from left to right, then top to bottom, using the Plexiglas template shown in **Figure 4.10**. Three measurements were taken from left to right, once on the far left, once in the middle and once on the far right. Three measurements were then taken from top to bottom, once on the top, once in the middle, and once on the bottom.

These measurements were taken in the same order, once every week. The measurements were taken weekly until the resistivity measurements became constant. However, due to time constraints, the duration of the test was limited to 24 weeks.

Figure 4.10 - Wenner Probe Grid

4.6. SCALING TEST

4.6.1. Introduction. When concrete is exposed to freezing and thawing temperatures and is subjected to de-icing salts, it can deteriorate in the form of scaling. Scaling is defined as a general loss of surface mortar or mortar surrounding the coarse aggregate particles on a concrete surface. This occurs most often on bridge decks and roadways in cold climates. Scaling deterioration reduces the appearance, smoothness, and, most importantly, resistance of the concrete to further degradation.

4.6.2. Fabrication. The specimens used for the scaling test were fabricated as specified by ASTM C 672–03, "Standard Test Method for Scaling Resistance of Concrete Surfaces Exposed to Deicing Chemicals." These specimens are required to be at least 75 in^2 (483.9 cm^2) in plan and at least 3 in. (76 mm.) in depth. The specimen form is shown in **Figure 4.11**. Three specimens were constructed for each concrete mix. It should be noted that scaling specimens were only fabricated for the HVFA concrete investigation. The molds used to fabricate these specimens were provided by the MoDOT

Construction Materials testing laboratory. The molds were formed from two steel channels connected by a steel pin. A plate was placed at the bottom of the channels.

Figure 4.11 - Scaling Specimen Form

The concrete was placed in the form in one lift and rodded 72 times. The concrete was placed with approximately one inch of the form remaining exposed. Once the concrete was placed into the mold and allowed to reach a firm state, the specimens were broom finished with a medium broom. Then, using the exposed 1 in. (25 mm) of form, a dike was constructed along the edges of the specimen. The dike was constructed using a mortar mix consisting of 3 parts fine aggregate, 2 parts Portland cement, and 1 part water. The dike was constructed by hand using putty knifes for forming. A 1 in. (25 mm.) guide line was pressed into the edge of the fresh concrete to indicate the boundary of the dike. Keyways were then placed into the concrete where the dike would be constructed. The mortar was then placed onto the specimen and the dike was formed. This process can be seen in **Figure 4.12**.

Figure 4.12 - Scaling Specimen Dike Keyway and Dike Construction

The dike and the specimen were allowed to cure for 24 hours before being removed from the forms. After form removal, specimens were moist cured for 14 days and then air cured for 14 days. A specimen ready for testing is shown in **Figure 4.13**.

Figure 4.13 - Completed Scaling Specimen and Dike

4.6.3. Testing & Procedure. The testing procedure consisted of subjecting the specimen to freezing and thawing cycles in the presence of a saltwater solution within the reservoir formed by the dikes. A chloride solution measuring approximately 0.25 in. (6

mm) deep was placed into the reservoir of the specimen. The specimen was then placed into a walk-in freezer where it remained for 16 to 18 hours at a temperature of 32°F (0°C). After that period of time, the specimen was removed from the freezer and placed in a temperature and humidity-controlled environment of 73.5± 3.5°F (23.05± 2°C) and 45 to 55% R.H. for a period of 6 to 8 hours. This sequence counted as one cycle. Chloride solution was periodically added as necessary to maintain the proper depth, and the solution was completely replaced every 5 cycles. After 50 cycles the surface of the specimens was inspected and the degree of scaling was reported based on the ASTM standard.

5. HARDENED PROPERTY AND DURABILITY RESULTS

5.1. COMPRESSIVE STRENGTH

The compressive strength was determined in accordance with ASTM C 39-11. A minimum of three replicate specimens were tested for each testing date for each experimental mix. The compressive strength was tested at 1 day, 7 days, and 28 days. The tests were averaged and reported as the compressive strength of the experimental mix. All the mixes were graphed on the same plot for comparison purposes. A strength profile was developed in order to analyze and compare the strength gain of each mix. The individual specimen results of the high volume fly ash mixes can be seen in **Table 5.1**.

Table 5.1 Individual Compressive Strength Results for HVFA Mixes

Batch ID	1 Day Compressive Strength (psi)			7 Day Compressive Strength (psi)			28 Day Compressive Strength (psi)		
Control	1,960	2,130	1,900	4,540	4,840	4,540	5,440	5,360	5,280
HVFA-70H	712	694	742	2,320	2,490	2,390	3,150	3,090	2,890
HVFA-70L	812	845	827	2,710	2,750	2,790	3,480	3,610	3,350
HVFA-70LA	578	702	621	1,730	1,680	1,610	2,330	2,260	2,590

1 psi = 6.89 kPa

The individual results were then averaged and reported as the compressive strength of the experimental mix. The averaged values can be seen in **Table 5.2**.

Table 5.2 Averaged Compressive Strength Results of HVFA Mixes

Batch ID	1 Day Strength (psi)	7 Day Strength (psi)	28 Day Strength (psi)
Control	2,000	4,640	5,360
HVFA-70H	716	2,400	3,100
HVFA-70L	828	2,750	3,480
HVFA-70LA	633	1,670	2,390

1 psi = 6.89 kPa

These values were then plotted in order to develop a strength gain profile for the HVFA mixes. The strength profiles for the HVFA mixes are shown in **Figure 5.1**.

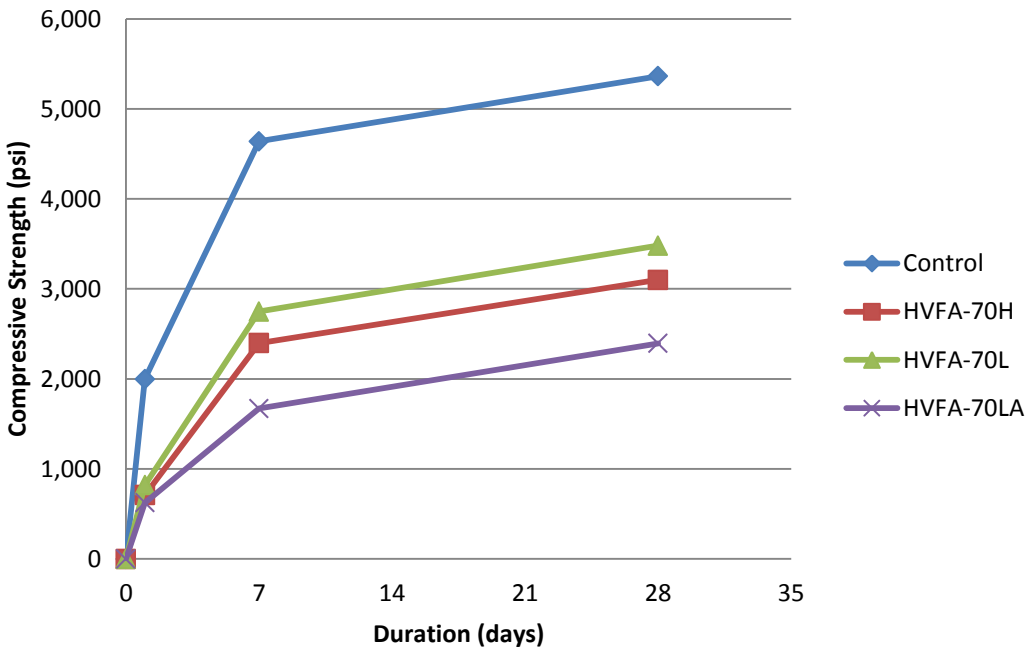

Figure 5.1 - Strength Profile of HVFA Mixes

The strength gain profile shows a large gap between the control mixes and the high-volume fly-ash mixes. The control mix also gained early strength at a much faster rate than any of the variation mixes. Both the HVFA mixes without air entrainment

performed very similar with the mix containing a low cement content doing slightly better. It should be noted that HVFA-70LA did poorly compared to the other mixes and did not even reach 3,000 psi (20.7 MPa).

5.2. MODULUS OF ELASTICITY

The modulus of elasticity was tested and calculated in accordance with ASTM C 469-10. Test specimens consisted of both 4 in. diameter x 8 in. long cylinder and 6 in. (152 mm) diameter x 12 in. (305 mm) long cylinders. The specimens were tested after 28 days. During testing both the load at 50 x 10^{-6} strain and the length change at 40% of the ultimate strength were measured. Using these values the modulus of elasticity was calculated using **Eq. 5.1**.

$$E = \frac{(S_2 - S_1)}{(\varepsilon_2 - 0.000050)} \qquad \textbf{(5.1)}$$

Where S_2 is the stress at 40% of the ultimate load, S_1 is the stress measured at 50 x 10^{-6} strain, and $\boldsymbol{\varepsilon_2}$ is the strain at S_2. The results for the control and HVFA-70L experimental mixes can be seen in **Table 5.3**.

The values for S_2 were based on results of the companion compressive strength tests. The modulus of elasticity test and compressive strength tests were performed back to back, so the values for S_2 vary slightly from test to test. Using this data and **Eq. 6.1**, the modulus of elasticity was calculated and averaged from the two tests. The modulus of elasticity for the HVFA-70H and HVFA-70LA mixes was calculated using a different apparatus. The apparatus was calibrated to calculate the modulus and report it on a

printout. For this apparatus to be used, 6 in. (152 mm) diameter x 12 in. (305) long cylindrical specimens were fitted with a special compressometer. This compressometer was also fitted with a LVDT to measure the length change of the specimen. Three replicate specimens were used for this mix. The individual results of the modulus of elasticity test can be seen in **Table 5.4**. These results were then averaged and can be seen in **Table 5.5**.

Table 5.3 Individual Modulus of Elasticity Results for Control and HVFA-70L Mixes

Mix Design ID	Specimen ID	Test 1			Test 2		
		S_2 (psi)	S_1 (psi)	ε_2 (x10^{-4})	S_2 (psi)	S_1 (psi)	ε_2 (x10^{-4})
Control	MOE-1	2181	154	6.6	2181	132	6.9
	MOE-2	2163	205	6.1	2163	214	6
HVFA-70L	MOE-1	1395	186	4.1	1395	187	4.1
	MOE-2	1420	152	4.6	1420	147	4.9

1 psi = 6.89 kPa

Table 5.4 Individual Modulus of Elasticity Results for HVFA-70H and HVFA-70LA Mixes

Mix Design ID	Specimen ID	Modulus of Elasticity (psi)
HVFA-70H	MOE-1	3,450,000
	MOE-2	3,500,000
HVFA-70LA	MOE-1	3,450,000
	MOE-2	3,400,000
	MOE-3	3,500,000

1 psi = 6.89 kPa

Table 5.5 Average Modulus of Elasticity for HVFA Mixes

Mix Design ID	Modulus of Elasticity (psi)
Control	3,390,000
HVFA-70H	3,475,000
HVFA-70L	3,163,000
HVFA-70LA	3,450,000

1 psi = 6.89 kPa

The results were also normalized using the respective measured compressive strengths. This step was performed in order to compare the coefficients with the ACI 318-08 recommended value of 57,000, as shown in **Eq. 5.2**.

$$E_c = 57{,}000\sqrt{f'c} \tag{5.2}$$

Where E_c is the modulus of elasticity and f'_c is the compressive strength of concrete. The measured modulus of elasticity was divided by the strength of the respective mix and the results can be seen in **Table 5.6**.

Table 5.6 Normalized Modulus of Elasticity for HVFA Mixes

Mix Design ID	Control	HVFA-70H	HVFA-70L	HVFA-70LA	ACI Coefficient
Normalized Results	46,250	62,420	53,610	70,410	57,000

The results of the modulus of elasticity were also compared to the AASHTO LRFD Bridge Design Specifications. The equation used for AASHTO to estimate the modulus of elasticity is shown in **Eq. 5.3.**

$$E_c = 33{,}000 w_c^{1.5} \sqrt{f_c'} \qquad (\mathbf{5.3})$$

For normal weight concrete w_c can be assumed as 0.145 kcf. The measured modulus of elasticity was divided by the strength of the respective mix and the results can be seen in **Table 6.7**.

Table 5.7 Normalized AASHTO Modulus of Elasticity for HVFA Mixes

Mix Design ID	Control	HVFA-70H	HVFA-70L	HVFA-70LA	AASHTO Coefficient
Normalized Results	1,463	1,974	1,694	2,232	1,820

5.3. MODULUS OF RUPTURE

The modulus of rupture test was performed in accordance with ASTM C 78-10. The modulus of rupture was calculated using the formula stated in section 3.5.3. The values used in the equation measured for each individual test can be seen in **Table 5.7**.

The modulus of rupture was calculated using the values in **Table 5.7** and then averaged for each concrete type. The average modulus of rupture for the high-volume fly ash mixes can be seen in **Table 5.8**.

Table 5.7 Individual Modulus of Rupture Results for HVFA Mixes

Batch ID	Specimen ID	L (in.)	Peak Load (lb.)	b_1 (in.)	b_2 (in.)	b_3 (in.)	d_1 (in.)	d_2 (in.)	d_3 (in.)
Control	MOR-1	18	4,561	6.15	6.18	6.15	5.91	5.99	5.93
	MOR-2	18	4,721	6.12	6.12	6.18	5.98	5.98	5.95
	MOR-3	18	5,494	6.19	6.23	6.34	5.90	5.87	5.83
HVFA-70H	MOR-1	18	4,314	6.21	6.26	6.25	5.93	5.96	5.99
	MOR-2	18	4,120	6.11	6.11	6.14	5.95	5.94	5.92
	MOR-3	18	4,085	6.18	6.18	6.17	5.97	5.96	5.94
HVFA-70L	MOR-1	18	5,292	6.22	6.24	6.23	6.09	6.07	5.97
	MOR-2	18	5,571	6.16	6.18	6.20	5.97	5.96	5.95
	MOR-3	18	5,137	6.22	6.18	6.16	6.00	5.95	5.91
HVFA-70LA	MOR-1	18	4,543	6.13	6.12	6.13	5.97	5.97	5.97
	MOR-2	18	5,009	6.19	6.19	6.19	5.95	5.94	5.94
	MOR-3	18	4,791	6.19	6.18	6.19	5.92	5.91	5.92

1 psi = 6.89 kPa
1 in. = 2.54 cm.

Table 5.8 Average Modulus of Rupture Results for HVFA Mixes

Batch ID	Modulus of Rupture (psi)
Control	405
HVFA-70H	343
HVFA-70L	433
HVFA-70LA	395

1 psi = 6.89 kPa

The results were also normalized using the respective measured compressive strengths. This step was done in order to compare the coefficients with the ACI 318-08 recommended coefficient of 7.5, which appears in the equation to estimate the modulus of rupture, as seen in **Eq. 5.4**.

$$f_r = 7.5\sqrt{f'c} \tag{5.4}$$

Where f_r is the modulus of rupture and f'_c is the compressive strength of concrete. While the coefficient of 7.5 is the most commonly used coefficient, ACI states that any values between 6 and 12 are acceptable. After the modulus was measured, the values were divided by the average measured strength of the respected mix. This normalized the results, and these results were compared to the ACI coefficient of 7.5. The results of the HVFA mixes can be seen in **Table 5.9**.

Table 5.9 Normalized Modulus of Rupture for HVFA Mixes

Mix Design ID	Control	HVFA-70H	HVFA-70L	HVFA-70LA	ACI Coefficient
Normalized Results	5.5	6.2	7.3	8.1	7.5

The results of the modulus of elasticity were also compared to the AASHTO LRFD Bridge Design Specifications. The equation used for AASHTO to estimate the modulus of rupture is shown in **Eq. 5.5.**

$$f_r = 0.24\sqrt{f_c'} \tag{5.5}$$

The normalized results of the HVFA mixes compared to the AASHTO coefficient can be seen in **Table 5.10**.

Table 5.10 Normalized AASHTO Modulus of Rupture for HVFA Mixes

Mix Design ID	Control	HVFA-70H	HVFA-70L	HVFA-70LA	AASHTO Coefficient
Normalized Results	0.17	0.19	0.23	0.40	0.24

5.4. SPLITTING TENSILE

The splitting-tensile strength of the concrete mixes was tested and calculated in accordance with ASTM C 496-11. This test was performed using 6 in. (152 mm) diameter by 12 in. (305 mm) long cylindrical specimens. These specimens were loaded into the testing apparatus a loaded until failure. The splitting tensile strength was then calculated using **Eq. 5.6**.

$$T = \frac{2P}{\pi l d} \tag{5.6}$$

Where P is the maximum load applied, l is the length of the specimen, and d is the diameter. A minimum of 3 specimens were tested for each mix. The individual test results for the normal strength mixes are shown in **Table 5.11**.

Table 5.11 Individual Splitting-Tensile Test Results for HVFA Concrete Mixes

Mix Design ID	Specimen Number	Length (in.)	Diameter (in.)	Load (lb.)	Splitting Tensile Strength (psi)
Control	1	12.0	6.05	45,560	400
	2	12.0	6.05	39,975	351
	3	12.0	6.07	38,760	339
HVFA-70H	1	12.0	6.03	31,635	279
	2	12.0	6.04	26,550	233
	3	12.0	6.03	32,865	289
	4	12.0	6.04	31,155	273
	5	12.0	6.01	27,165	240
HVFA-70L	1	12.0	6.0	34,530	305
	2	12.0	6.0	35,235	312
	3	12.0	6.0	33,075	292
HVFA-70LA	1	8.0	4.0	7,410	147
	2	8.0	4.0	12,435	248
	3	8.0	4.0	13,980	278

1 in. = 2.54 cm.
1 lb = 0.45 kg
1 psi = 6.89 kPa

The individual splitting-tensile data was then averaged for each mix. The averaged splitting-tensile strength can be seen in **Table 5.12**.

Table 5.12 Averaged Splitting-Tensile Strength for HVFA Mixes

Mix Design ID	Splitting-Tensile Strength (psi)
Control	363
HVFA-70H	263
HVFA-70L	303
HVFA-70LA	224

1 psi = 6.89 kPa

The results were also normalized using the respective measured compressive strengths. This step was done in order to compare the coefficients with the ACI coefficient of 6.7, which comes from the equation to estimate the splitting-tensile strength as seen in **Eq. 5.7**.

$$f_t = 6.7\sqrt{f'c} \tag{5.7}$$

Where f_t is the splitting-tensile strength and f'_c is the compressive strength of concrete. The measured modulus of elasticity was divided by the strength of the respected mix and the results can be seen in **Table 5.13**.

Table 5.13 Normalized Splitting-Tensile Strength for HVFA Mixes

Mix Design ID	Control	HVFA-70H	HVFA-70L	HVFA-70LA	ACI Coefficient
Normalized Results	8.6	4.7	5.1	4.6	6.7

5.5. RAPID FREEZING & THAWING

The concrete's resistance to freezing and thawing was tested and calculated in accordance to ASTM C 666-08. During the freezing and thawing cycles, the relative dynamic modulus of elasticity was measured for each of the specimens using the equation stated in Section 4.2.3. Using this data, the durability factor of the specimen could be calculated using the equation stated in Section 4.2.3. The relative dynamic modulus of elasticity and durability factor of each specimen was calculated every 36

cycles. The complete data for all test specimens can be found in Appendix B. The minimum calculated durability factor was reported as the durability factor for that specimen, and the values for the individual specimens of HVFA mixes can be seen in **Table 5.14**.

Table 5.14 Individual Results of Freezing and Thawing Test for HVFA Mixes

Batch ID	Specimen ID	Initial Frequency	Terminal Frequency	Durability Factor	% Weight Change	Notes
Control	FT-1	1800	1080	20.3	0.02	-
	FT-2	1893	1136	23.5	0.02	-
	FT-3	1942	1165	20.9	0.02	-
HVFA-70H	FT-1	1782	1069	1.83	0.27	corner fell off
	FT-2	1787	1072	2.22	0.27	corner fell off
	FT-3	1739	1043	2.39	0.31	corner fell off
HVFA-70L	FT-1	1881	1129	85.7	-0.004	-
	FT-2	1882	1129	77.8	0.007	-
	FT-3	1886	1132	82.1	0.005	-
HVFA-70LA	FT-1	1761	1057	81.52	-0.683	-
	FT-2	1763	1058	79.61	-0.371	-
	FT-3	1739	1043	44.4	0.18	-

It should be noted that corner of all the freeze-thaw specimens for the HVFA-70H experimental mix fell off during the testing procedure. This shows the extremely poor durability performance of this particular mix. The average durability factor was reported using the three replicate specimens for each experimental mix. The higher the measured durability factor of the specimen, the better the mix will perform when exposed to cyclic

freezing and thawing. The calculated durability factors for the conventional mixes can be seen in **Table 5.15**.

Table 5.15 Average Durability Factors for HVFA Mixes

Batch ID	Durability Factor
Control	21.6
HVFA-70H	2.1
HVFA-70L	81.8
HVFA-70LA	68.5

5.6. ELECTRICAL INDICATION TO RESIST CHLORIDE PENETRATION

The testing and calculations for this test were performed in accordance with ASTM C 1202-10. After the testing was complete, the measured current vs. time was plotted. A trend line was drawn through the graph and was integrated to calculate the area under the curve. The graphs plotted for each specimen can be found in Appendix B. An example of this graph can be seen in **Figure 5.2**.

This area gives the total charge in coulombs to pass through the specimen during the 6 hour test. Since the diameter of the specimens used did not measure 3.75 in. (95 mm) the charge had to be adjusted using **Eq. 6.8**.

$$Q_s = Q_x \times \left(\frac{3.75}{x}\right)^2 \tag{6.8}$$

Where Q_S is the total charge through a 3.75 in. (95 mm) specimen, Q_X is the total charge passed through a specimen measuring x inches in diameter, and x is the diameter of the

specimen that is tested. The total charge was then compared to Table 4.1 in ASTM C 1202 to assign a permeability rating, with a range from negligible (indicating the highest resistance to chloride penetration) to high (indicating the lowest resistance to chloride penetration). The corrected results of the individual specimens for the HVFA mixes are shown in **Table 5.16**.

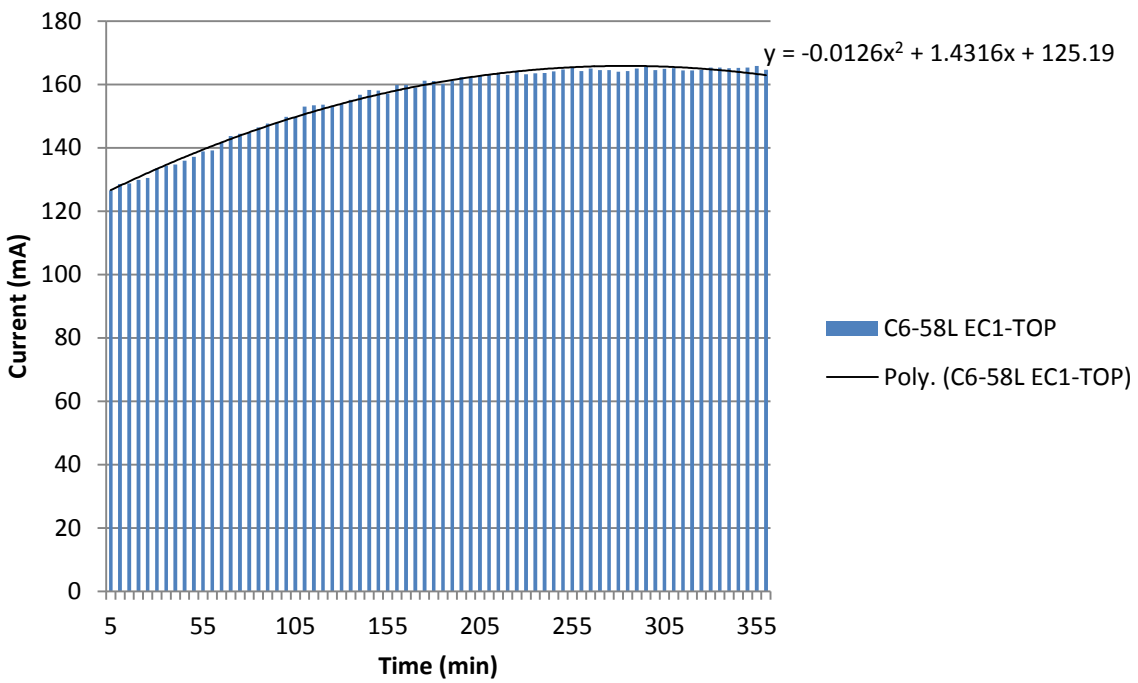

Figure 5.2 - Example of RCT Results

Table 5.16 Individual Results of RCT for HVFA Mixes

	Corrected Charge Passed (Coulombs)				
Batch ID	EC1-TOP	EC1-MID	EC2-TOP	EC2-MID	Notes
Control	4939	4660	4163	4877	-
HVFA-70H	778	583	1445	690	test stopped
HVFA-70L	1067	652	7576	999	test stopped
HVFA-70LA	967	791	1067	652	test stopped

It should be noted that the tests for all specimens for the high-volume fly ash mixes except the control were halted due to excessive voltage or excessive mA. This occurs when the concrete is excessively permeable. While the total charge may appear to be a good indication of permeability, the excessive voltage or mA indicates a high permeability class. The results were then averaged and used to assign a permeability class. The results are shown in **Table 5.17**.

Table 5.17 Averaged Results of RCT and Permeability Class of HVFA Mixes

Batch ID	Charge Passed (Coulombs)	Permeability Class	Notes
Control	4660	High	-
HVFA-70H	874	Very Low	test stopped
HVFA-70L	2573	Moderate	test stopped
HVFA-70LA	869	Very Low	test stopped

The ranges for the classes are as follows; 0-100 for negligible, 100-1000 for very low, 1000-2000 for low, 2000-4000 for moderate, >4000 for high. All three of the high volume fly ash experimental mixes, while showing low permeability class, are actually extremely permeable due to the excessive voltage or mA.

5.7. PONDING TEST

The ponding test was performed in accordance with ASTM C 1543-10. After the ponding duration was complete, cores were taken from the specimens and powder samples collected at specified depths. A chloride analysis was performed on each powder sample to determine the chloride concentration. For each experimental mix, a total of 3

cores were taken from the three individual test specimens, with 5 powder samples taken from each core. This approach would determine an average chloride profile for each experimental mix. Using a scale set forth by Broomfield in 2007, the risk of corrosion in concrete can be determined by the amount of chloride present in concrete. The scale can be seen in **Table 5.18**.

Table 5.18 Correlation Between Percent Chloride by Mass of Concrete and Corrosion Risk [Broomfield, 2007]

% Chloride by mass of concrete	Corrosion Risk
<0.03	Negligible
0.03-0.06	Low
0.06-0.14	Moderate
>0.14	High

Using this scale, the concrete mixes were assigned corrosion risk based on the data collected in the chloride analysis. The averaged data for the HVFA mixes can be seen in Table **5.19**. The complete table of data can be found in the appendix. This data was also plotted in **Figure 6.3** with a line indicating negligible corrosion risk.

Table 5.19 Average Chloride Content at Specified Depths of HVFA Mixes

Mix Design ID	Depth (in.)	Chloride Content (%)	Corrosion Risk
Control	Surface	0.045	Low
	0.25	0.047	Low
	0.75	0.039	Low
	1.5	0.031	Low
	2.0	0.033	Low
HVFA-70H	Surface	0.17	High
	0.25	0.37	High
	0.75	0.093	Moderate
	1.5	0.034	Low
	2.0	0.030	Negligible
HVFA-70L	Surface	0.14	High
	0.25	0.24	High
	0.75	0.059	Low
	1.5	0.022	Negligible
	2.0	0.012	Negligible
HVFA-70LA	Surface	0.28	High
	0.25	0.21	High
	0.75	0.13	Moderate
	1.5	0.024	Negligible
	2.0	0.017	Negligible

1 in. = 2.54 cm

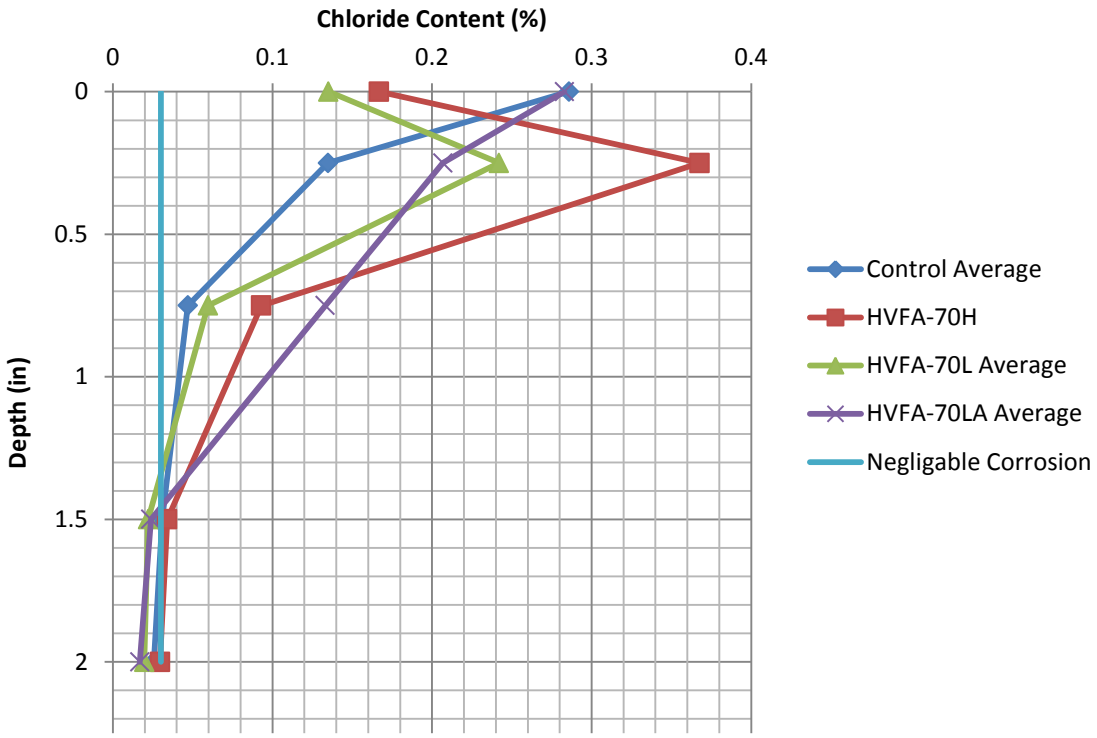

Figure 5.3 – Averaged Chloride Profile for HVFA Mixes

5.8. CONCRETE RESISTIVITY

The concrete resistivity test was a non-ASTM test method. It is, however, an industry standard, and is used quite frequently. The resistivity measurements were measured over a period of 24 weeks. These measurements can be found in Appendix B. The test was performed on three replicate specimens with the results averaged to determine the response of the individual concrete mixes. The averages for each mix were then compared. The individual specimen for the Control, HVFA-70H, HVFA-70L, and HVFA-70LA mixes can be seen in **Figures 5.4**, **5.5**, **5.6**, and **5.7,** respectively.

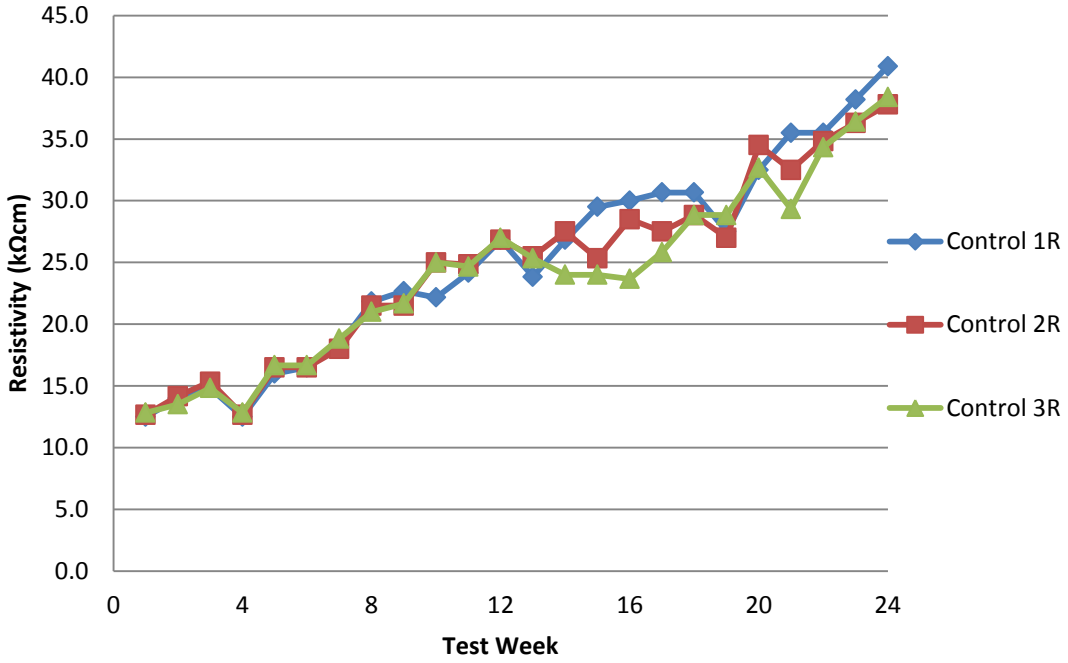

Figure 5.4 – Individual Specimen Results for Concrete Resistivity of Control Mix

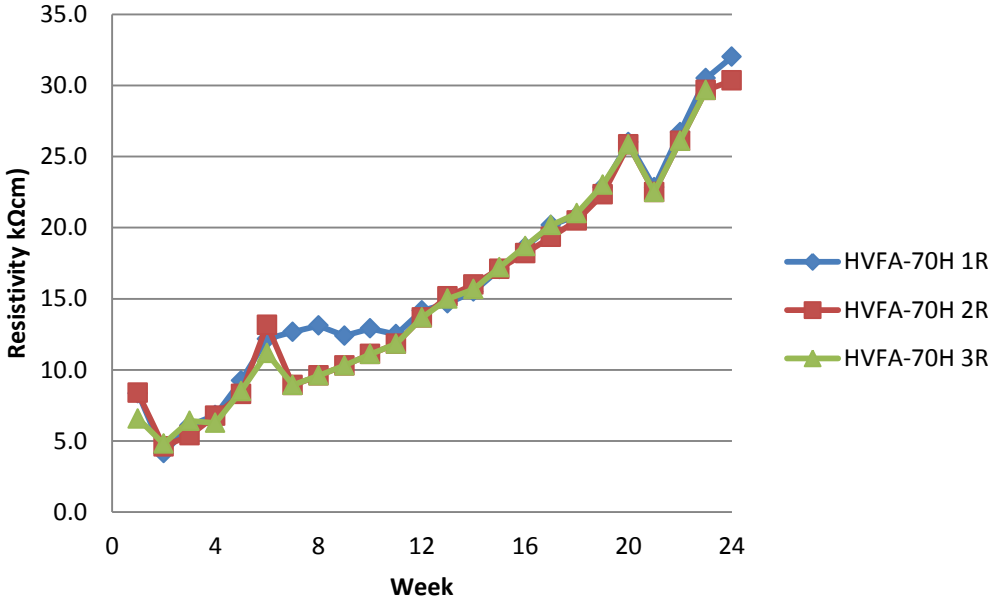

Figure 5.5 – Individual Specimen Results for Concrete Resistivity of HVFA-70H Mix

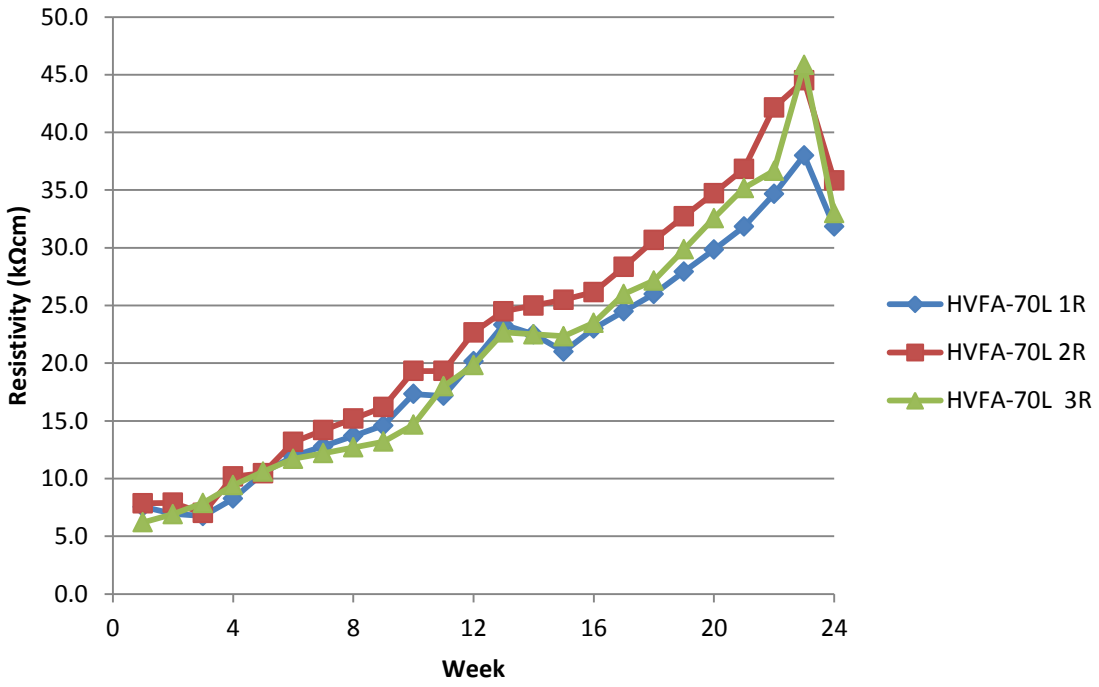

Figure 5.6 – Individual Specimen Results for Concrete Resistivity of HVFA-70H Mix

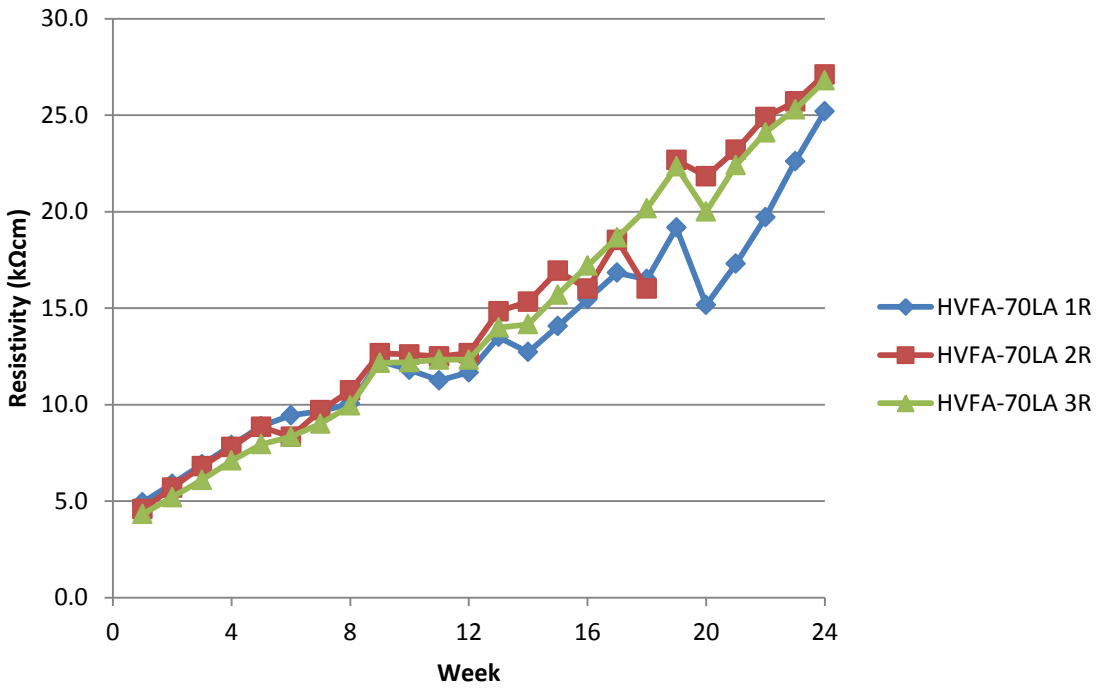

Figure 5.7 – Individual Specimen Results for Concrete Resistivity of HVFA-70LA Mix

The individual results were then averaged and graphed on the same plot for comparison purposes, which are shown in **Figure 5.8**. According to Broomfield, any concrete that has a resistivity greater than 20kΩcm is considered to have low corrosion potential. The final readings were taken at 24 weeks and can be seen in **Table 5.20**.

Table 5.20 Final Resistivity of HVFA Mixes

Mix Design ID	Resistivity (kΩcm)
Control	39.1
HVFA-70H	30.9
HVFA-70L	33.6
HVFA-70LA	26.4

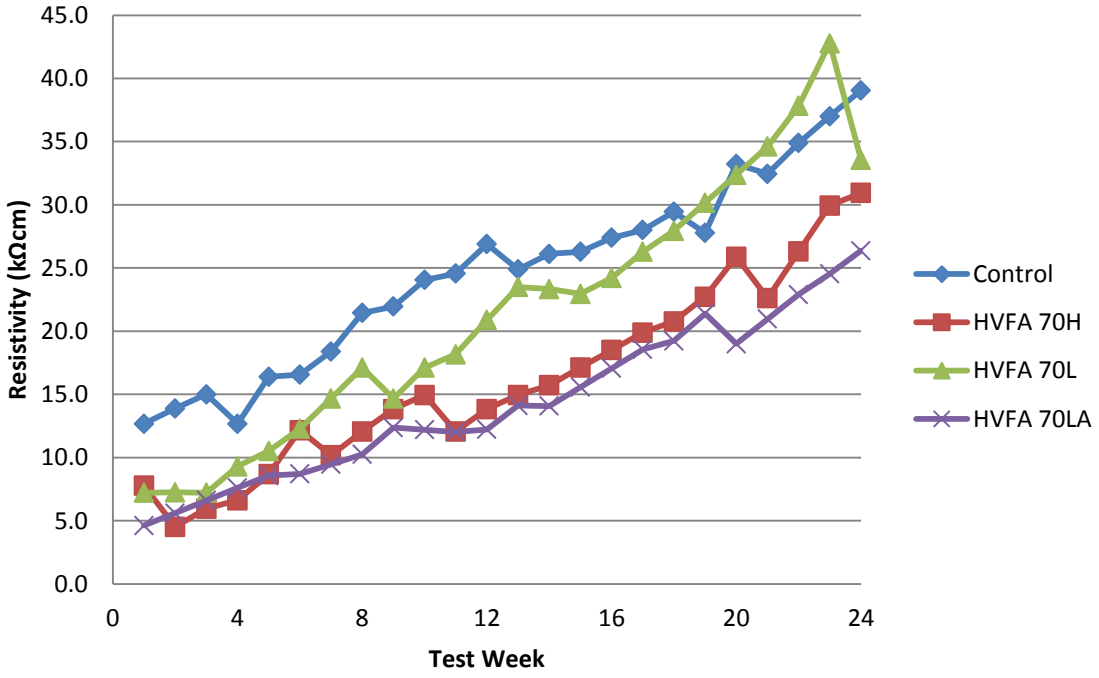

Figure 5.8 – Averaged Resistivity Results for HVFA Mixes

5.9. SCALING

The scaling resistance test was performed in accordance with ASTM C 672-03. After being subjected to 50 freezing and thawing cycles while being ponded with chloride solution, the surface of the specimens were inspected and the appearance assigned a number depending on deterioration. The scale can be seen in **Table 5.21**.

Table 5.21 Scaling Deterioration Classes [MoDOT]

Rating	Condition of Surface
1	No Scaling
2	Very Slight Scaling
3	Slight to Moderate Scaling
4	Moderate Scaling
5	Moderate to Severe Scaling

This scale is determined by ASTM C 672. The deterioration of the surface is evaluated by investigators and is assigned at their discretion. Three specimens were tested for each mix. Each specimen was given a deterioration class and the results of the test were averaged. In the case specimens having different classes, the numbers were averaged and the rounded up to stay conservative. The specimens were subjected to the tests and the results can be seen in **Table 5.22.**

Table 5.22 Averaged Scaling Performance for HVFA Mixes

Batch ID	Condition of Surface
Control	4
HVFA-70H	5
HVFA-70L	5
HVFA-70LA	5

6. EVALUATION OF HIGH-VOLUME FLY ASH CONCRETE

As stated in previous sections, both the Control mix and the HVFA concrete mixes were subjected to the same mechanical property and durability tests. In this way, it was possible to evaluate the performance of the HVFA concrete relative to a benchmark – the conventional mix. If the HVFA concrete mix performed as well or better than the conventional concrete, than it could be reasoned that, due to the positive environmental impact, it would be beneficial to use HVFA concrete in the construction of transportation infrastructure. The results of the mechanical property and durability tests can be found in Chapter 6. An outline of these results can be seen in **Table 6.1**. As stated in previous chapters, the HVFA-70H, HVFA-70L, and HVFA-70LA mix design IDs represent the relatively high total cementitious content HVFA concrete mix, the relatively low total cementitious content HVFA concrete mix, and the relatively low total cementitious content HVFA concrete mix with an air-entraining admixture, respectively. All three HVFA mixes contained a 70 percent replacement of total cementitious material with fly ash.

6.1. MECHANICAL PROPERTIES

For compressive strength, all four mixes were designed to reach 4,000 psi (27.6 MPa) after 28 days. However, only the Control mix reached this goal. All of the mixes containing fly ash showed relatively low early strength gains compared to the Control mix. This behavior is due to the relatively slow pozzolanic reaction typical of fly ash. A statistical t-test was performed on the compressive strength data in order to determine if

there is any statistical difference between the four mixes. The t-test was used to compare each HVFA concrete mix to the Control mix. The P values between the Control mix and the HVFA-70H, HVFA-70L, and HVFA-70LA mixes were 0.0002, 0.001, and 0.002, respectively. Any P value less than 0.05 means the data is statistically different. In other words, the compressive strength of the Control mix exceeded the compressive strength of all the HVFA concrete mixes.

Table 6.1 Outline of Results of HVFA Investigation

	Mix Design ID			
Test ID	Control	HVFA-70H	HVFA-70L	HVFA-70LA
28 Day Compressive Strength (psi)	5,363	3,100	3,480	2,394
Modulus of Elasticity (psi)	3,390,000	3,475,000	3,160,000	3,450,000
Modulus of Rupture (psi)	405	343	433	395
Splitting Tensile (psi)	363	263	303	224
Rapid Freezing – Thawing (durability factor)	21.6	2.1	81.8	68.5
RCT (coulombs)	4,660	874	2,573	879
Ponding (Depth at 0.03% Chloride Content, in.)	1.5	2.0	1.3	1.45
Concrete Resistivity (kΩcm)	39.1	30.9	33.6	26.4
Scaling	4	5	5	5

1 psi = 6.89 kPa
1 in. = 2.54 cm

The modulus of rupture, modulus of elasticity, and splitting-tensile strengths are typically estimated in design using equations based on previous research. These equations were mentioned in Chapter 6. The results of the modulus of rupture, modulus of elasticity, and splitting-tensile strengths were subsequently normalized using the

respective compressive strengths of each mix and the resulting coefficients were then compared to recommended values within ACI standards. A summary of these results can be seen in **Table 6.2**.

Table 6.2 Normalized Mechanical Properties Compared to Respective ACI Coefficients

	Control	HVFA-70H	HVFA-70L	HVFA-70LA	ACI Coefficient
Modulus of Elasticity	46,250	62,420	53,610	70,410	57,000
Modulus of Rupture	5.5	6.2	7.3	8.1	7.5
Splitting-Tensile Strength	4.9	4.7	5.1	4.6	6.7

The Control mix and the HVFA-70L mix fell considerably short of the empirical relationship recommended for modulus of elasticity. This result means that in the design of concrete structures constructed with these concretes, the modulus of elasticity for either mix would be overestimated. This situation can have negative effects on estimating deflection and serviceability of concrete in the field. However, both the HVFA-70H and HVFA-70LA mixes exceeded the empirical relationship. These concrete mixes would likely perform better in the field than estimated. A statistical t-test was performed on the modulus of elasticity coefficient data in order to determine if there is a statistical difference between the four mixes. The t-test was used to compare each HVFA concrete mix to the control. The P values between the Control mix and the HVFA-70H, HVFA-70L, HVFA-70LA mixes were 0.045, 0.41, and 0.048, respectively. Any P value less than 0.05 means the data is statistically different. In other words, the modulus of

elasticity of the Control and all of the HVFA mixes are statistically different. The modulus of elasticity of each specimen was also plotted against compressive strength for comparison with the ACI recommended relationship. Also included in the plot for comparison is data from another HVFA concrete study completed at Missouri S&T. The graph can be seen in **Figure 6.1**.

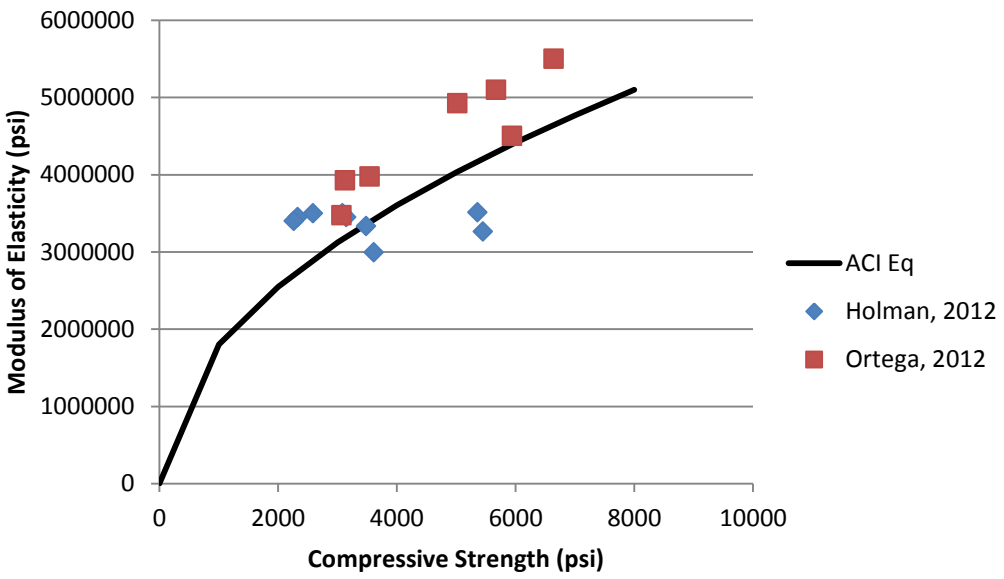

Figure 6.1 - Compressive Strength vs. Modulus of Elasticity

For the modulus of rupture, the Control, HVFA-70H, and HVFA-70L mixes fell below the ACI coefficient of 7.5, although the HVFA-70L was very close (7.3). However, the HVFA-70LA mix exceeded the ACI coefficient of 7.5. It is important to note, however, that the modulus of rupture is highly variable as the coefficient can vary between 6 and 12 [Neville, 1997]. A statistical t-test was performed on the modulus of rupture coefficient data in order to determine if there is a statistical difference between

the four mixes. The t-test was used to compare each HVFA mix to the control. The P value between the Control and the HVFA-70H, HVFA-70L, and HVFA-70LA mixes were 0.18, 0.04, and 0.04, respectively. Any P value greater than 0.05 means the data is statistically equal. In other words, the modulus of rupture of the Control and HVFA-70H are essentially identical. The P values for the HVFA-70L and HVFA-70LA were less than 0.05. This means the data is statistically different. The modulus of rupture for each specimen was plotted against the compressive strength for comparison with the ACI recommended relationship. Also included in the plot for comparison is data from other HVFA concrete studies completed at Missouri S&T. The graph can be seen in **Figure 6.2**.

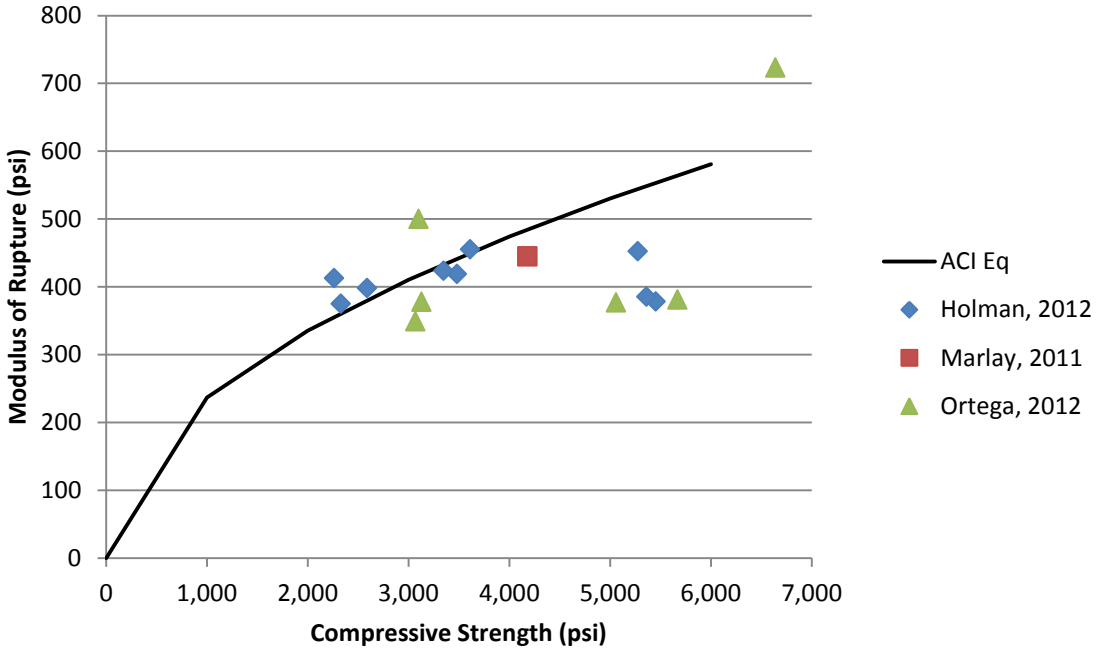

Figure 6.2 – Compressive Strength vs. Modulus of Rupture

For the splitting-tensile strength, all the mixes except for the Control fell below the ACI coefficient used to estimate the splitting-tensile strength. All of the HVFA concrete mixes performed similarly with the calculated coefficients being very close in value. However, splitting-tensile strength is also highly variable with values ranging from 5 to 9.5 [Oluokun, 1991]. A statistical t-test was performed on the splitting-tensile coefficient data in order to determine if there is a statistical difference between the four mixes. The t-test was used to compare each HVFA mix to the control. The P value between the Control and the HVFA-70H, HVFA-70L, and HVFA-70LA mixes were 0.81, 0.48, and 0.74. Any P value greater than 0.05 means the data is statistically equal. In other words, the splitting-tensile strengths of the four mixes are essentially identical. The splitting-tensile strength of the specimens was also plotted against the compressive strength of the concrete. Also included in the plot for comparison is data from other HVFA concrete studies completed at Missouri S&T. The graph can be seen in **Figure 6.3**.

The measured modulus of elasticity and modulus of rupture were also compared to the AASHTO LRFD Design equations used to estimate these mechanical properties. These properties were normalized by dividing the measured values by the respective compressive strength and then compared to the AASHTO equations as mentioned in Chapter 5. A summary of these coefficients can be seen in **Table 6.3**.

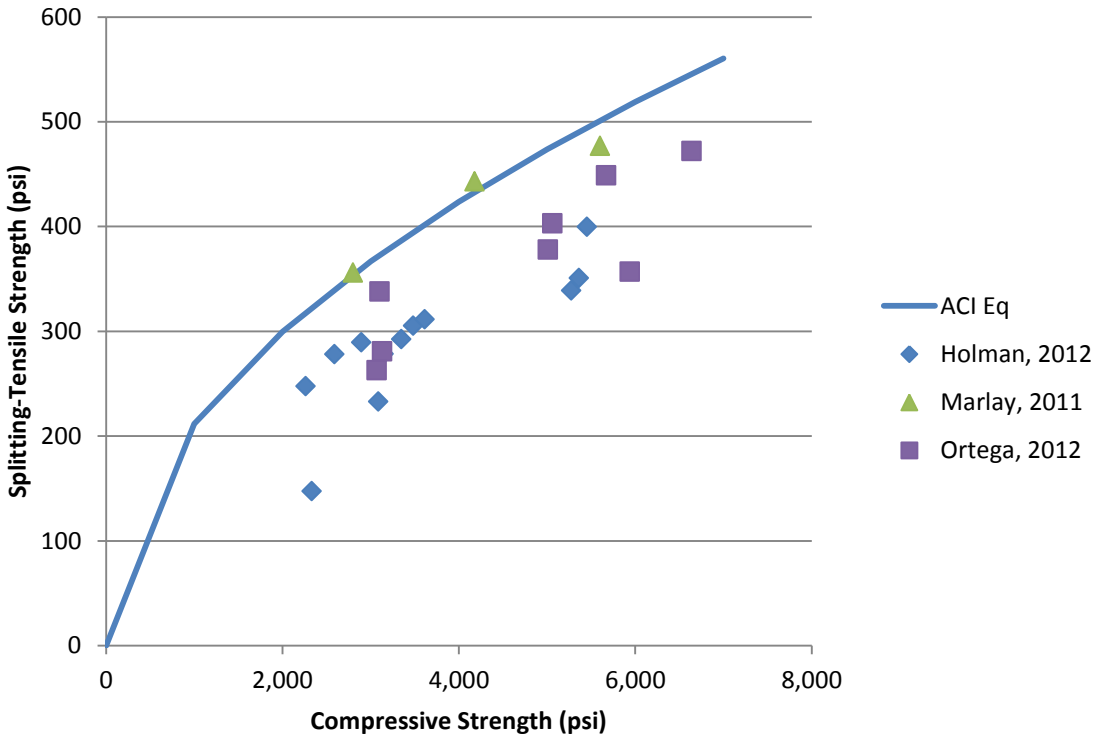

Figure 6.3 – Compressive Strength vs. Splitting-Tensile Strength

Table 6.3 Normalized Mechanical Properties Compared to Respective AASHTO Coefficients

	Control	HVFA-70H	HVFA-70L	HVFA-70LA	AASHTO Coefficient
Modulus of Elasticity	1,463	1,974	1,694	2,232	1,820
Modulus of Rupture	0.17	0.19	0.23	0.40	0.24

These results also followed a very similar trend as the ACI coefficient comparison. For the modulus of elasticity, both the HVFA-70H and HVFA-70LA showed higher coefficients than the AASHTO recommended coefficient. Only the HVFA-70LA showed a higher coefficient than the AASHTO coefficient.

6.2. DURABILITY PERFORMANCE.

For resistance to freeze-thaw most of the mixes performed very poorly when compared to the minimum set forth by MoDOT, including the Control mix. MoDOT specifies a minimum durability factor of 75, which only the HVFA-70L exceeded. The HVFA-70H mix performed extremely poorly, recording a durability factor of 2.1. Both the HVFA-70L and HVFA-70LA mixes showed much higher performance when compared to the Control mix. Consequently, except for the HVFA-70L mix, the poor freeze-thaw performance was probably more a function of the particular limestone coarse aggregate used in the mixes (Jefferson City dolomite).

With regard to permeability, the mixes showed variable results. The Control mix received a high permeability rating while the HVFA mixes all showed very low permeability. However, all of the tests performed on the mixes containing fly ash were forced to stop due to excessive current or voltage build-up after less than an hour. While the total coulombs passed for these mixes indicate a low permeability, these low numbers are due to early termination of the tests. Two tests performed on specimens containing fly ash did reach the specified test duration of 6 hours and these specimens showed an extremely high total charge passed, indicating high permeability. This result further confirms what other researchers have reported; namely that the RCT indicates false results for concrete mixes contain fly ash [Shi, 2002].

The ponding test also indicated unusual performance of the HVFA concrete mixes. The control mix reached a chloride content of 0.03% at approximately 1.5 in. (38 mm) in depth. This chloride content indicates a negligible corrosion risk. The Control mix also showed a typical chloride profile, with the surface containing the highest

chloride content and decreasing as the depth increases. Both HVFA-70H and HVFA-70L mixes did not show this type of behavior. Both mixes revealed relatively low chloride concentrations at the surface and relatively high chloride concentrations at 0.25 in. (6.4 mm) in depth. These results suggest that mixes containing high amounts of fly ash have higher capillary action than conventional concrete. Also the chloride content decreased significantly after 0.25 in. (6.4 mm) in depth, reaching the 0.03% chloride content goal at approximately 1.5 in. (38 mm). This characteristic would suggest that while HVFA concrete may have high capillary action, these mixes have low diffusion. This was not seen in the HVFA-70LA mix, which showed a relatively typical chloride profile. This mix also reached the 0.03% chloride content goal at approximately 1.5 in. (38 mm). The average chloride profile for all the mixes can be seen in **Figure 6.4**.

With regard to concrete resistivity using the Wenner probe, all of the concrete mixes showed adequate performance. According to Broomfield [2007], any concrete indicating resistivity over 20kΩcm is to be classified as having a low rate of corrosion. All the mixes exceeded this value, with the Control mix having the highest resistivity at 39.1 kΩcm after 24 weeks of testing. HVFA-70L showed the seconded highest resistivity at 33.6 kΩcm, performing slightly higher than HVFA-70H at 30.9 kΩcm, both after 24 weeks of testing. It appears that the addition of an air entraining admixture significantly reduces the resistivity of concrete. The HVFA-70LA mix showed the lowest resistivity at 26.4 kΩcm after 24 weeks of testing, although still above the 20kΩcm standard for a low rate of corrosion. All of the mixes also showed an increase in resistivity over time at approximately the same rate of increase. The average results of this test can be seen in **Figure 6.5**.

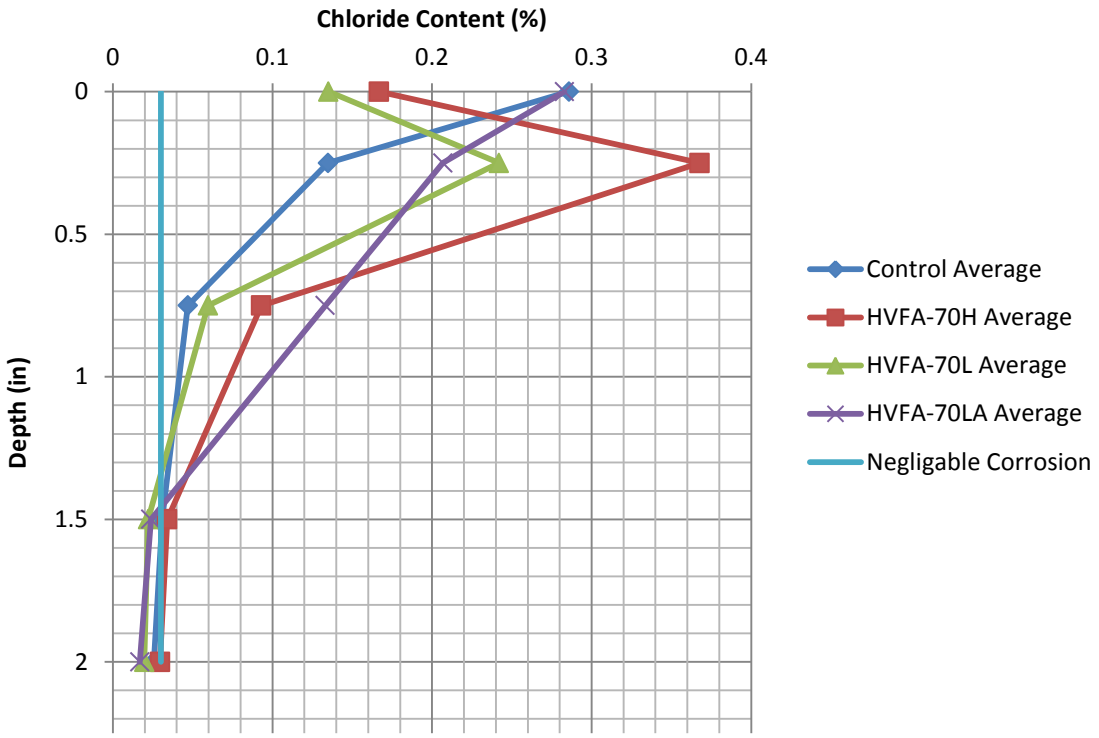

Figure 6.4 – Average Chloride Content vs. Depth of HVFA Mixes
1 in. = 2.54 cm

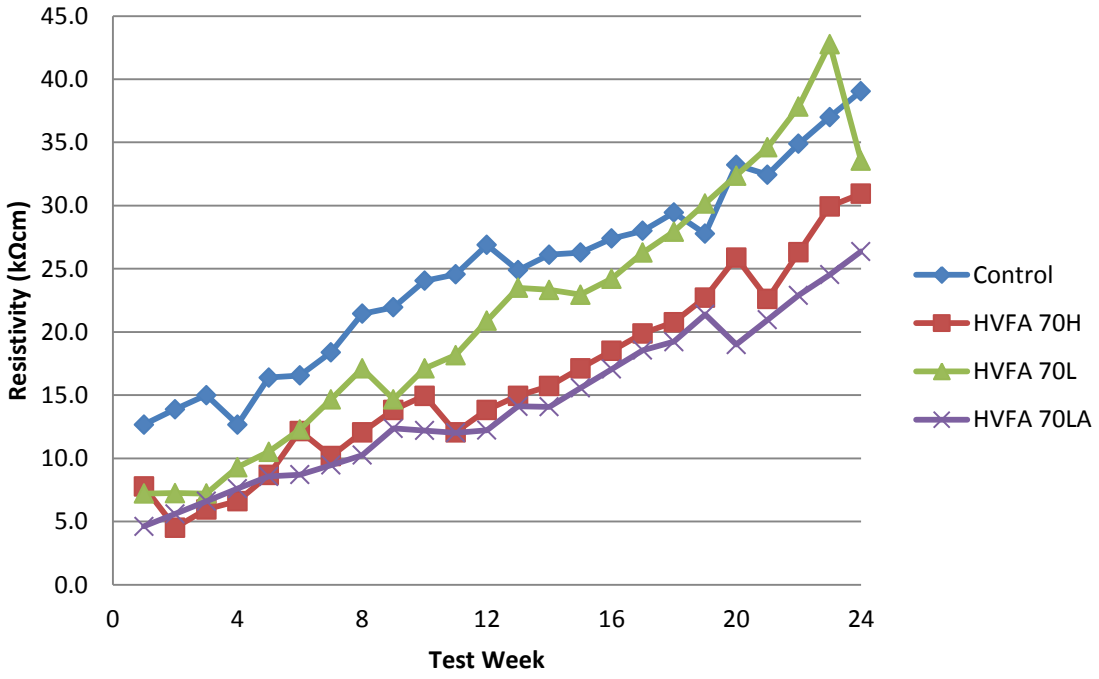

Figure 6.5 – Average Resistivity of HVFA Concrete Mixes

With regard to scaling, all of the HVFA concrete mixes showed very low resistance. All of the mixes containing fly ash reached a rating of 5 within a relatively low number of cycles. This agrees with previous research performed on HVFA concrete, which has consistently shown poor scaling resistance. The Control mix did slightly better, reaching a rating of 4 in deterioration, although the Control completed the 50 cycles of testing while the HVFA concrete mixes did not reach that point in testing due to their rapid rate of deterioration. Many of the scaling panels constructed with HVFA concrete showed deterioration up to 0.25 in. (6.4 mm) in depth. This observation in conjunction with the observations made in the ponding test seems to suggest that HVFA concrete absorbs a high amount of water through capillary action. Two of the three HVFA mixes contained higher chloride concentrations at 0.25 in. (6.4 mm) in depth than at the surface. A highly absorptive concrete would explain both the unusually high chloride concentrations at 0.25 in. (6.4 mm) as well as the severe deterioration of the salt scaling panels.

7. FINDINGS, CONCLUSIONS, AND RECOMMENDATIONS

7.1. FINDINGS AND CONCLUSIONS

The HVFA concretes tested in this investigation showed mixed results relative to the material property and durability testing. All of the concrete mixes containing fly ash showed relatively slow strength gains, including an inability to reach the target strength of 4,000 psi (27.6 MPa) at 28 days. A slow rate of strength gain may be a significant problem in some aspects of construction, although in others, the 28 or 56-day strength is the critical aspect and early age strength is relatively unimportant.

Both the Control and the HVFA-70L mix showed comparable modulus of elasticity. However, both the HVFA-70H and HVFA-70LA showed higher values than the Control mix. When comparing the normalized data, all three HVFA mixes exceeded the Control mix, with only the HVFA-70L mix falling below the recommended ACI coefficient. In regard to the modulus of rupture, only the Control and HVFA-70H mix showed comparable results, with the HVFA-70L and HVFA-70LA mixes performing above the control. In fact, only the HVFA-70L and HVFA-70LA mixes exceeded the recommended ACI coefficient used to estimate the modulus of rupture. In regard to splitting-tensile strength, all three of the HVFA concrete mixes showed comparable results with the Control mix. While all the mixes fell short of the recommended ACI coefficient, all the calculated coefficients for the mixes were comparable; indicating that the HVFA concrete mixes did not suffer any decrease in capacity compared to the conventional concrete.

The mixes containing fly ash all showed variable performance in many of the durability tests. The Control and HVFA-70H showed poor performance for resistance to

freeze-thaw. Both the HVFA-70L and HVFA-70LA significantly exceeded the performance of the Control mix, with the HVFA-70L mix showing slightly better performance than the HVFA-70LA mix. Typically, air entrainment improves a concrete's resistance to freeze-thaw. However, with the higher carbon content of fly ash, the air void system created by air entraining admixtures may be difficult to maintain.

The HVFA concrete mixes all showed poor test results when subjected to the RCT. A majority of the tests performed on the HVFA concrete mixes were terminated before the appropriate time, due to excessive mA or voltage. However, one study has indicated that this test is believed to be invalid for HVFA concrete. The chemical composition of fly ash impacts the test in such a way that excessive mA or voltage can build up during the procedure, forcing the test to be terminated. All of the HVFA mixes showed better performance than the Control mix in the ponding test. All of the concrete mixes containing fly ash reached a chloride content of 0.03% at approximately 1.5 in. (38 mm) in depth, while the Control mix reached a chloride concentration of 0.03% at approximately 2.0 in. (51 mm). However, both the HVFA-70H and HVFA-70L mixes showed very unique chloride content profiles. Both mixes showed lower chloride concentrations at the surface and higher chloride concentrations at 0.25 in. (6 mm) in depth. This observation could indicate that concrete mixes containing high amounts of fly ash have an unusually high amount of capillary action but diffusion characteristics consistent with conventional concrete. HVFA-70LA showed a more typical chloride content profile when compared to the Control mix.

All of the mixes in this investigation showed excellent performance in the aspect of concrete resistivity performance. The Control mix showed the highest resistivity after

24 weeks of testing, measuring 39.1 kΩcm. The HVFA-70H and HVFA-70L mixes both performed similarly, measuring 30.9 kΩcm and 33.6 kΩcm, respectively. The HVFA-70LA performed the lowest, measuring 26.4 kΩcm at 24 weeks, yet still measuring a resistivity higher than that needed to be classified as low rate of corrosion. All of the HVFA concrete mixes showed very poor performance in scaling resistance. All three mixes reached the lowest rating of 5 very early in the testing cycles. This result indicates extremely low durability when exposed to deicing salts in freezing weather.

7.2. RECOMMENDATIONS

After thorough mechanical property and durability testing, it is recommended that HVFA concrete should only be used in applications that are not exposed to salt scaling, such as bridge decks. However, except for the aspect of rate of compressive strength gain, HVFA concrete was comparable in all other aspects of hardened properties tested in this investigation. Unfortunately, HVFA concrete showed very inadequate performance with regard to scaling and inconsistent performance involving chloride penetration. The areas in which HVFA concrete showed adequate durability performance was resistance to freeze-thaw deterioration and concrete resistivity. For freeze-thaw, both the HVFA-70L and HVFA-70LA mixes showed higher performance than the Control mix. The HVFA-70H mix showed extremely low performance, with the specimens falling apart before the end of the test duration. While all of the HVFA mixes measured resistivity lower than the Control mix, all the HVFA mixes performed higher than the level indicating low corrosion risk. While the HVFA mixes showed similar chloride profiles, the observation of higher chloride content at 0.25 in. (6 mm) may suggest that the mechanism of capillary

action and diffusion within HVFA concrete is variable and should be investigated further. It is recommended that HVFA concrete be used in applications where high early strengths are not necessary and the concrete elements are not exposed to any environmental conditions that may cause salt scaling. Alternatively, lower levels of cement replacement with fly ash – up to 50% – are recommended for the majority of applications involving transportation-related infrastructure.

APPENDIX

HVFA DURABILITY TEST RESULTS DATA

Table A.1 Control-R1 (Weeks 1-7)

Date	7/19/2011	7/26/2011	8/2/2011	8/9/2011	8/16/2011	8/23/2011	8/30/2011
A1	13	14	16	13	17	17	20
A2	12	13	13	12	15	15	17
A3	14	15	16	14	17	18	20
B1	13	15	15	13	16	17	18
B2	11	13	14	11	15	15	16
B3	12	14	15	12	16	17	19
Average	12.5	14.0	14.8	12.5	16.0	16.5	18.3

Table A.2 Control-R1 (Weeks 8-14)

Date	9/6/2011	9/13/2011	9/20/2011	9/27/2011	10/4/2011	10/11/2011	10/18/2011
A1	23	24	19	25	27	27	27
A2	20	20	20	21	23	21	24
A3	24	25	26	26	30	22	29
B1	24	24	25	25	30	23	28
B2	19	21	19	23	24	23	24
B3	21	22	24	25	27	27	29
Average	21.8	22.7	22.2	24.2	26.8	23.8	26.8

Table A.3 Control-R1 (Weeks 15-21)

Date	10/25/2011	11/1/2011	11/8/2011	11/15/2011	11/22/2011	11/29/2011	12/6/2011
A1	32	32	32	33	32	35	36
A2	26	26	30	29	22	25	31
A3	30	33	34	34	26	38	41
B1	33	32	32	34	33	36	38
B2	26	26	26	27	24	31	30
B3	30	31	30	27	28	30	37
Average	29.5	30.0	30.7	30.7	27.5	32.5	35.5

Table A.4 Control-R1 (Weeks 22-24)

Date	12/16/2011	12/16/2011	12/16/2011
A1	34	36	39
A2	30	33	36
A3	41	44	45
B1	40	42	44
B2	33	36	38
B3	35	38	43
Average	35.5	38.2	40.9

Table A.5 Control-R2 (Weeks 1-7)

Date	7/19/2011	7/26/2011	8/2/2011	8/9/2011	8/16/2011	8/23/2011	8/30/2011
A1	13	14	16	13	17	17	18
A2	11	13	14	11	15	15	17
A3	14	16	17	14	19	18	20
B1	14	16	16	14	17	17	19
B2	11	12	13	11	14	15	16
B3	13	14	16	13	17	17	18
Average	12.7	14.2	15.3	12.7	16.5	16.5	18.0

Table A.6 Control-R2 (Weeks 8-14)

Date	9/6/2011	9/13/2011	9/20/2011	9/27/2011	10/4/2011	10/11/2011	10/18/2011
A1	21	22	25	25	28	26	30
A2	19	19	22	22	23	23	24
A3	24	24	28	26	30	27	30
B1	23	24	26	27	28	28	30
B2	21	19	23	22	28	23	24
B3	21	21	26	27	24	26	27
Average	21.5	21.5	25.0	24.8	26.8	25.5	27.5

Table A.7 Control-R2 (Weeks 15-21)

Date	10/25/2011	11/1/2011	11/8/2011	11/15/2011	11/22/2011	11/29/2011	12/6/2011
A1	27	26	26	28	36	32	35
A2	20	27	25	24	25	27	28
A3	27	35	30	35	28	41	34
B1	31	30	28	34	28	37	36
B2	22	25	24	23	20	28	28
B3	25	28	32	29	25	42	34
Average	25.3	28.5	27.5	28.8	27.0	34.5	32.5

Table A.8 Control-2R (Weeks 22-24)

Date	12/16/2011	12/16/2011	12/16/2011
A1	38	39	41
A2	30	33	34
A3	42	43	44
B1	36	38	39
B2	27	29	31
B3	36	36	38
Average	34.8	36.3	37.8

Table A.9 Control-3R (Weeks 1-7)

Date	7/19/2011	7/26/2011	8/2/2011	8/9/2011	8/16/2011	8/23/2011	8/30/2011
A1	15	15	17	15	17	19	20
A2	12	13	14	12	15	16	18
A3	12	13	15	12	18	17	18
B1	14	14	15	14	18	18	21
B2	11	11	13	11	15	15	18
B3	13	15	15	13	17	15	18
Average	12.8	13.5	14.8	12.8	16.7	16.7	18.8

Table A.10 Control-3R (Weeks 8-14)

Date	9/6/2011	9/13/2011	9/20/2011	9/27/2011	10/4/2011	10/11/2011	10/18/2011
A1	23	24	29	26	28	24	24
A2	21	20	22	23	24	25	19
A3	22	21	25	24	26	22	25
B1	21	25	27	28	30	29	31
B2	20	19	22	23	27	29	24
B3	19	21	25	24	27	23	21
Average	21.0	21.7	25.0	24.7	27.0	25.3	24.0

Table A.11 Control-3R (Weeks 15-21)

Date	10/25/2011	11/1/2011	11/8/2011	11/15/2011	11/22/2011	11/29/2011	12/6/2011
A1	24	25	25	29	35	38	28
A2	20	21	23	23	26	27	21
A3	28	23	34	33	36	37	33
B1	24	27	26	33	30	39	36
B2	20	20	24	31	23	26	28
B3	28	26	23	24	23	29	30
Average	24.0	23.7	25.8	28.8	28.8	32.7	29.3

Table A.12 Control-3R (Weeks 22-24)

Date	12/16/2011	12/16/2011	12/16/2011
A1	36	37	39
A2	26	28	29
A3	35	36	37
B1	46	48	49
B2	32	35	36
B3	31	34	40
Average	34.3	36.4	38.4

Table A.13 HVFA-70H-1R (Weeks 1-7)

Date	10/31/2011	11/7/2011	11/14/2011	11/21/2011	11/28/2011	12/5/2011	12/12/2011
A1	9.4	5.1	7.1	7.1	10	13	14
A2	7.8	3.8	5.4	6.2	9.0	12	12
A3	7.9	4.3	5.0	6.5	8.7	10	11
B1	7.8	3.3	6.6	7.0	11	13	16
B2	7.8	4.3	5.8	7.1	8.0	12	11
B3	9.4	4.0	6.6	7.0	8.7	13	12
Average	8.4	4.1	6.1	6.8	9.2	12.2	12.7

Table A.14 HVFA-70H-1R (Weeks 8-14)

Date	12/19/2011	12/26/2011	1/2/2012	1/9/2012	1/16/2012	1/23/2012	1/30/2012
A1	14	13	13	12	15	16	18
A2	13	12	13	12	13	14	15
A3	12	11	12	12	14	14	14
B1	15	14	13	14	16	15	16
B2	12	10	11	11	12	12	14
B3	13	14	15	14	15	17	16
Average	13.1	12.4	12.9	12.5	14.2	14.7	15.5

Table A.15 HVFA-70H-1R (Weeks 15-21)

Date	2/6/2012	2/13/2012	2/20/2012	2/27/2012	3/5/2012	3/12/2012	3/19/2012
A1	19	21	22	24	24	26	25
A2	16	17	19	21	22	25	21
A3	17	18	19	19	22	27	21
B1	16	19	22	21	23	27	25
B2	15	16	16	17	20	23	19
B3	20	21	23	23	26	28	26
Average	17.1	18.6	20.2	20.8	22.8	26.0	22.8

Table A.16 HVFA-70H-1R (Weeks 22-24)

Date	3/26/2012	4/2/2012	4/9/2012
A1	32	35	33
A2	26	29	31
A3	27	30	30
B1	28	31	33
B2	22	25	28
B3	25	33	37
Average	26.7	30.5	32.0

Table A.17 HVFA-70H-2R (Weeks 1-7)

Date	10/31/2011	11/7/2011	11/14/2011	11/21/2011	11/28/2011	12/5/2011	12/12/2011
A1	7.3	4.7	5.7	7.1	7.9	12	8.1
A2	7.6	4.8	4.8	6	6.2	11	7.4
A3	9.3	4.9	6.1	7.2	9.5	13	9.8
B1	8.5	4.9	6	7	10	14	10
B2	7.6	4.2	4.3	6.4	7.6	13	9
B3	10	4.2	5.4	6.9	8.6	16	9.2
Average	8.4	4.6	5.4	6.8	8.3	13.2	8.9

Table A.18 HVFA-70H-2R (Weeks 8-14)

Date	12/19/2011	12/26/2011	1/2/2012	1/9/2012	1/16/2012	1/23/2012	1/30/2012
A1	9.3	11	12	11	12	15	16
A2	8.1	9.7	10	10	12	13	14
A3	10	12	13	13	14	16	17
B1	11	11	11	12	14	18	19
B2	9.3	10	10	11	13	14	15
B3	9.9	8	11	14	17	15	15
Average	9.6	10.3	11.1	11.8	13.7	15.2	16.0

Table A.19 HVFA-70H-2R (Weeks 15-21)

Date	2/6/2012	2/13/2012	2/20/2012	2/27/2012	3/5/2012	3/12/2012	3/19/2012
A1	17	18	18	20	23	26	23
A2	14	15	17	18	20	20	20
A3	18	19	20	21	21	26	22
B1	21	22	21	23	23	29	24
B2	15	16	19	19	22	25	22
B3	18	19	21	22	25	29	24
Average	17.1	18.2	19.3	20.5	22.3	25.8	22.5

Table A.20 HVFA-70H-2R (Weeks 22-24)

Date	3/26/2012	4/2/2012	4/9/2012
A1	29	31	31
A2	21	23	24
A3	26	30	30
B1	29	31	31
B2	23	26	29
B3	29	37	37
Average	26.1	29.7	30.3

Table A.21 HVFA-70H-3R (Weeks 1-7)

Date	10/31/2011	11/7/2011	11/14/2011	11/21/2011	11/28/2011	12/5/2011	12/12/2011
A1	7.4	4.8	6.4	6.4	8.6	12	9.7
A2	5.7	3.8	6.2	5.2	7.4	10	9.0
A3	6.6	4.2	6	6	9.1	12	7.0
B1	6.6	6.6	6	6.5	8.4	11	9.4
B2	6.5	5	6.2	6.4	8.4	10	8.7
B3	6.6	4.4	7.7	7.1	9.1	12	9.8
Average	6.6	4.8	6.4	6.3	8.5	11.2	8.9

Table A.22 HVFA-70H-3R (Weeks 8-14)

Date	12/19/2011	12/26/2011	1/2/2012	1/9/2012	1/16/2012	1/23/2012	1/30/2012
A1	11	12	12	13	14	15	16
A2	9.6	10	11	11	12	14	15
A3	8.1	9.4	10	11	14	16	16
B1	11	12	12	11	14	15	16
B2	9.5	9.8	10	12	13	14	15
B3	8.4	8.6	12	13	15	16	16
Average	9.6	10.3	11.1	11.8	13.7	15.0	15.7

Table A.23 HVFA-70H-3R (Weeks 15-21)

Date	2/6/2012	2/13/2012	2/20/2012	2/27/2012	3/5/2012	3/12/2012	3/19/2012
A1	18	19	21	21	22	25	23
A2	16	18	18	20	21	24	20
A3	16	17	20	21	24	28	27
B1	17	18	20	21	24	26	22
B2	17	18	19	20	22	24	21
B3	19	22	23	23	25	28	22
Average	17.2	18.7	20.2	21.0	23.0	25.8	22.5

Table A.24 HVFA-70H-3R (Weeks 22-24)

Date	3/26/2012	4/2/2012	4/9/2012
A1	26	29	29
A2	25	28	29
A3	29	32	31
B1	28	29	31
B2	26	27	30
B3	23	33	33
Average	26.1	29.7	30.5

Table A.25 HVFA-70L-1R (Weeks 1-7)

Date	11/11/2011	11/18/2011	11/25/2011	12/2/2011	12/9/2011	12/16/2011	12/23/2011
A1	8.7	6.9	7.5	9.8	11	10	11
A2	7.5	5.7	6.4	6.9	9.7	8.6	9.7
A3	7.6	8.5	6.6	8.4	9.5	12	12
B1	8.4	8.1	5.9	9.6	12	13	13
B2	7	6.7	6.6	5.8	9.8	11	12
B3	6.1	5.8	7.5	9.1	11	17	19
Average	7.6	7.0	6.8	8.3	10.5	11.9	12.8

Table A.26 HVFA-70L-1R (Weeks 8-14)

Date	12/30/2011	1/13/2012	1/20/2012	1/27/2012	2/3/2012	2/10/2012	2/17/2012
A1	12	13	17	18	20	22	21
A2	10	11	14	16	19	19	20
A3	13	14	19	18	22	26	24
B1	14	15	18	19	23	28	27
B2	13	15	13	14	18	21	21
B3	20	20	23	18	19	24	22
Average	13.7	14.6	17.3	17.2	20.2	23.3	22.5

Table A.27 HVFA-70L-1R (Weeks 15-21)

Date	2/24/2012	3/2/2012	3/9/2012	3/16/2012	3/23/2012	3/30/2012	4/6/2012
A1	20	23	26	26	27	29	31
A2	19	19	23	23	25	27	26
A3	22	24	24	25	26	29	33
B1	22	26	26	30	32	32	34
B2	19	21	22	23	25	27	28
B3	24	25	26	29	32	35	39
Average	21.0	23.0	24.5	26.0	27.9	29.8	31.8

Table A.28 HVFA-70L-1R (Weeks 22-24)

Date	4/13/2012	4/20/2012	4/27/2012
A1	34	35	31
A2	32	36	28
A3	35	38	31
B1	36	40	34
B2	30	35	32
B3	41	44	35
Average	34.7	38.0	31.8

Table A.29 HVFA-70L-2R (Weeks 1-7)

Date	11/11/2011	11/18/2011	11/25/2011	12/2/2011	12/9/2011	12/16/2011	12/23/2011
A1	8.1	7.7	7.3	11	11	16	15
A2	7.1	7.2	5.6	9.5	7	12	13
A3	7.9	8.5	9	11	13	12	12
B1	7.1	8.5	6.4	9.6	11	13	14
B2	7	6.2	6	9	8.8	12	13
B3	10	9.3	7.8	11	12	14	18
Average	7.9	7.9	7.0	10.2	10.5	13.2	14.2

Table A.30 HVFA-70L-2R (Weeks 8-14)

Date	12/30/2011	1/13/2012	1/20/2012	1/27/2012	2/3/2012	2/10/2012	2/17/2012
A1	16	17	25	19	22	27	26
A2	13	14	24	17	21	23	24
A3	14	15	26	21	24	26	27
B1	16	17	24	20	23	24	25
B2	15	16	23	19	21	21	22
B3	17	18	23	20	25	26	26
Average	15.2	16.2	24.2	19.3	22.7	24.5	25.0

Table A.31 HVFA-70L-2R (Weeks 15-21)

Date	2/24/2012	3/2/2012	3/9/2012	3/16/2012	3/23/2012	3/30/2012	4/6/2012
A1	27	26	26	31	32	34	39
A2	24	25	25	29	31	32	34
A3	26	27	30	32	33	34	39
B1	25	26	30	30	32	33	37
B2	24	25	26	28	30	32	32
B3	27	28	33	34	37	43	40
Average	25.5	26.2	28.3	30.7	32.7	34.7	36.8

Table A.32 HVFA-70L-2R (Weeks 22-24)

Date	4/13/2012	4/20/2012	4/27/2012
A1	44	46	35
A2	40	38	35
A3	42	47	35
B1	41	43	35
B2	40	41	35
B3	46	52	40
Average	42.2	44.5	35.8

Table A.33 HVFA-70L-3R (Weeks 1-7)

Date	11/11/2011	11/18/2011	11/25/2011	12/2/2011	12/9/2011	12/16/2011	12/23/2011
A1	6.6	7.2	8.7	9.8	11	12	13
A2	5.3	6	6.6	7.2	9.2	10	11
A3	7.1	8.2	7.9	11	11	13	14
B1	5.9	6.1	8.7	8.8	9.7	9.3	10
B2	5.4	5.4	7.2	8.8	8.7	10	11
B3	7	8.6	8.2	11	14	16	14
Average	6.2	6.9	7.9	9.4	10.6	11.7	12.2

Table A.34 HVFA-70L-3R (Weeks 8-14)

Date	12/30/2011	1/13/2012	1/20/2012	1/27/2012	2/3/2012	2/10/2012	2/17/2012
A1	13	14	13	18	20	24	23
A2	12	12	11	14	16	20	20
A3	14	13	13	19	22	23	23
B1	10	14	10	21	20	22	22
B2	12	13	14	16	17	20	19
B3	15	13	27	20	24	27	28
Average	12.7	13.2	14.7	18.0	19.8	22.7	22.5

Table A.35 HVFA-70L-3R (Weeks 15-21)

Date	2/24/2012	3/2/2012	3/9/2012	3/16/2012	3/23/2012	3/30/2012	4/6/2012
A1	20	24	25	28	31	35	34
A2	19	20	24	24	26	31	29
A3	23	24	27	28	30	33	37
B1	22	22	25	26	29	32	32
B2	21	22	23	23	27	31	32
B3	29	29	32	34	36	34	47
Average	22.3	23.5	26.0	27.2	29.9	32.6	35.2

Table A.36 HVFA-70L-3R (Weeks 22-24)

Date	4/13/2012	4/20/2012	4/27/2012
A1	39	45	33
A2	34	39	29
A3	41	50	33
B1	33	40	28
B2	33	41	34
B3	40	60	41
Average	36.7	45.8	33.0

Table A.37 HVFA-70LA-1R (Weeks 1-7)

Date	12/16/2011	12/23/2011	12/30/2011	1/6/2012	1/13/2012	1/20/2012	1/27/2012
A1	5.2	6.2	7.2	8.2	9.2	11	9.4
A2	3.2	4.2	5.2	6.2	8.1	7.1	8.6
A3	5.3	6.3	7.3	8.3	10	9.8	10
B1	5.9	6.9	7.9	8.9	9.2	11	11
B2	4.6	5.6	6.6	7.6	7.6	8.6	9
B3	5.4	6.4	7.4	8.4	9.2	9.2	10
Average	4.9	5.9	6.9	7.9	8.9	9.5	9.7

Table A.38 HVFA-70LA-1R (Weeks 8-14)

Date	2/3/2012	2/10/2012	2/17/2012	2/24/2012	3/2/2012	3/9/2012	3/16/2012
A1	10	12	11	11	13	14	14
A2	7.7	9.6	8.7	8.9	8.6	14	9.3
A3	11	13	12	13	13	14	13
B1	12	14	13	11	14	14	14
B2	8.6	11	11	9.6	9.4	12	11
B3	11	14	15	14	12	13	15
Average	10.1	12.3	11.8	11.3	11.7	13.5	12.7

Table A.39 HVFA-70LA-1R (Weeks 15-21)

Date	3/23/2012	3/30/2012	4/6/2012	4/13/2012	4/20/2012	4/27/2012	5/4/2012
A1	15	18	19	19	22	16	18
A2	13	14	12	13	16	12	14
A3	14	14	17	18	21	16	18
B1	15	16	20	20	22	18	20
B2	13	15	14	13	15	13	15
B3	15	16	19	16	19	16	18
Average	14.1	15.5	16.8	16.5	19.2	15.2	17.3

Table A.40 HVFA-70LA-1R (Weeks 22-24)

Date	5/11/2012	5/18/2012	5/25/2012
A1	20	23	26
A2	16	19	24
A3	21	24	26
B1	22	25	27
B2	17	20	23
B3	22	25	25
Average	19.7	22.6	25.2

Table A.41 HVFA-70LA-2R (Weeks 1-7)

Date	12/16/2011	12/23/2011	12/30/2011	1/6/2012	1/13/2012	1/20/2012	1/27/2012
A1	4.8	5.8	6.8	7.8	8.1	8.2	10
A2	3.7	4.7	5.7	6.7	8.4	7.5	9.3
A3	4.7	5.7	6.7	7.7	9.3	8.2	10
B1	5.3	6.3	7.3	8.3	11	9.2	12
B2	3.6	4.6	5.6	6.6	8.3	7.4	5.9
B3	5.4	6.4	7.4	8.4	8	9.5	11
Average	4.6	5.7	6.8	7.8	8.9	8.3	9.7

Table A.42 HVFA-70LA-2R (Weeks 8-14)

Date	2/3/2012	2/10/2012	2/17/2012	2/24/2012	3/2/2012	3/9/2012	3/16/2012
A1	12	13	13	13	13	19	16
A2	9.2	11	11	11	11	12	13
A3	10	13	13	12	13	15	16
B1	13	14	14	14	14	16	18
B2	9.2	11	11	11	12	12	13
B3	11	14	14	14	13	15	16
Average	10.7	12.7	12.6	12.5	12.7	14.8	15.3

Table A.43 HVFA-70LA-2R (Weeks 15-21)

Date	3/23/2012	3/30/2012	4/6/2012	4/13/2012	4/20/2012	4/27/2012	5/4/2012
A1	18	20	21	21	24	26	28
A2	15	17	17	18	20	19	21
A3	17	19	20	21	22	22	25
B1	19	21	23	24	26	22	24
B2	15	17	18	18	21	19	21
B3	17	17	22	24	23	23	25
Average	16.9	18.5	20.2	21.0	22.7	21.8	23.2

Table A.44 HVFA-70LA-2R (Weeks 22-24)

Date	12/30/2011	1/6/2012	1/13/2012
A1	30	31	33
A2	22	23	25
A3	26	27	29
B1	25	26	28
B2	24	25	27
B3	22	23	20
Average	24.9	25.7	27.1

Table A.45 HVFA-70LA-3R (Weeks 1-7)

Date	12/16/2011	12/23/2011	12/30/2011	1/6/2012	1/13/2012	1/20/2012	1/27/2012
A1	4.4	5.7	6.6	7.6	8.8	8.1	9.3
A2	4	4.4	5.4	6.4	6.8	8.1	7.6
A3	5.2	5.5	6.6	7.5	7.9	10	9.5
B1	4.7	6.3	7.1	8.1	9.2	9.2	11
B2	3.4	4.5	5.5	6.3	6.7	6.4	7.6
B3	4.3	6.1	7.3	8.4	8.3	8.2	9.1
Average	4.3	5.2	6.1	7.1	8.0	8.3	9.0

Table A.46 HVFA-70LA-3R (Weeks 8-14)

Date	2/3/2012	2/10/2012	2/17/2012	2/24/2012	3/2/2012	3/9/2012	3/16/2012
A1	10	13	13	13	12	14	13
A2	9.4	12	12	11	12	13	13
A3	12	12	12	13	13	14	16
B1	11	15	15	14	14	16	17
B2	7.3	10	10	11	11	14	13
B3	10	11	11	12	12	13	13
Average	10.0	12.2	12.2	12.3	12.3	14.0	14.2

Table A.47 HVFA-70LA-3R (Weeks 15-21)

Date	3/23/2012	3/30/2012	4/6/2012	4/13/2012	4/20/2012	4/27/2012	5/4/2012
A1	15	18	17	18	20	19	21
A2	14	16	18	20	21	18	20
A3	18	20	20	22	24	21	23
B1	19	21	22	23	27	24	26
B2	14	15	17	19	22	17	19
B3	14	13	18	19	20	21	23
Average	15.7	17.2	18.7	20.2	22.3	20.0	22.4

Table A.48 HVFA-70LA-3R (Weeks 22-24)

Date	12/30/2011	1/6/2012	1/13/2012
A1	23	24	25
A2	22	23	24
A3	25	26	27
B1	28	29	30
B2	21	22	23
B3	25	26	32
Average	24.1	25.3	26.8

PROOVE it

ASTM C 1202-97

ST CO.

Test-compagny
Testing street 45
CompagnyCity
Some Country

Test report

Voltage Used:	60
Testing time:	06:00 hour
Charge passed:	5473
Adjusted Charge passed:	4939
Permeability class:	High
Instrument number:	071401
Channel number:	1
Report date:	7/12/2011
Testing by:	TP-SJ
Reference:	B1-EC1 TOP
Sample diameter:	100
Comment:	28 DAY

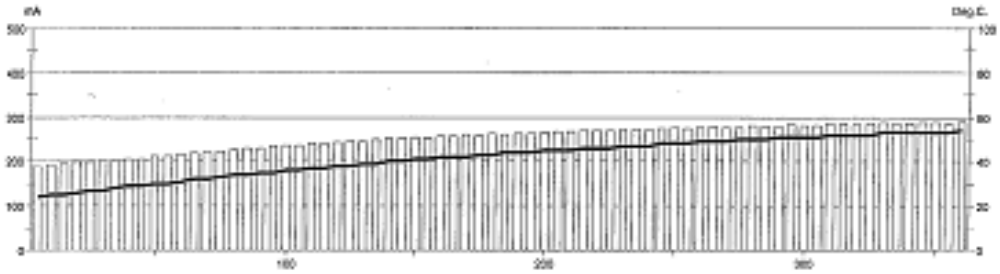

Time	°C	mA	Time	°C	mA	Time	°C	mA	Time	°C	mA
00:05	24	188.8	01:35	35	234.0	03:05	44	261.2	04:35	50	277.7
00:10	25	193.0	01:40	36	236.0	03:10	44	264.3	04:40	50	280.8
00:15	25	194.3	01:45	36	236.8	03:15	44	264.0	04:45	50	279.7
00:20	26	199.0	01:50	37	241.4	03:20	45	264.7	04:50	51	279.0
00:25	27	198.4	01:55	37	240.7	03:25	45	268.1	04:55	51	283.3
00:30	27	201.6	02:00	38	242.2	03:30	45	266.8	05:00	51	282.2
00:35	28	200.5	02:05	38	245.9	03:35	46	269.4	05:05	51	281.1
00:40	29	205.4	02:10	39	245.3	03:40	46	270.3	05:10	52	284.6
00:45	29	205.7	02:15	39	249.0	03:45	46	269.5	05:15	52	284.8
00:50	30	211.1	02:20	40	251.7	03:50	47	272.6	05:20	52	284.0
00:55	30	211.8	02:25	40	252.5	03:55	47	273.0	05:25	52	285.3
01:00	31	217.1	02:30	41	254.4	04:00	47	272.2	05:30	53	287.2
01:05	32	218.1	02:35	41	253.3	04:05	48	275.2	05:35	53	286.4
01:10	32	221.4	02:40	42	257.3	04:10	48	275.7	05:40	53	286.1
01:15	33	224.0	02:45	42	257.4	04:15	48	274.5	05:45	53	288.0
01:20	34	225.2	02:50	42	260.4	04:20	49	276.8	05:50	53	288.9
01:25	34	230.2	02:55	43	258.9	04:25	49	278.3	05:55	53	284.5
01:30	35	230.1	03:00	43	263.1	04:30	49	277.1	06:00	54	289.7

Figure A.1 – Control-EC1TOP RCT Data

PROOVE it

ASTM C 1202-97

TEST CO.

Test-compagny
Testing street 45
CompagnyCity
Some Country

Test report

Voltage Used:	60
Testing time:	06:00 hour
Charge passed:	5163
Adjusted Charge passed:	4650
Permeability class:	High
Instrument number:	071401
Channel number:	2
Report date:	7/12/2011
Testing by:	TP-SJ
Reference:	B1-EC1 MIDDLE
Sample diameter:	100
Comment:	28 DAY

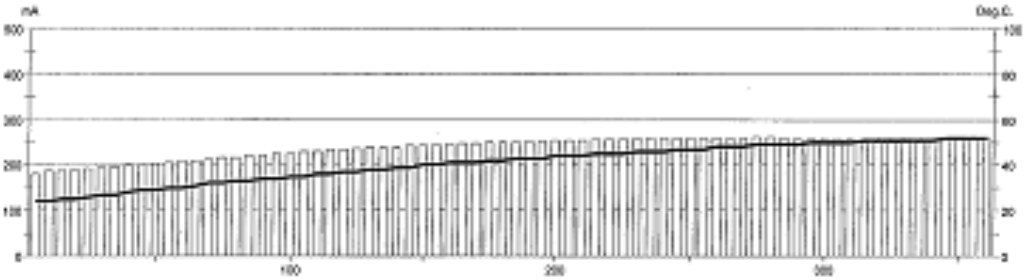

Time	°C	mA	Time	°C	mA	Time	°C	mA	Time	°C	mA
00:05	24	181.4	01:35	34	224.9	03:05	43	251.4	04:35	49	260.4
00:10	24	187.7	01:40	35	225.4	03:10	43	252.2	04:40	49	260.1
00:15	25	189.1	01:45	35	229.2	03:15	43	252.7	04:45	49	259.7
00:20	25	188.8	01:50	36	229.1	03:20	44	254.5	04:50	49	257.5
00:25	26	191.3	01:55	36	233.5	03:25	44	255.1	04:55	50	257.2
00:30	27	193.1	02:00	37	233.7	03:30	44	254.7	05:00	50	257.2
00:35	27	195.5	02:05	37	235.5	03:35	45	257.0	05:05	50	257.5
00:40	28	199.1	02:10	38	238.1	03:40	45	256.6	05:10	50	257.2
00:45	29	199.9	02:15	38	238.6	03:45	45	258.3	05:15	51	256.7
00:50	29	204.2	02:20	39	239.6	03:50	46	257.9	05:20	51	257.3
00:55	30	205.0	02:25	39	242.2	03:55	46	258.0	05:25	51	257.5
01:00	30	208.8	02:30	40	243.2	04:00	46	258.5	05:30	51	257.7
01:05	31	210.9	02:35	40	244.8	04:05	47	258.7	05:35	51	257.5
01:10	32	211.9	02:40	41	245.7	04:10	47	259.7	05:40	51	257.8
01:15	32	216.1	02:45	41	247.1	04:15	47	259.4	05:45	52	257.6
01:20	33	216.0	02:50	41	248.2	04:20	48	260.0	05:50	52	257.9
01:25	33	221.6	02:55	42	249.7	04:25	48	260.0	05:55	52	258.5
01:30	34	221.2	03:00	42	250.6	04:30	48	260.0	06:00	52	259.0

Figure A.2 – Control-EC1MIDDLE RCT Data

PROOVE it

ASTM C 1202-97

ST CO.

Test-compagny
Testing street 45
CompagnyCity
Some Country

Test report

Voltage Used:	60
Testing time:	06:00 hour
Charge passed:	4613
Adjusted Charge passed:	4163
Permeability class:	High
Instrument number:	071401
Channel number:	3
Report date:	7/12/2011
Testing by:	TP-SJ
Reference:	B1-EC2 TOP
Sample diameter:	100
Comment:	28 DAY

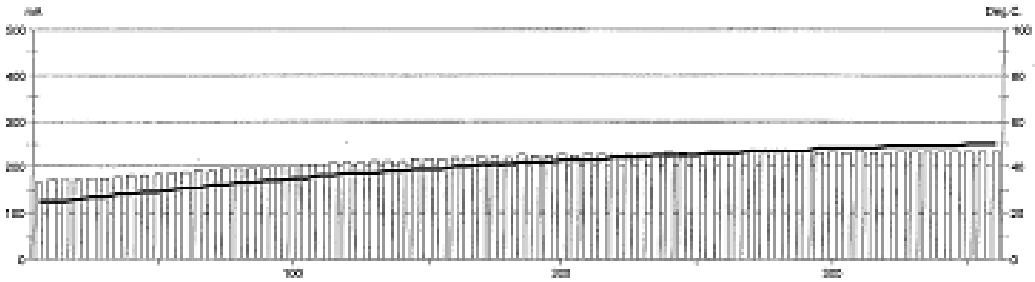

Time	°C	mA	Time	°C	mA	Time	°C	mA	Time	°C	mA
00:05	25	164.3	01:35	34	200.9	03:05	42	224.8	04:35	47	230.1
00:10	25	171.5	01:40	35	201.0	03:10	42	223.0	04:40	47	229.5
00:15	25	170.8	01:45	35	205.4	03:15	42	223.8	04:45	47	234.6
00:20	26	171.8	01:50	36	204.9	03:20	43	226.4	04:50	47	231.6
00:25	27	173.2	01:55	36	206.7	03:25	43	224.0	04:55	48	229.5
00:30	27	174.4	02:00	37	209.5	03:30	43	227.6	05:00	48	234.9
00:35	28	175.6	02:05	37	208.3	03:35	43	226.5	05:05	48	230.9
00:40	28	180.4	02:10	37	212.2	03:40	44	224.8	05:10	48	233.9
00:45	29	180.3	02:15	38	212.9	03:45	44	227.6	05:15	48	230.5
00:50	29	184.0	02:20	38	212.0	03:50	44	229.3	05:20	49	230.2
00:55	30	185.6	02:25	39	216.8	03:55	45	227.0	05:25	49	231.2
01:00	31	187.7	02:30	39	215.8	04:00	45	231.6	05:30	49	233.0
01:05	31	190.9	02:35	39	216.4	04:05	45	228.8	05:35	49	231.2
01:10	32	190.8	02:40	40	219.6	04:10	45	227.5	05:40	49	232.6
01:15	32	193.4	02:45	40	218.0	04:15	46	231.5	05:45	49	231.5
01:20	33	194.6	02:50	41	220.6	04:20	46	231.7	05:50	50	231.6
01:25	33	195.8	02:55	41	221.9	04:25	46	229.9	05:55	50	231.7
01:30	34	199.5	03:00	41	219.7	04:30	47	233.1	06:00	50	232.1

Figure A.3 – Control-EC2TOP RCT Data

PROOVE it

ASTM C 1202-97

ST CO.

Test-compagny
Testing street 45
CompagnyCity
Some Country

Test report

Voltage Used:	60
Testing time:	06:00 hour
Charge passed:	5404
Adjusted Charge passed:	4877
Permeability class:	High
Instrument number:	071401
Channel number:	4
Report date:	7/12/2011
Testing by:	TP SJ
Reference:	B1-EC2 MIDDLE
Sample diameter:	100
Comment:	28 DAY

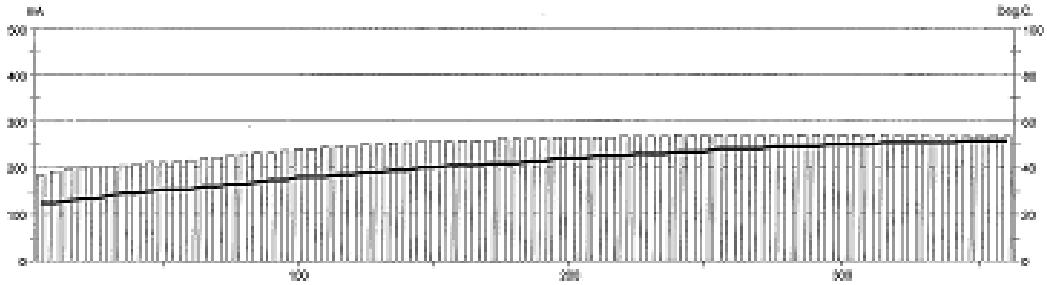

Time	°C	mA	Time	°C	mA	Time	°C	mA	Time	°C	mA
00:05	25	185.3	01:35	35	236.3	03:05	43	263.1	04:35	49	270.1
00:10	25	191.8	01:40	36	239.5	03:10	43	264.1	04:40	49	270.3
00:15	26	195.9	01:45	36	240.0	03:15	44	264.8	04:45	49	270.1
00:20	27	198.5	01:50	36	243.3	03:20	44	265.7	04:50	49	270.4
00:25	27	200.4	01:55	37	245.8	03:25	44	266.0	04:55	50	270.4
00:30	28	203.1	02:00	37	245.7	03:30	45	266.7	05:00	50	270.5
00:35	29	206.2	02:05	38	249.6	03:35	45	266.1	05:05	50	270.4
00:40	29	208.9	02:10	38	250.6	03:40	45	268.4	05:10	50	270.3
00:45	30	211.2	02:15	39	251.6	03:45	46	268.1	05:15	51	270.3
00:50	31	213.1	02:20	39	254.4	03:50	46	268.2	05:20	51	269.9
00:55	31	214.9	02:25	40	256.5	03:55	46	268.9	05:25	51	269.5
01:00	31	216.7	02:30	40	258.9	04:00	47	269.5	05:30	51	269.1
01:05	32	221.9	02:35	41	256.8	04:05	47	269.5	05:35	51	268.3
01:10	32	224.0	02:40	41	259.3	04:10	47	269.5	05:40	51	267.8
01:15	33	225.2	02:45	41	259.5	04:15	48	269.0	05:45	52	266.9
01:20	33	230.0	02:50	42	259.8	04:20	48	269.7	05:50	52	267.1
01:25	34	232.2	02:55	42	262.3	04:25	48	270.4	05:55	52	269.2
01:30	35	233.1	03:00	42	262.9	04:30	48	270.2	06:00	52	268.4

Figure A.4 – Control-EC2MIDDLE RCT Data

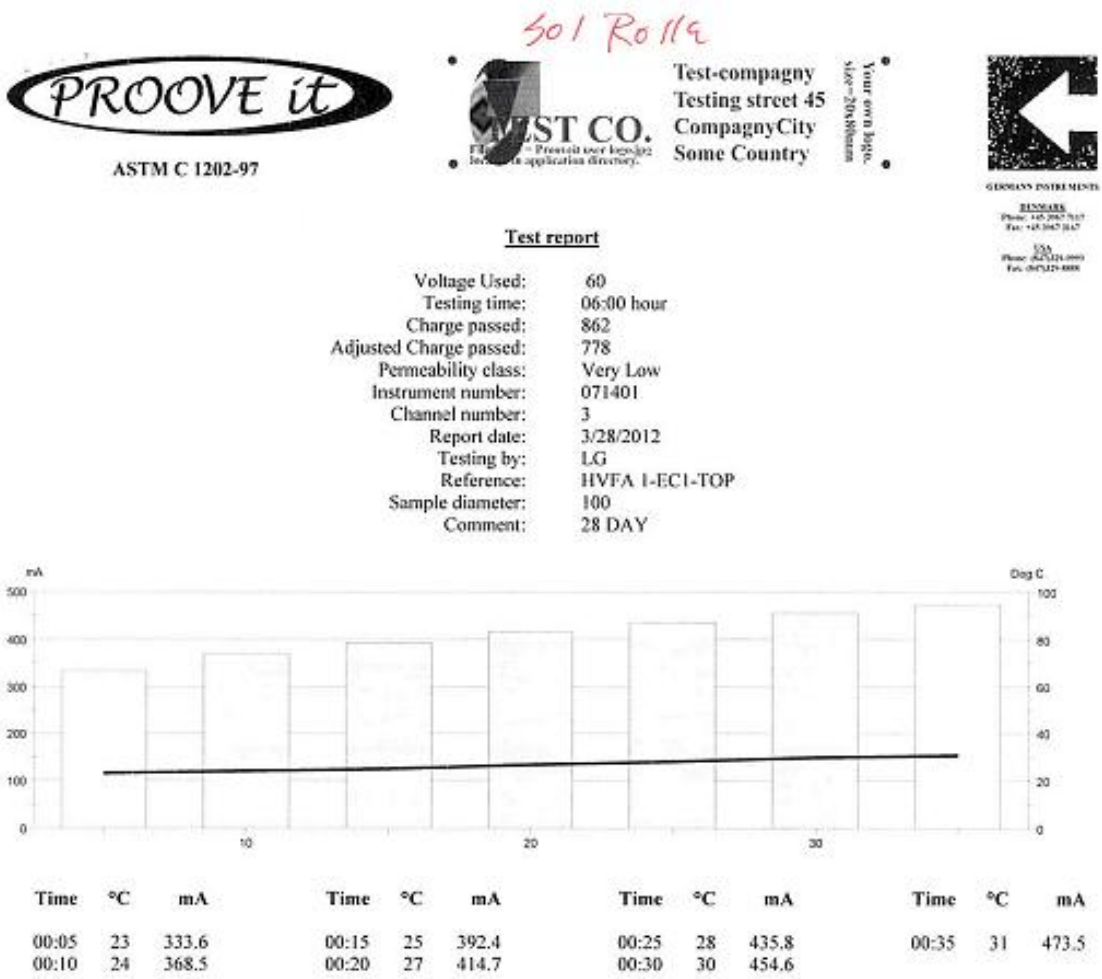

PROOVE it

ASTM C 1202-97

Test-compagny
Testing street 45
CompagnyCity
Some Country

Test report

Voltage Used:	60
Testing time:	06:00 hour
Charge passed:	862
Adjusted Charge passed:	778
Permeability class:	Very Low
Instrument number:	071401
Channel number:	3
Report date:	3/28/2012
Testing by:	LG
Reference:	HVFA 1-EC1-TOP
Sample diameter:	100
Comment:	28 DAY

Time	°C	mA	Time	°C	mA	Time	°C	mA	Time	°C	mA
00:05	23	333.6	00:15	25	392.4	00:25	28	435.8	00:35	31	473.5
00:10	24	368.5	00:20	27	414.7	00:30	30	454.6			

Figure A.5 – HVFA-70H-EC1TOP RCT Data

PROOVE it

ASTM C 1202-97

Test-compagny
Testing street 45
CompagnyCity
Some Country

Test report

Voltage Used:	60
Testing time:	06:00 hour
Charge passed:	646
Adjusted Charge passed:	583
Permeability class:	Very Low
Instrument number:	071401
Channel number:	4
Report date:	3/28/2012
Testing by:	LG
Reference:	HVFA I-EC1-MIDDLE
Sample diameter:	100
Comment:	28 DAY

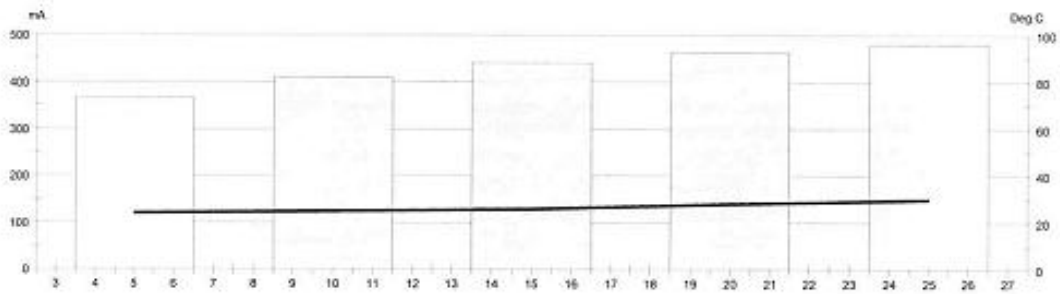

Time	°C	mA	Time	°C	mA	Time	°C	mA	Time	°C	mA
00:05	24	365.4	00:15	26	439.2	00:25	30	479.0			
00:10	25	407.9	00:20	28	462.5						

Figure A.6 – HVFA-70H-EC1MIDDLE RCT Data

PROOVE it

ASTM C 1202-97

501 Kolla

TEST CO.

Test-compagny
Testing street 45
CompagnyCity
Some Country

Your own logo, size=20x80mm

GERMANN INSTRUMENTS

Test report

Voltage Used:	60
Testing time:	06:00 hour
Charge passed:	1601
Adjusted Charge passed:	1445
Permeability class:	Low
Instrument number:	071401
Channel number:	1
Report date:	3/28/2012
Testing by:	LG
Reference:	HVFA1-EC2-TOP
Sample diameter:	100
Comment:	28 DAY

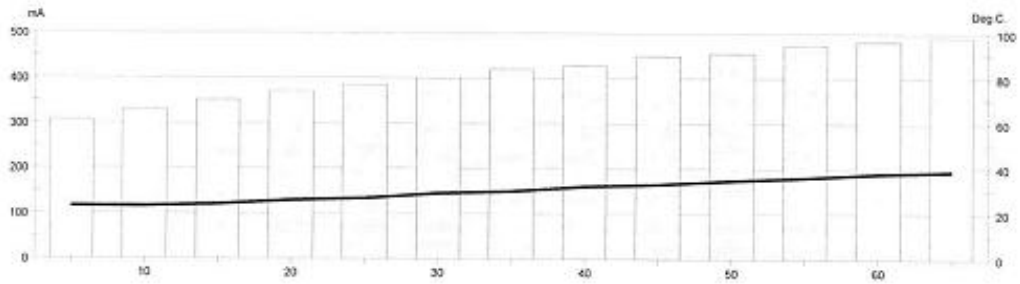

Time	°C	mA	Time	°C	mA	Time	°C	mA	Time	°C	mA
00:05	23	306.9	00:25	27	384.3	00:45	33	448.2	01:05	39	490.7
00:10	23	327.2	00:30	29	399.7	00:50	35	455.0			
00:15	24	350.5	00:35	30	420.1	00:55	36	472.2			
00:20	26	370.6	00:40	32	427.4	01:00	38	482.3			

Figure A.7 – HVFA-70H-EC2TOP RCT Data

PROOVE it

ASTM C 1202-97

Test-compagny
Testing street 45
CompagnyCity
Some Country

Test report

Voltage Used:	60
Testing time:	06:00 hour
Charge passed:	765
Adjusted Charge passed:	690
Permeability class:	Very Low
Instrument number:	071401
Channel number:	2
Report date:	3/28/2012
Testing by:	LG
Reference:	HVFA 1-EC 2-MIDDLE
Sample diameter:	100
Comment:	28 DAY

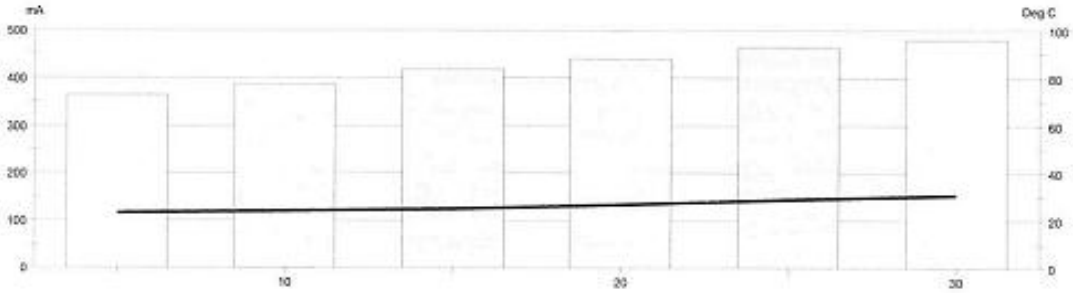

Time	°C	mA	Time	°C	mA	Time	°C	mA	Time	°C	mA
00:05	23	363.0	00:15	25	417.2	00:25	29	463.4			
00:10	24	386.4	00:20	27	440.6	00:30	31	481.0			

Figure A.8 – HVFA-70H-EC2MIDDLE RCT Data

PROOVE it

ASTM C 1202-97

ST CO.

Test-compagny
Testing street 45
Compagny City
Some Country

Test report

Voltage Used:	60
Testing time:	06:00 hour
Charge passed:	7822
Adjusted Charge passed:	7059
Permeability class:	High
Instrument number:	071401
Channel number:	1
Report date:	11/4/2011
Testing by:	LG
Reference:	HVFA-EC1-28 DAY-TOP
Sample diameter:	100
Comment:	---

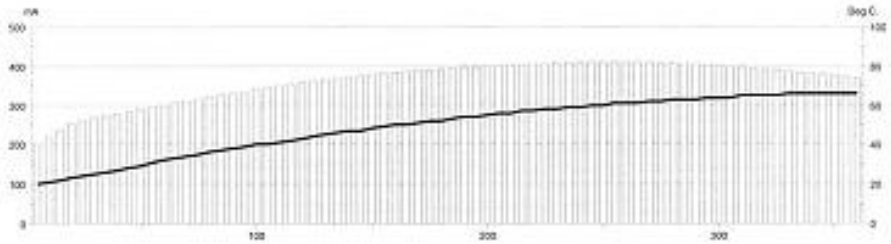

Time	°C	mA	Time	°C	mA	Time	°C	mA	Time	°C	mA
00:05	20	200.3	01:35	39	335.3	03:05	53	394.8	04:35	62	409.3
00:10	21	219.1	01:40	40	340.5	03:10	54	397.0	04:40	63	408.4
00:15	22	237.5	01:45	40	345.5	03:15	54	398.4	04:45	63	407.3
00:20	23	251.6	01:50	41	350.8	03:20	55	400.4	04:50	63	405.9
00:25	24	261.4	01:55	42	354.6	03:25	56	401.1	04:55	64	404.3
00:30	25	268.3	02:00	43	358.0	03:30	56	403.0	05:00	64	402.3
00:35	26	273.0	02:05	44	361.8	03:35	57	404.1	05:05	64	400.0
00:40	27	277.7	02:10	45	366.6	03:40	57	405.6	05:10	65	397.6
00:45	28	283.3	02:15	46	368.9	03:45	58	406.4	05:15	65	395.0
00:50	29	289.7	02:20	47	373.0	03:50	58	407.5	05:20	65	392.5
00:55	31	295.0	02:25	47	375.7	03:55	59	408.9	05:25	65	389.9
01:00	32	300.2	02:30	48	379.5	04:00	59	410.2	05:30	66	387.6
01:05	33	305.6	02:35	49	382.4	04:05	60	410.5	05:35	66	384.8
01:10	34	311.2	02:40	50	384.2	04:10	60	411.1	05:40	66	382.0
01:15	35	315.6	02:45	50	386.7	04:15	61	411.1	05:45	66	379.0
01:20	36	321.1	02:50	51	389.8	04:20	61	410.9	05:50	66	376.3
01:25	37	326.4	02:55	52	391.1	04:25	61	410.5	05:55	66	373.3
01:30	38	330.8	03:00	52	393.6	04:30	62	410.2	06:00	66	370.3

Figure A.9 – HVFA-70L-EC1TOP RCT Data

PROOVE it

ASTM C 1202-97

TEST CO.

Test-compagny
Testing street 45
Compagny City
Some Country

Test report

Voltage Used:	60
Testing time:	05:00 hour
Charge passed:	1245
Adjusted Charge passed:	1124
Permeability class:	Low
Instrument number:	071401
Channel number:	2
Report date:	11/4/2011
Testing by:	LG
Reference:	HVFA-EC1-28 DAY-MIDDLE
Sample diameter:	100
Comment:	SHUT OFF AFTER 50 MINUTES DUE TO HIGH mA

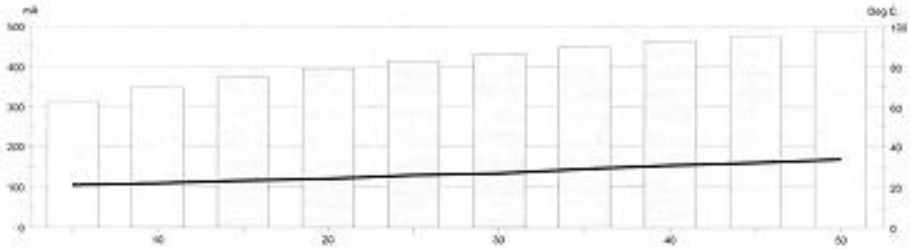

Time	°C	mA	Time	°C	mA	Time	°C	mA	Time	°C	mA
00:05	21	310.4	00:20	24	394.2	00:35	29	448.1	00:50	34	488.7
00:10	22	347.9	00:25	26	414.3	00:40	31	463.7			
00:15	23	373.8	00:30	27	432.0	00:45	32	476.4			

Figure A.10 – HVFA-70L-EC1MIDDLE RCT Data

PROOVE it

ASTM C 1202-97

ST CO.

Test-compagny
Testing street 45
Compagny City
Some Country

Test report

Voltage Used:	60
Testing time:	06:00 hour
Charge passed:	8394
Adjusted Charge passed:	7576
Permeability class:	High
Instrument number:	071401
Channel number:	3
Report date:	11/4/2011
Testing by:	LG
Reference:	HVFA-EC2-TOP-28 DAY
Sample diameter:	100
Comment:	---

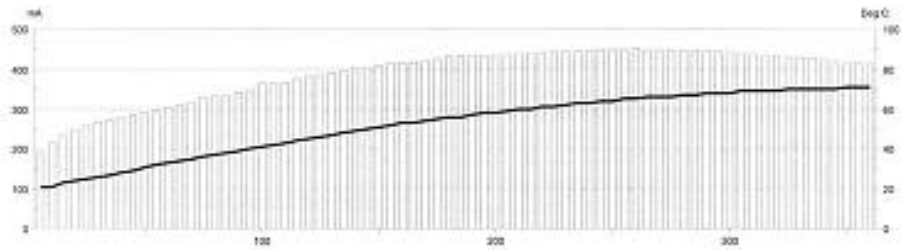

Time	°C	mA	Time	°C	mA	Time	°C	mA	Time	°C	mA
00:05	21	193.5	01:35	40	346.2	03:05	56	432.6	04:35	66	448.6
00:10	21	217.2	01:40	41	363.0	03:10	57	435.1	04:40	67	447.4
00:15	23	235.9	01:45	42	363.1	03:15	58	433.8	04:45	67	446.9
00:20	24	249.8	01:50	43	367.0	03:20	58	435.9	04:50	68	445.0
00:25	25	260.2	01:55	44	373.9	03:25	59	437.4	04:55	68	444.2
00:30	26	267.7	02:00	45	381.1	03:30	60	438.6	05:00	68	441.6
00:35	27	272.5	02:05	46	386.2	03:35	60	440.3	05:05	69	440.1
00:40	28	279.2	02:10	47	390.1	03:40	61	441.8	05:10	69	438.1
00:45	29	285.7	02:15	48	395.4	03:45	61	443.1	05:15	69	435.4
00:50	31	289.9	02:20	49	401.0	03:50	62	444.2	05:20	69	433.6
00:55	32	296.5	02:25	50	404.0	03:55	63	445.3	05:25	70	431.2
01:00	33	302.6	02:30	51	407.8	04:00	63	447.0	05:30	70	428.9
01:05	34	309.9	02:35	52	412.3	04:05	64	448.4	05:35	70	426.5
01:10	35	317.1	02:40	53	414.5	04:10	64	449.4	05:40	70	423.6
01:15	36	327.2	02:45	53	416.7	04:15	65	449.5	05:45	70	420.7
01:20	37	332.0	02:50	54	420.2	04:20	65	450.1	05:50	71	418.0
01:25	38	333.7	02:55	55	423.0	04:25	66	449.6	05:55	71	415.9
01:30	39	340.7	03:00	56	432.5	04:30	66	449.4	06:00	71	413.3

Figure A.11 – HVFA-70L-EC2TOP RCT Data

PROOVE it

ASTM C 1202-97

Test-compagny
Testing street 45
Compagny City
Some Country

Test report

Voltage Used:	60
Testing time:	06:00 hour
Charge passed:	1107
Adjusted Charge passed:	999
Permeability class:	Very Low
Instrument number:	071401
Channel number:	4
Report date:	11/4/2011
Testing by:	LG
Reference:	HVFA-EC2-MIDDLE-28 DAY
Sample diameter:	100
Comment:	SHUT OFF 45 MIN DUE TO HIGH mA

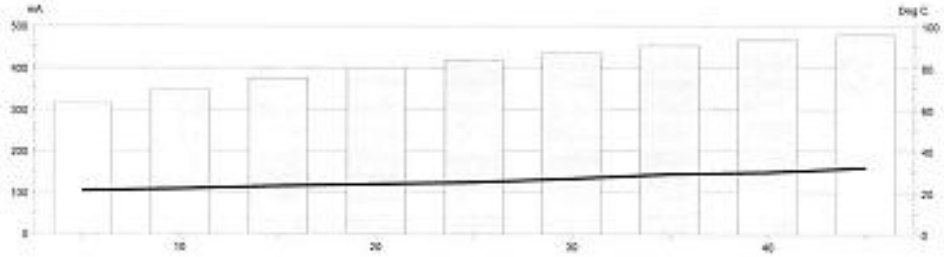

Time	°C	mA	Time	°C	mA	Time	°C	mA	Time	°C	mA
00:05	21	314.0	00:20	24	398.5	00:35	29	452.2			
00:10	22	348.2	00:25	25	418.4	00:40	30	467.2			
00:15	23	374.8	00:30	27	436.2	00:45	32	480.5			

Figure A.12 – HVFA-70L-EC2MIDDLE RCT Data

PROOVE it

ASTM C 1202-97

TEST CO.

Test-compagny
Testing street 45
CompagnyCity
Some Country

Your own logo.
size=26x50mm

GERMANN INSTRUMENTS

Test report

Voltage Used:	60
Testing time:	06:00 hour
Charge passed:	1072
Adjusted Charge passed:	967
Permeability class:	Very Low
Instrument number:	071401
Channel number:	3
Report date:	12/13/2011
Testing by:	LG/SB
Reference:	EC1 HVFA3-top 30day
Sample diameter:	100
Comment:	Turned off due excessive voltage.

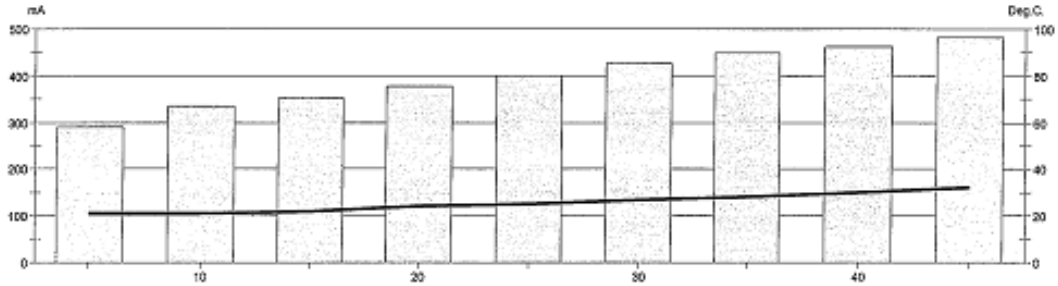

Time	°C	mA	Time	°C	mA	Time	°C	mA	Time	°C	mA
00:05	21	290.3	00:20	24	376.2	00:35	28	448.4			
00:10	21	333.8	00:25	25	399.8	00:40	30	462.8			
00:15	22	351.7	00:30	27	426.7	00:45	32	482.9			

Figure A.13 – HVFA-70LA-EC1TOP RCT Data

PROOVE it

ASTM C 1202-97

ST CO.

Test-compagny
Testing street 45
CompagnyCity
Some Country

Your own logo.

GERMANN INSTRUMENTS

Test report

Voltage Used:	60
Testing time:	06:00 hour
Charge passed:	876
Adjusted Charge passed:	791
Permeability class:	Very Low
Instrument number:	071401
Channel number:	4
Report date:	12/13/2011
Testing by:	LG/SB
Reference:	EC1 HVFA3-middle 30day
Sample diameter:	100
Comment:	Turned off due to excessive voltage.

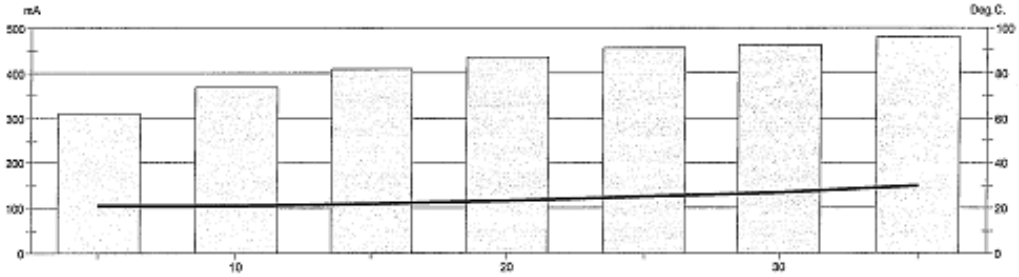

Time	°C	mA	Time	°C	mA	Time	°C	mA	Time	°C	mA
00:05	21	310.0	00:15	22	408.2	00:25	25	455.3	00:35	30	479.5
00:10	21	368.6	00:20	23	436.0	00:30	27	462.3			

Figure A.14 – HVFA-70LA-EC1MIDDLE RCT Data

PROOVE it

ASTM C 1202-97

TEST CO.

Test-compagny
Testing street 45
CompagnyCity
Some Country

Your own logo

GERMANN INSTRUMENTS

Test report

Voltage Used:	60
Testing time:	06:00 hour
Charge passed:	1182
Adjusted Charge passed:	1067
Permeability class:	Low
Instrument number:	071401
Channel number:	1
Report date:	12/13/2011
Testing by:	LG/SB
Reference:	EC2 HVFA-top 30day
Sample diameter:	100
Comment:	Turned off due to excessive voltage.

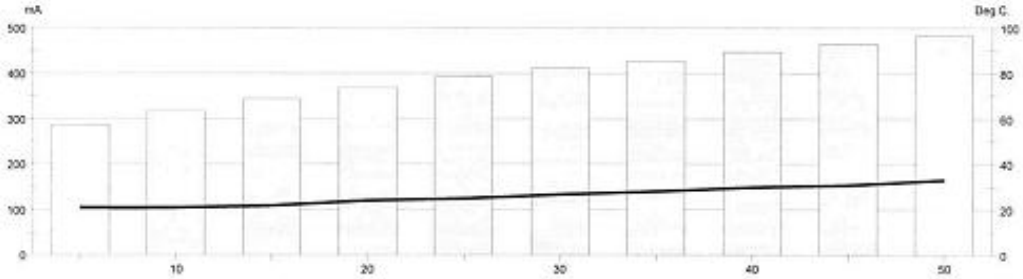

Time	°C	mA	Time	°C	mA	Time	°C	mA	Time	°C	mA
00:05	21	285.7	00:20	24	369.1	00:35	28	427.2	00:50	33	483.2
00:10	21	316.4	00:25	25	391.8	00:40	30	446.9			
00:15	22	344.1	00:30	27	410.0	00:45	31	464.3			

Figure A.15 – HVFA-70LA-EC2TOP RCT Data

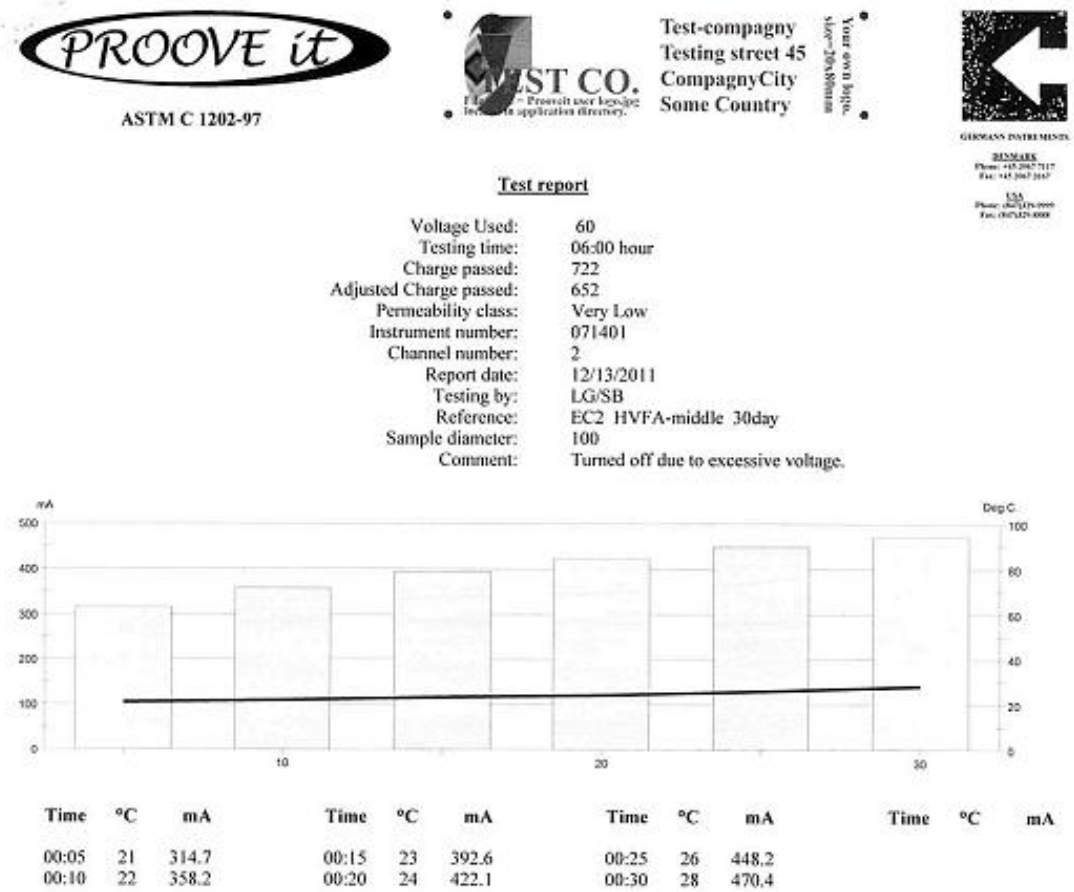

PROOVE it

ASTM C 1202-97

Test-compagny
Testing street 45
CompagnyCity
Some Country

Test report

Voltage Used:	60
Testing time:	06:00 hour
Charge passed:	722
Adjusted Charge passed:	652
Permeability class:	Very Low
Instrument number:	071401
Channel number:	2
Report date:	12/13/2011
Testing by:	LG/SB
Reference:	EC2 HVFA-middle 30day
Sample diameter:	100
Comment:	Turned off due to excessive voltage.

Time	°C	mA	Time	°C	mA	Time	°C	mA	Time	°C	mA
00:05	21	314.7	00:15	23	392.6	00:25	26	448.2			
00:10	22	358.2	00:20	24	422.1	00:30	28	470.4			

Figure A.16 – HVFA-70LA-EC2MIDDLE RCT Data

Table A.49 Control Chloride Content Data

Depth (in)	Chloride Content (%)		
	Control-1P	Control-2P	Control-3P
0	0.28	0.26	0.31
0.25	0.14	0.15	0.12
0.75	0.06	0.05	0.04
1.5	0.03	0.03	0.03
2.0	0.03	0.03	0.02

Table A.50 HVFA-70H Chloride Content Data

Depth (in)	Chloride Content (%)		
	HVFA-70H-1P	HVFA-70H-2P	HVFA-70H-3P
0	0.16	0.16	0.18
0.25	0.36	0.46	0.31
0.75	0.09	0.07	0.13
1.5	0.05	0.03	0.03
2.0	0.03	0.03	0.03

Table A.51 HVFA-70L Chloride Content Data

Depth (in)	Chloride Content (%)		
	HVFA-70L-1P	HVFA-70L-2P	HVFA-70L-3P
0	0.17	0.14	0.10
0.25	0.22	0.25	0.25
0.75	0.06	0.04	0.08
1.5	0.03	0.02	0.02
2.0	0.02	0.02	0.02

Table A.52 HVFA-70LA Chloride Content Data

Depth (in)	Chloride Content (%)		
	HVFA-70LA-1P	HVFA-70LA-2P	HVFA-70LA-3P
0	0.32	0.30	0.24
0.25	0.18	0.21	0.23
0.75	0.12	0.12	0.17
1.5	0.03	0.03	0.02
2.0	0.02	0.01	0.02

GM23		FREEZE & THAW LEDGER				Preliminary Testing Results @ Zero Cycles					
LAB NO:	UMR-B1		BEAM ID NO:		1	Agg. Description					
	35 Day Cure										
Initial Weight in Air		9445.5					Starting Cycle Count		12710		
					Initial bar reading		0				
Initial Gage Reading							Date Test Started		7/19/11		
					Completion Date		8/21/11				
Initial Frequency		1800				TERMINAL FREQUENCY			1080		
DATE	CYCLE # machine	Actual cycles	Weight	Ref. Bar	Gage reading	Corr. gage reading	Frqncy	RDM	Durab. Factor	% Gage Length Change	%Wght Change
7/20/11	12719	9	9447.6				1715	90.78	2.72		0.022
7/21/11	12728	18	9453.8				1676	86.70	5.20		0.088
7/22/11	12736	26	9457.8				1655	84.54	7.33		0.130
7/25/11	12763	53	9477.5				1574	76.47	13.51		0.339
7/27/11	12781	71	9491.2				1497	69.17	16.37		0.484
7/29/11	12799	89	9498.2				1457	65.52	19.44		0.558
8/1/11	12828	118	9505.2				1293	51.60	20.30		0.632
8/3/11	12844	134	9511.2				1104	37.62	16.80		0.696
	Flexural Strength = 356 psi										
	Tangent Modulus = 0.1416 Msi										
	Maximum Strain = 0.0055 in/in										
Totals		134						37.62	20.30	0.00	0.02

Initial Measurements		Post Break Measurments					
WIDTH	DEPTH	WIDTH		DEPTH			
		4.567		3.304		21.59	Avg. DF bms 1,2,3
		4.576		3.295		1.71257	Std. dev.
		4.575		3.228			
0.000	0.000	4.573		3.276	Avg.		

Initial Measurements not taken per Steve Jackson

Figure A.17 – Control-FT1 Data

GM23		FREEZE & THAW LEDGER				Preliminary Testing Results @ Zero Cycles					
LAB NO:	UMR-B1		BEAM ID NO:		2	Agg. Description		0			
	35 Day Cure										
Initial Weight in Air		9974.5					Starting Cycle Count			12710	
					Initial bar reading		0				
Initial Gage Reading							Date Test Started		7/19/11		
					Completion Date		8/21/11				
Initial Frequency		1893				TERMINAL FREQUENCY			1136		
DATE	CYCLE # machine	Actual cycles	Weight	Ref. Bar	Gage reading	Corr. gage reading	Frqncy	RDM	Durab. Factor	% Gage Length Change	%Wght Change
7/20/11	12719	9	9976.6	0			1787	89.11	2.67		0.021
7/21/11	12728	18	9984.6	0			1771	87.53	5.25		0.101
7/22/11	12736	26	9988.7	0			1759	86.34	7.48		0.142
7/25/11	12763	53	10007.7	0			1703	80.93	14.30		0.333
7/27/11	12781	71	10019.8	0			1644	75.42	17.85		0.454
7/29/11	12799	89	10028.9	0			1577	69.40	20.59		0.545
8/1/11	12828	118	10038.8	0			1423	56.51	22.23		0.645
8/3/11	12844	134	10040.8	0			1374	52.68	23.53		0.665
	Flexural Strength = 248 psi										
	Tangent Modulus = 0.0806 Msi										
	Maximum Strain = 0.0049 in/in										
Totals		134						52.68	23.53	0.00	0.02

Initial Measurements		Post Break Measurments			
WIDTH	DEPTH	WIDTH		DEPTH	
		4.656		3.373	
		4.675		3.413	
		4.694		3.478	
0.000	0.000	4.675		3.421	Avg.

Initial Measurements not taken per Steve Jackson

Figure B.18 – Control-FT2 Data

GM23		FREEZE & THAW LEDGER				Preliminary Testing Results @ Zero Cycles					
LAB NO:	UMR-B1		BEAM ID NO:		3	Agg. Description		0			
	35 Day Cure										
Initial Weight in Air		9195.0					Starting Cycle Count			12710	
					Initial bar reading		0				
Initial Gage Reading							Date Test Started		7/19/11		
					Completion Date		8/21/11				
Initial Frequency		1942				TERMINAL FREQUENCY			1165		
DATE	CYCLE # machine	Actual cycles	Weight	Ref. Bar	Gage reading	Corr. gage reading	Frqncy	RDM	Durab. Factor	% Gage Length Change	%Wght Change
7/20/11	12719	9	9197.0	0			1835	89.28	2.68		0.022
7/21/11	12728	18	9203.9	0			1813	87.16	5.23		0.097
7/22/11	12736	26	9210.1	0			1787	84.67	7.34		0.164
7/25/11	12763	53	9229.5	0			1696	76.27	13.47		0.375
7/27/11	12781	71	9239.3	0			1617	69.33	16.41		0.482
7/29/11	12799	89	9247.1	0			1540	62.88	18.66		0.567
8/1/11	12828	118	9255.9	0			1417	53.24	20.94		0.662
8/3/11	12844	134	9257.3	0			1263	42.30	18.89		0.678
	Flexural Strength = 350 psi										
	Tangent Modulus = 0.1226 Msi										
	Maximum Strain = 0.0040 in/in										
Totals		134						42.30	20.94	0.00	0.02
	Initial Measurements				Post Break Measurments						
	WIDTH	DEPTH			WIDTH		DEPTH				
					4.261		3.515				
					4.247		3.514				
					4.221		3.525				
	0.000	0.000			4.243		3.518	Avg.			
	Initial Measurements not taken per Steve Jackson										

Figure A.19 – Control-FT3 Data

GM23		FREEZE & THAW LEDGER				Preliminary Testing Results @ Zero Cycles					
LAB NO:	HV FA1 ROLLA		BEAM ID NO:		1	Agg. Description					
	35 Day Cure										
Initial Weight in Air		9788.0					Starting Cycle Count			13611	
					Initial bar reading		0.2527				
Initial Gage Reading		0.2751					Date Test Started		10/31/11		
					Completion Date		12/3/11				
Initial Frequency		1782				TERMINAL FREQUENCY			1069		
DATE	CYCLE # machine	Actual cycles	Weight	Ref. Bar	Gage reading	Corr. gage reading	Frqncy	RDM	Durab. Factor	% Gage Length Change	%Wght Change
11/1/11	13620	9	9814.1	0.2534	0.2896	0.2889	1390	60.84	1.83	0.0862	0.267
11/3/11	13638	27	9856.8	0.2530	0.3299	0.3296	758	18.09	1.63	0.3406	0.703
Totals		27									

Initial Measurements		Post Break Measurments				
WIDTH	DEPTH	WIDTH		DEPTH		
4.538	3.518	4.515		3.526	#DIV/0!	Avg. DF bms 1,2,3
4.530	3.521	4.521		3.517	#DIV/0!	Std. dev.
4.543	3.515	4.538		3.553		
4.518	3.511					
4.532	3.516	4.525		3.532	Avg.	

11/3 CORNER FELL OFF

Figure A.20 – HVFA-70H-FT1 Data

GM23		FREEZE & THAW LEDGER				Preliminary Testing Results @ Zero Cycles					
LAB NO:	HV FA1 ROLLA		BEAM ID NO:		2	Agg. Description		0			
	35 Day Cure										
Initial Weight in Air		9917.5					Starting Cycle Count			13611	
					Initial bar reading		0.2527				
Initial Gage Reading		0.2505					Date Test Started		10/31/11		
					Completion Date		12/3/11				
Initial Frequency		1787				TERMINAL FREQUENCY			1072		
DATE	CYCLE # machine	Actual cycles	Weight	Ref. Bar	Gage reading	Corr. gage reading	Frqncy	RDM	Durab. Factor	% Gage Length Change	%Wght Change
11/1/11	13620	9	9944.7	0.2534	0.2640	0.2633	1304	53.25	1.60	0.0800	0.274
11/3/11	13638	27	9968.6	0.253	0.3018	0.3015	888	24.69	2.22	0.3188	0.515
Totals		27									

Initial Measurements		Post Break Measurments		
WIDTH	DEPTH	WIDTH		DEPTH
4.555	3.518	4.588		3.523
4.578	3.511	4.560		3.526
4.551	3.503	4.574		3.514
4.558	3.502			
4.561	3.509	4.574		3.521 Avg.

Figure A.21 – HVFA-70H-FT2 Data

GM23		FREEZE & THAW LEDGER				Preliminary Testing Results @ Zero Cycles					
LAB NO:	HV FA1 ROLLA		BEAM ID NO:		3	Agg. Description		0			
	35 Day Cure										
Initial Weight in Air		9825.6					Starting Cycle Count			13611	
					Initial bar reading		0.2527				
Initial Gage Reading		0.1937					Date Test Started		10/31/11		
					Completion Date		12/3/11				
Initial Frequency		1739				TERMINAL FREQUENCY			1043		
DATE	CYCLE # machine	Actual cycles	Weight	Ref. Bar	Gage reading	Corr. gage reading	Frqncy	RDM	Durab. Factor	% Gage Length Change	%Wght Change
11/1/11	13620	9	9856.3	0.2534	0.2080	0.2073	1229	49.95	1.50	0.0850	0.312
11/3/11	13638	27	9891.9	0.253	0.2459	0.2456	878	25.49	2.29	0.3244	0.675
Totals		27									

Initial Measurements		Post Break Measurments		
WIDTH	DEPTH	WIDTH		DEPTH
4.548	3.504	4.570		3.504
4.542	3.492	4.570		3.502
4.547	3.494	4.569		3.522
4.569	3.507			
4.552	3.499	4.570		3.509 Avg.

11/3 corner fell off

Figure A.22 – HVFA-70H-FT3 Data

GM23		FREEZE & THAW LEDGER				Preliminary Testing Results @ Zero Cycles					
LAB NO:	HV FA -2		BEAM ID NO:		1	Agg. Description		ROLLA			
	35 Day Cure										
Initial Weight in Air		9956.7					Starting Cycle Count			13703	
					Initial bar reading		0.2528				
Initial Gage Reading		0.3387					Date Test Started		11/10/11		
					Completion Date		12/13/11				
Initial Frequency		1881				TERMINAL FREQUENCY			1129		
DATE	CYCLE # machine	Actual cycles	Weight	Ref. Bar	Gage reading	Corr. gage reading	Frqncy	RDM	Durab. Factor	% Gage Length Change	%Wght Change
11/14/11	13737	34	9952.3	0.2523	0.3350	0.3355	1845	96.21	10.90	-0.0200	-0.044
11/16/11	13756	53	9952.4	0.2531	0.3356	0.3353	1845	96.21	17.00	-0.0212	-0.043
11/18/11	13776	73	9953.8	0.2530	0.3340	0.3338	1849	96.63	23.51	-0.0306	-0.029
11/21/11	13801	98	9955.6	0.2535	0.3370	0.3363	1845	96.21	31.43	-0.0150	-0.011
11/23/11	13819	116	9956.3	0.2533	0.3374	0.3369	1840	95.69	37.00	-0.0112	-0.004
11/25/11	13837	134	9919.0	0.2526	0.3386	0.3388	1842	95.90	42.83	0.0006	-0.379
11/28/11	13864	161	9918.1	0.2530	0.3396	0.3394	1842	95.90	51.46	0.0044	-0.388
11/29/11	13873	170	9918.4	0.2536	0.3406	0.3398	1862	97.99	55.53	0.0069	-0.385
12/2/11	13899	196	9849.6	0.2527	0.3419	0.342	1895	101.49	66.31	0.0206	-1.076
12/5/11	13928	225	9721.7	0.2524	0.3439	0.3443	1910	103.11	77.33	0.0350	-2.360
12/7/11	13944	241	9566.9	0.2521	0.3387	0.3394	1892	101.17	81.28	0.0044	-3.915
12/9/11	13956	253	9556.1	0.2523	0.3478	0.3483	1883	100.21	84.51	0.0600	-4.023
12/12/11	13985	282	9558.8	0.2526	0.3503	0.3505	1757	87.25	82.02	0.0737	-3.996
12/14/11	14003	300	6450.0	0.2533	0.3599	0.3594	1742	85.77	85.77	0.1294	-35.220
Totals		300									

Initial Measurements		Post Break Measurments				
WIDTH	DEPTH	WIDTH		DEPTH		
4.578	3.480	4.591		3.480	#DIV/0!	Avg. DF bms 1,2,3
4.579	3.487	4.616		3.500	#DIV/0!	Std. dev.
4.535	3.486	4.577		3.487		
4.515	3.483					
4.552	3.484	4.595		3.489	Avg.	

Figure A.23 – HVFA-70L-FT1 Data

GM23		FREEZE & THAW LEDGER				Preliminary Testing Results @ Zero Cycles					
LAB NO:	HV FA -2		BEAM ID NO:		2	Agg. Description		ROLLA			
	35 Day Cure										
Initial Weight in Air		10025.6					Starting Cycle Count			13703	
					Initial bar reading		0.2528				
Initial Gage Reading		0.2417					Date Test Started		11/10/11		
					Completion Date		12/13/11				
Initial Frequency		1882				TERMINAL FREQUENCY			1129		
DATE	CYCLE # machine	Actual cycles	Weight	Ref. Bar	Gage reading	Corr. gage reading	Frqncy	RDM	Durab. Factor	% Gage Length Change	%Wght Change
11/14/11	13737	34	10022.2	0.2523	0.2446	0.2451	1845	96.11	10.89	0.0213	-0.034
11/16/11	13756	53	10022.1	0.2531	0.2452	0.2449	1841	95.69	16.91	0.0200	-0.035
11/18/11	13776	73	10022.3	0.253	0.2434	0.2432	1851	96.73	23.54	0.0094	-0.033
11/21/11	13801	98	10023.5	0.2535	0.2460	0.2453	1848	96.42	31.50	0.0225	-0.021
11/23/11	13819	116	10023.9	0.2533	0.2461	0.2456	1856	97.26	37.61	0.0244	-0.017
11/25/11	13837	134	10025.8	0.2526	0.2466	0.2468	1855	97.15	43.39	0.0319	0.002
11/28/11	13864	161	10026.3	0.253	0.2482	0.248	1854	97.05	52.08	0.0394	0.007
11/29/11	13873	170	10027.9	0.2536	0.2484	0.2476	1856	97.26	55.11	0.0369	0.023
12/2/11	13899	196	10030.4	0.2527	0.2503	0.2504	1846	96.21	62.86	0.0544	0.048
12/5/11	13928	225	10034.0	0.2524	0.2519	0.2523	1836	95.17	71.38	0.0663	0.084
12/7/11	13944	241	10016.8	0.2521	0.2507	0.2514	1829	94.45	75.87	0.0606	-0.088
12/9/11	13956	253	10018.1	0.2523	0.2530	0.2535	1805	91.98	77.57	0.0738	-0.075
12/12/11	13985	282	10027.0	0.2526	0.2608	0.261	1696	81.21	76.34	0.1206	0.014
12/14/11	14003	300	9962.0	0.2533	0.2645	0.264	1660	77.80	77.80	0.1394	-0.634
1/0/00	0	####		0							
1/0/00	0	####		0							
1/0/00	0	####		0							
1/0/00	0	####		0							
1/0/00	0	####		0							
1/0/00	0	####		0							
1/0/00	0	####		0							
1/0/00	0	####		0							
Totals		300									

Initial Measurements		Post Break Measurments		
WIDTH	DEPTH	WIDTH		DEPTH
4.569	3.480	4.565		3.486
4.578	3.481	4.563		3.473
4.549	3.487	4.555		3.472
4.533	3.474			
4.557	3.481	4.561		3.477 Avg.

Figure A.24 – HVFA-70L-FT2 Data

GM23		FREEZE & THAW LEDGER				Preliminary Testing Results @ Zero Cycles					
LAB NO:	HV FA -2		BEAM ID NO:		3	Agg. Description		ROLLA			
	35 Day Cure										
Initial Weight in Air		10153.3					Starting Cycle Count			13703	
					Initial bar reading		0.2528				
Initial Gage Reading		0.2511					Date Test Started		11/10/11		
					Completion Date		12/13/11				
Initial Frequency		1886				TERMINAL FREQUENCY			1132		
DATE	CYCLE # machine	Actual cycles	Weight	Ref. Bar	Gage reading	Corr. gage reading	Frqncy	RDM	Durab. Factor	% Gage Length Change	%Wght Change
11/14/11	13737	34	10149.6	0.2523	0.2534	0.2539	1870	98.31	11.14	0.0175	-0.036
11/16/11	13756	53	10149.5	0.2531	0.2521	0.2518	1865	97.79	17.28	0.0044	-0.037
11/18/11	13776	73	10151.2	0.253	0.2503	0.2501	1875	98.84	24.05	-0.0062	-0.021
11/21/11	13801	98	10151.8	0.2535	0.2535	0.2528	1862	97.47	31.84	0.0106	-0.015
11/23/11	13819	116	10152.2	0.2533	0.2536	0.2531	1879	99.26	38.38	0.0125	-0.011
11/25/11	13837	134	10154.4	0.2526	0.2538	0.254	1876	98.94	44.19	0.0181	0.011
11/28/11	13864	161	10153.8	0.253	0.2548	0.2546	1877	99.05	53.16	0.0219	0.005
11/29/11	13873	170	10156.6	0.2536	0.2559	0.2551	1871	98.42	55.77	0.0250	0.033
12/2/11	13899	196	10157.2	0.2527	0.2604	0.2605	1862	97.47	63.68	0.0588	0.038
12/5/11	13928	225	10163.3	0.2524	0.2641	0.2645	1836	94.77	71.08	0.0838	0.098
12/7/11	13944	241	10132.3	0.2521	0.2650	0.2657	1842	95.39	76.63	0.0913	-0.207
12/9/11	13956	253	10059.1	0.2523	0.2654	0.2659	1842	95.39	80.44	0.0925	-0.928
12/12/11	13985	282	10066.2	0.2526	0.2757	0.2759	1715	82.69	77.73	0.1550	-0.858
12/14/11	14003	300	9992.9	0.2533	0.2776	0.2771	1709	82.11	82.11	0.1625	-1.580
1/0/00	0	####		0							
1/0/00	0	####		0							
1/0/00	0	####		0							
1/0/00	0	####		0							
1/0/00	0	####		0							
1/0/00	0	####		0							
1/0/00	0	####		0							
1/0/00	0	####		0							
Totals		300									

Initial Measurements		Post Break Measurments		
WIDTH	DEPTH	WIDTH		DEPTH
4.629	3.494	4.620		3.495
4.633	3.489	4.598		3.491
4.620	3.503	4.562		3.495
4.633	3.501			
4.629	3.497	4.593		3.494 Avg.

Figure A.25 – HVFA-70L-FT3 Data

GM23		FREEZE & THAW LEDGER				Preliminary Testing Results @ Zero Cycles					
LAB NO:	HV FA3		BEAM ID NO:		1	Agg. Description		ROLLA			
Initial Weight in Air		10102.4					Starting Cycle Count			888	
					Initial bar reading		0.2523				
Initial Gage Reading		0.4134					Date Test Started		3/5/12		
					Completion Date		4/7/12				
Initial Frequency		1761				TERMINAL FREQUENCY			1057		
DATE	CYCLE # machine	Actual cycles	Weight	Ref. Bar	Gage reading	Corr. gage reading	Frqncy	RDM	Durab. Factor	% Gage Length Change	%Wght Change
3/7/12	901	13	10102.6	0.2532	0.4143	0.4134	1676	90.58	3.93	0.0000	0.002
3/9/12	917	29	10092.7	0.2521	0.4132	0.4134	1669	89.82	8.68	0.0000	-0.096
3/13/12	953	65	10093.9	0.2523	0.4149	0.4149	1663	89.18	19.32	0.0094	-0.084
3/16/12	979	91	10094.7	0.2507	0.4141	0.4157	1656	88.43	26.82	0.0144	-0.076
3/26/12	1015	127	10088.6	0.2516	0.4167	0.4174	1648	87.58	37.07	0.0250	-0.137
3/28/12	1033	145	10089.6	0.2519	0.4168	0.4172	1633	85.99	41.56	0.0238	-0.127
3/29/12	1043	155	10090.2	0.2515	0.4172	0.418	1636	86.31	44.59	0.0288	-0.121
4/4/12	1081	193	10092.0	0.2513	0.4172	0.4182	1610	83.59	53.77	0.0300	-0.103
4/6/12	1087	199	10094.0	0.2495	0.4169	0.4197	1609	83.48	55.38	0.0394	-0.083
4/9/12	1113	225	10094.1	0.2518	0.4196	0.4201	1613	83.90	62.92	0.0419	-0.082
4/13/12	1128	240	10065.3	0.2513	0.4183	0.4193	1594	81.93	65.55	0.0369	-0.367
4/16/12	1156	268	10061.2	0.2520	0.4204	0.4207	1598	82.34	73.56	0.0456	-0.408
4/19/12	1179	291	10059.4	0.2524	0.4220	0.4219	1593	81.83	79.38	0.0531	-0.426
4/20/12	1188	300	10033.4	0.2515	0.4208	0.4216	1590	81.52	81.52	0.0513	-0.683
Totals		300						81.52	81.52	0.05	0.00

Initial Measurements		Post Break Measurments					
WIDTH	DEPTH	WIDTH		DEPTH			
4.590	3.512	4.558		3.511		68.52	Avg. DF bms 1,2,3
4.601	3.512	4.578		3.508		20.8907	Std. dev.
4.601	3.512	4.581		3.510			
4.615	3.513						
4.602	3.512	4.572		3.510	Avg.		

3/20/12 Equipment failure the beams had to be put in the walk in freezer for 6 days.

Figure A.26 – HVFA-70LA-FT1 Data

GM23		FREEZE & THAW LEDGER				Preliminary Testing Results @ Zero Cycles					
LAB NO:	HV FA3		BEAM ID NO:		2	Agg. Description		ROLLA			
Initial Weight in Air		10005.7					Starting Cycle Count			888	
					Initial bar reading		0.2523				
Initial Gage Reading		0.2670					Date Test Started		3/5/12		
					Completion Date		4/7/12				
Initial Frequency		1763				TERMINAL FREQUENCY			1058		
DATE	CYCLE # machine	Actual cycles	Weight	Ref. Bar	Gage reading	Corr. gage reading	Frqncy	RDM	Durab. Factor	% Gage Length Change	%Wght Change
3/7/12	901	13	10003.1	0.2532	0.2679	0.267	1694	92.33	4.00	0.0000	-0.026
3/9/12	917	29	10003.3	0.2521	0.2667	0.2669	1689	91.78	8.87	-0.0006	-0.024
3/13/12	953	65	10003.6	0.2523	0.2690	0.269	1691	92.00	19.93	0.0125	-0.021
3/16/12	979	91	10005.5	0.2507	0.2690	0.2706	1675	90.27	27.38	0.0225	-0.002
3/26/12	1015	127	10000.1	0.2516	0.2711	0.2718	1662	88.87	37.62	0.0300	-0.056
3/28/12	1033	145	9997.2	0.2519	0.2716	0.272	1656	88.23	42.64	0.0313	-0.085
3/29/12	1043	155	9998.0	0.2515	0.2721	0.2729	1643	86.85	44.87	0.0369	-0.077
4/4/12	1081	193	9995.5	0.2513	0.2726	0.2736	1618	84.23	54.19	0.0413	-0.102
4/6/12	1087	199	9991.9	0.2495	0.2723	0.2751	1626	85.06	56.42	0.0506	-0.138
4/9/12	1113	225	9990.1	0.2518	0.2762	0.2767	1613	83.71	62.78	0.0606	-0.156
4/13/12	1128	240	9970.3	0.2513	0.2748	0.2758	1578	80.11	64.09	0.0550	-0.354
4/16/12	1156	268	9971.2	0.252	0.2772	0.2775	1592	81.54	72.84	0.0656	-0.345
4/19/12	1179	291	9969.3	0.2524	0.2780	0.2779	1580	80.32	77.91	0.0681	-0.364
4/20/12	1188	300	9968.6	0.2515	0.2781	0.2789	1573	79.61	79.61	0.0744	-0.371
Totals		300						79.61	79.61	0.07	0.00

Initial Measurements		Post Break Measurments			
WIDTH	DEPTH	WIDTH		DEPTH	
4.569	3.491	4.611		3.477	
4.618	3.501	4.616		3.482	
4.613	3.496	4.610		3.492	
4.601	3.495				
4.600	3.496	4.612		3.484	Avg.

3/20/12 Equipment failure the beams had to be put in the walk in freezer for 6 days.

Figure A.27 – HVFA-70LA-FT2 Data

GM23		FREEZE & THAW LEDGER				Preliminary Testing Results @ Zero Cycles					
LAB NO:	HV FA3		BEAM ID NO:		3	Agg. Description		ROLLA			
Initial Weight in Air		9969.8					Starting Cycle Count			888	
					Initial bar reading		0.2523				
Initial Gage Reading		0.3015					Date Test Started		3/5/12		
					Completion Date		4/7/12				
Initial Frequency		1739				TERMINAL FREQUENCY			1043		
DATE	CYCLE # machine	Actual cycles	Weight	Ref. Bar	Gage reading	Corr. gage reading	Frqncy	RDM	Durab. Factor	% Gage Length Change	%Wght Change
3/7/12	901	13	9971.1	0.2532	0.3025	0.3016	1672	92.44	4.01	0.0006	0.013
3/9/12	917	29	9974.1	0.2521	0.3014	0.3016	1659	91.01	8.80	0.0006	0.043
3/13/12	953	65	9977.6	0.2523	0.3044	0.3044	1640	88.94	19.27	0.0181	0.078
3/16/12	979	91	9982.5	0.2507	0.3039	0.3055	1607	85.40	25.90	0.0250	0.127
3/26/12	1015	127	9987.2	0.2516	0.3086	0.3093	1563	80.78	34.20	0.0487	0.175
3/28/12	1033	145	9987.6	0.2519	0.3103	0.3107	1516	76.00	36.73	0.0575	0.179
3/29/12	1043	155	9982.0	0.2515	0.3111	0.3119	1506	75.00	38.75	0.0650	0.122
4/4/12	1081	193	9976.9	0.2513	0.3132	0.3142	1441	68.66	44.17	0.0794	0.071
4/6/12	1087	199	9976.9	0.2495	0.3129	0.3157	1440	68.57	45.48	0.0888	0.071
4/9/12	1113	225	9978.0	0.2518	0.3192	0.3197	1368	61.88	46.41	0.1138	0.082
4/13/12	1128	240	9932.4	0.2513	0.3185	0.3195	1310	56.75	45.40	0.1125	-0.375
4/16/12	1156	268	9933.0	0.252	0.3223	0.3226	1267	53.08	47.42	0.1319	-0.369
4/19/12	1179	291	9901.1	0.2524	0.3236	0.3235	1210	48.41	46.96	0.1375	-0.689
4/20/12	1188	300	9895.9	0.2515	0.3275	0.3283	1159	44.42	44.42	0.1675	-0.741
Totals		300						44.42	44.42	0.17	0.18

Initial Measurements		Post Break Measurments		
WIDTH	DEPTH	WIDTH		DEPTH
4.568	3.538	4.576		3.491
4.592	3.504	4.566		3.492
4.581	3.501	4.557		3.502
4.589	3.515			
4.583	3.515	4.566		3.495 Avg.

3/20/12 Equipment failure the beams had to be put in the walk in freezer for 6 days.

Figure A.28 – HVFA-70LA-FT3 Data

REFERENCES

ASTM C 39 (2010). Standard Test Method for Compressive Strength of Cylindrical Concrete Specimens. *American Society of Testing and Materials,* West Conshohocken, PA.

ASTM C 78 (2010). Standard Test Method for Flexural Strength of Concrete (Using Simple Beam with Third-Point Loading) *American Society of Testing and Materials,* West Conshohocken, PA.

ASTM C 192 (2007). Standard Test Method for Making and Curing Concrete Test Specimens in the Laboratory. *American Society of Testing and Materials,* West Conshohocken, PA.

ASTM C 469 (2002). Standard Test Method for Static Modulus of Elasticity and Poissons Ratio of Concrete in Compression. *American Society of Testing and Materials,* West Conshohocken, PA.

ASTM C 496 (2004). Standard Test Method for Splitting Tensile Strength of Cylindrical Concrete Specimens. *American Society of Testing and Materials,* West Conshohocken, PA.

ASTM C 618 (2004). Standard Guide for Coal Fly Ash and Raw or Calcined Natural Pozzolan for Use in Concrete. *American Society of Testing and Materials,* West Conshohocken, PA.

ASTM C 666 (2008). Standard Test Method for Resistance of Concrete to Rapid Freezing and Thawing. *American Society of Testing and Materials,* West Conshohocken, PA.

ASTM C 672 (2008). Standard Test Method for Scaling Resistance of Concrete Surfaces Exposed to Deicing Chemicals. *American Society of Testing and Materials,* West Conshohocken, PA.

ASTM C 1202 (2010). Standard Test Method for Electrical Indication of Concrete's Ability to Resist Chloride Ion Penetration. *American Society of Testing and Materials*, West Conshohocken, PA.

ASTM C 1543 (2010). Standard Test Method for Determining the Penetration of Chloride Ion into Concrete by Ponding. *American Society of Testing and Materials,* West Conshohocken, PA.

Office of Research, Development, and Technology, Office of Safety, RDT. (1997). "User Guidelines for Waste and Byproduct Materials in Pavement Construction," *Report No. FHWA-RD-97-148*. Federal Highway Administration, Cortest Columbus Technologies.

V.M. Malhotra and P.K. Mehta (2008). *High-Performance, High-Volume Fly Ash Concrete for Building Sustainable and Durable Structures*. (Third Editon).

Mindess, Sidney, Young, J. Francis, and Darwin, David (2003). *Concrete*. Pearson Education, Inc. (Second Editon)

Powers, T.C., "Freezing Effects in Concrete," in *Durability of Concrete*, SP-47, American Concrete Institute, Detroit, MI, pp. 1-12 (1975)

Shi, Caijun, "Another Look at the Rapid Chloride Permeability Test (ASTM C1202 or AASHTO T277)

Bentz, Dale P. and Ferraris, Chiara F. (2001). Rheology and Setting of High Volume Fly Ash Mixtures. *National Institute of Standards and Technology*. Gaithersburg, MD.

Broomfield, John P. (2007). *Corrosion of Steel in Concrete: Understanding, Investigation and Repair*. Taylor & Francis (Second Edition).

Hopkins, D.S., Thomas, M.D.A., Oates, D.B., Girn, G., Munro, R. (2003). York University uses High-Volume Fly Ash Concrete for Green Building. Department of Civil Engineering, University of Toronto, Canada.

Huffman, Morris and ACI Committee 232. (2003). "Use of Fly Ash in Concrete," *Report No. ACI 232.2R-03*. American Concrete Institute, Farmington Hills, MI.

Sengul, O. and Gjørv, O. (2009). Effect of Embedded Steel on Electrical Resistivity Measurements on Concrete Structures. *ACI Materials Journal, 106(1),* 11-18.

Whiting, D.A. and Nagi, M.A. (2003). *Electrical Resistivity of Concrete - A Literature Review,* R&D Serial No. 2457. Portland Cement Association, Skokie, IL.

Mansfield, F. "Recording and Analysis of AC Impedance Data for *Corrosion* Studies," *Corrosion*, Vol. *37*, No. *5*, *1981*, pp. *301-307*

Berke, N.S. and Hicks, M.C., "Predicting Times to Corrosion from Field and Laboratory Data," Techniques to Assess the Corrosion Activity of Steel Reinforced Concrete Structures, ASTM STP 1276. Neal S. Berke, Edward Escalante, Charles K. Nmai, and David Whiting, Eds., American Society for Testing and Materials, 1996.

Marlay, Kyle M. *Hardened Concrete Properties and Durability Assessment of High Volume Fly Ash Concrete*. Report. Missouri University of Science and Technology, 2011. Print.

Ortega, Carlos A. *Shear and Fracture Behavior of High-Volume Fly Ash Reinforced Concrete for Sustainable Construction.* Report. Missouri University of Science and Technology, 2012. Print.

A. M. Neville (1997). *Properties of Concrete*. John Wiley and Sons, Inc. (Fourth Edition).

Oluokun, Francis A (1991). "Prediciton of Concrete Tensile Strength from Its Compressive Strength: Evaluation of Existing Relations for Normal Weight Concrete." *ACI Materials Journal*, Vol. 88, No. 3, pp. 302-309.